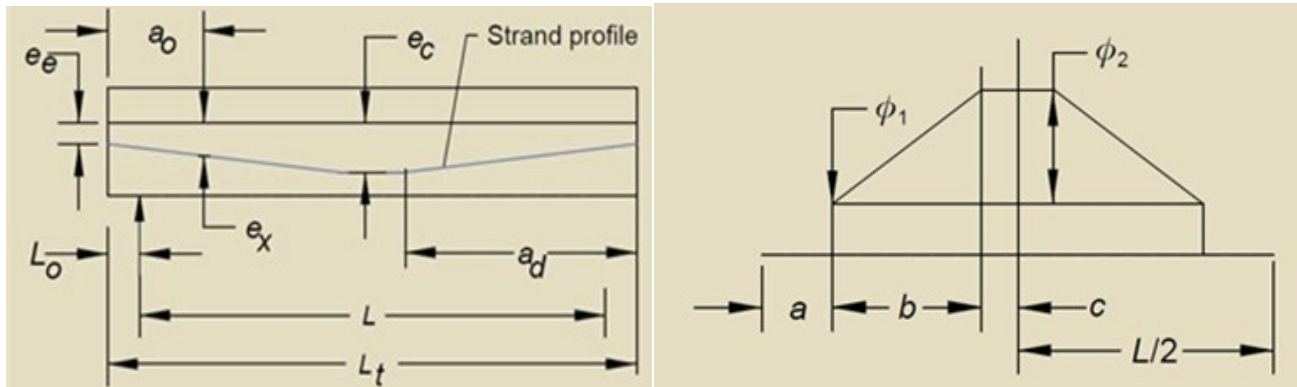


Enhanced Camber Calculations for Prestressed Concrete Bridge Girders



December 2021
Final Report

Project number TR202101
MoDOT Research Report number cmr 21-011

PREPARED BY:

Dr. Sarah Orton

Dr. Vellore Gopalaratnam

Ali Elawadi

John Holt

Dr. Maria Lopez

Dr. Thomas Murphy

University of Missouri-Columbia

PREPARED FOR:

Missouri Department of Transportation

Construction and Materials Division, Research Section

TECHNICAL REPORT DOCUMENTATION PAGE

1. Report No. cmr 21-011	2. Government Accession No.	3. Recipient's Catalog No.	
4. Title and Subtitle Enhanced Camber Calculations for Prestressed Concrete Bridge Girders		5. Report Date November 2021 Published: December 2021	
		6. Performing Organization Code	
7. Author(s) Dr. Sarah Orton, Dr. Vellore Gopalaratnam, Ali Elawadi, John Holt, Dr. Maria Lopez, Dr. Thomas Murphy		8. Performing Organization Report No.	
9. Performing Organization Name and Address Department of Civil and Environmental Engineering University of Missouri-Columbia E2509 Lafferre Hall Columbia, MO 65201		10. Work Unit No.	
		11. Contract or Grant No. MoDOT project # TR202101	
12. Sponsoring Agency Name and Address Missouri Department of Transportation (SPR-B) Construction and Materials Division P.O. Box 270 Jefferson City, MO 65102		13. Type of Report and Period Covered Final Report (September 2020-November 2021)	
		14. Sponsoring Agency Code	
15. Supplementary Notes Conducted in cooperation with the U.S. Department of Transportation, Federal Highway Administration. MoDOT research reports are available in the Innovation Library at https://www.modot.org/research-publications .			
16. Abstract The objective of this study was to develop accurate prestressed girder camber calculations and validate them with available data. The project team conducted a thorough literature review and analyzed recent girder camber research efforts in other states. The project collected existing data on 189 Missouri bridge girders. The project also collected field data and cylinder samples from four girders during fabrication. The camber prediction equations and parameters were evaluated and compared to the field data. The study found that the current prediction method under-predicted the initial camber measured in the field on average by about 25%. However, investigation also found that the field measurements may have had error due to sag in the measurement string line. The study found that the effect of the overhang (girder length past storage support locations) affects the camber. Temperature effects were found to be another source of camber error. The current camber calculations were modified to include the effect of the girder overhang and a continuous time-dependent prediction of camber. In addition, guidelines for camber measurement were developed. The modifications to the camber prediction reduced the underprediction of camber to less than 4% on average and decreased the variability to within $\pm 25\%$. The proposed method was implemented into a computer spreadsheet for easy calculation.			
17. Key Words Camber research, Girder bridges, Literature reviews, Prestressed concrete		18. Distribution Statement No restrictions. This document is available through the National Technical Information Service, Springfield, VA 22161.	
19. Security Classif. (of this report) Unclassified.	20. Security Classif. (of this page) Unclassified.	21. No. of Pages 170	22. Price

Report

Enhanced Camber Calculations for Prestressed Concrete Bridge Girders

Prepared for
Missouri Department of Transportation
Construction and Materials

By:

Dr. Sarah Orton, Dr. Vellore Gopalaratnam, Ali Elawadi

University of Missouri

John Holt, Dr. Maria Lopez, Dr. Thomas Murphy

Modjeski and Masters, Inc.

November 2021

Table of Contents

ABSTRACT.....	xvi
EXECUTIVE SUMMARY	xvii
CHAPTER 2: INTRODUCTION.....	1
2.1 Research Objectives and Methodology.....	2
2.2 Organization of Report.....	2
CHAPTER 3: BACKGROUND.....	4
3.1 Previous Studies.....	5
3.1.1 Tadros (2011).....	6
3.1.2 Tadros (2015).....	7
3.1.3 Gilbertson and Ahlborn (2004).....	7
3.1.4 Nguyen et al. (2015)	8
3.1.5 Washington Study; Rosa et al. (2007)	9
3.1.6 North Carolina Study; Rizkalla et al. (2011)	10
3.1.7 Minnesota Study; French and O’Neill (2012)	11
3.1.8 Iowa Study; Honarvar et al. (2015).....	11
3.1.9 Alabama Study; Stallings et al. (2003)	12
3.1.10 Arkansas Study; Mohammedi and Hale (2018), Feedle (2017)	13

3.1.11	Idaho Study; Brown (1998)	13
3.1.12	Mississippi Study; Tomley (2019).....	14
3.1.13	Oklahoma Study; Jayaseelan and Russell (2007)	14
3.1.14	Summary of Previous Literature	14
3.2	Camber Prediction Overview	15
3.2.1	Multiplier Method.....	16
3.2.2	Refined/Approximate Method	16
3.2.3	Incremental Time-Step Approach.....	17
3.2.4	Camber Prediction Methods in Other States.....	17
3.3	Camber Measurement	18
CHAPTER 4: MISSOURI BRIDGE CAMBER FIELD DATA.....		20
4.1	Girder Properties	20
4.2	Camber Measurements and Predictions	22
4.2.1	Camber Measurement Method.....	26
4.3	Field Measured Cambers.....	30
4.3.1	Field Camber.....	33
4.4	Summary	36
CHAPTER 5: CAMBER CALCULATION – A PARAMETRIC ANALYSIS OF RELATIVE SENSITIVITY		37
5.1	Effect of Overhang	38

5.2	Effect of Concrete Modulus of Elasticity.....	47
5.3	Effect of Concrete Age/Strength at Prestress Transfer	52
5.4	Effect of Temperature	57
5.5	Effect of Prestressing Force	59
5.5.1	Elastic Shortening.....	60
5.5.2	Relaxation Losses	60
5.6	Transformed vs. Gross Section Properties	63
5.7	Temperature Due to Concrete Curing	65
5.8	Effect of Concrete Density.....	66
5.9	Strand Eccentricity	67
5.10	Effect of Creep	69
5.10.1	Effect of Concrete Creep	69
5.11	Effect of Concrete Shrinkage	77
5.12	Effect of Humidity	78
5.13	Effect of the Long-Term Prediction Method.....	79
5.14	Conclusions and Recommendations.....	84
CHAPTER 6: PROPOSED CAMBER PREDICTION		89
6.1	Calculation of Deflection and Camber.....	89
6.1.1	Initial Camber at Transfer at Midspan	89

6.1.2	Camber at Midspan After Strand Release.....	90
6.1.3	Final Camber at Midspan After Slab is Poured	91
6.1.4	Final Camber Along Span Length	91
6.1.5	Calculation of Camber (Upward) Using Transformed Properties	92
6.1.6	Calculations of Deflections (Downward)	94
6.1.7	Creep Coefficient	96
6.1.8	Prestress Losses	97
6.1.9	Elastic Shortening	97
6.1.10	Modulus of Elasticity	101
6.1.11	Temperature Due to Concrete Curing.....	101
6.1.12	Change in Camber Due to Daily Temperature Variation	102
6.2	Camber Prediction Spreadsheet	102
6.2.1	Overview of the Spreadsheet	103
6.2.2	Time Camber Estimates (Discrete Time-Step).....	117
6.2.3	Time Camber Estimates (Time-Step)	117
6.2.4	Sensitivity Analysis	119
6.3	Spreadsheet Verification	119
6.4	Proposed Camber Measurement.....	122
CHAPTER 7:	SUMMARY AND CONCLUSIONS.....	124

REFERENCES	129
Appendix A.....	1
A-1 Current MoDOT Method	1
Initial Camber at Transfer	1
Camber at Midspan After Strand Release (Estimated at 7 days)	2
Camber at Midspan After Erection (Estimated at 90 days)	2
Final Camber at Midspan After Pouring the Slab	2
Calculation of Camber (Upward) Using Transformed Properties.	3
Calculations of Deflections (Downward).....	5
Creep Coefficient	6
A-2 PGSuper Method	7
Initial Camber at Transfer	8
Camber at Hauling (Estimated at 90 days).....	10
A-3 Incremental time-step approach Stallings et al. (2003)	12
A-4 Incremental time-step approach Tadros et al. (2011)	13
A-5 Incremental time-step approach Naaman (2012).....	15

List of Figures

Figure 3-1. Number of bridges in study for each girder type	20
Figure 3-2. Inventory of Missouri bridges based on girder type	21
Figure 3-3. Distribution of girder length in the study database	22
Figure 3-4. Seam line in beam for precast Plant #1	23
Figure 3-5. Comparison of camber at 7 days on bridge plans and measured camber	24
Figure 3-6. Comparison of camber at 90 days on bridge plans and measured camber	25
Figure 3-7. Camber prediction at transfer using current MoDOT method	26
Figure 3-8. Comparison of predicted and measured camber from precast Plant #1	27
Figure 3-9. Comparison of predicted and measured camber from precast Plant #2	27
Figure 3-10. Comparison of predicted and measured camber from precast Plant #2 correcting for the line sag	30
Figure 3-11. Concrete creep test setup.....	32
Figure 3-12. Creep testing results	33
Figure 3-13. Measured vs. calculated camber for Bridge #1 girders.....	35
Figure 3-14. Measured vs. calculated camber for Bridge #2 girders.....	35
Figure 4-1. Bending moment diagram due to girder's weight (Tadros et al. 2001).....	39
Figure 4-2. Optimum strand arrangement used in Tadros method (Tadros et al. 2001).....	39
Figure 4-3. Debond and transfer length (Tadros et al. 2001).....	40
Figure 4-4. The curvature distribution due to the initial prestress (Tadros et al. 2001)	40
Figure 4-5. Girder self-weight deflection during lifting	42
Figure 4-6. Girder dimensions (Brice 2020).....	42
Figure 4-7. Strand eccentricities (Brice 2020).....	42
Figure 4-8. Camber including overhang length equal to girder depth per Tadros (2011)	44
Figure 4-9. Camber including overhang length equal to girder depth per PGSuper method	45
Figure 4-10. Camber including overhang length equal to lifting location per PGSuper method .	46
Figure 4-11. Sensitivity of overhang length on camber per PGSuper method	46
Figure 4-12. Effect of k_1 modulus factor on camber prediction	50

Figure 4-13. Camber using AASHTO (2010) equation for concrete modulus.....	51
Figure 4-14. Camber using ACI 363 equation for concrete modulus.....	51
Figure 4-15. Camber using CEB-FIP Model Code 1990 equation for concrete modulus.....	52
Figure 4-16. Concrete age at release for the available field data.....	54
Figure 4-17. Reported cylinder strengths vs ACI predictions using design compressive strength	55
Figure 4-18. Field measured compressive strength of concrete vs. the expected compressive strength using ACI 209R-92 formula	55
Figure 4-19. Field measured compressive strength of concrete vs. the expected compressive strength modified ACI 209R-92 formula.....	56
Figure 4-20. Predicted camber using the measured initial concrete strength	56
Figure 4-21. Predicted camber considering 20°F temperature variation	58
Figure 4-22. Predicted camber considering actual daily temperature variation	59
Figure 4-23. Predicted camber when increasing the jacking force by 6 ksi	62
Figure 4-24. Predicted camber when decreasing the jacking force by 6 ksi.....	62
Figure 4-25. Predicted camber when decreasing the initial prestress force by 5%	63
Figure 4-26. Predicted camber using transformed properties.....	64
Figure 4-27. Predicted camber using gross properties.....	64
Figure 4-28. Predicted camber including prestress reduction due to increased concrete temperature at curing	66
Figure 4-29. Predicted camber when decreasing the concrete density by 5%.....	67
Figure 4-30. Predicted camber when considering strand eccentricity of (+1/16 in.).....	68
Figure 4-31. Predicted camber when considering strand eccentricity of (-1/16 in.).....	68
Figure 4-32. Comparison of the different creep models with the tested concrete cylinders	74
Figure 4-33. Change in 90-day camber due to the creep coefficient	75
Figure 4-34. Camber prediction at later time using the current MoDOT method.....	76
Figure 4-35. Camber prediction at later time when increasing the creep coefficient by 20%.....	76
Figure 4-36. Change in 90-day camber due to shrinkage strain	77
Figure 4-37. Camber prediction at later times when increasing the shrinkage strain by 50%	78

Figure 4-38. Camber prediction at later times when using relative humidity as 50%.....	79
Figure 4-39. Time-dependent camber growth prediction vs. measured for Bridge #1.....	81
Figure 4-40. Time-dependent camber growth prediction vs. measured for Bridge #2.....	81
Figure 4-41. Time-dependent camber growth prediction vs. measured for bridge monitored by Gopalaratnam and Eatherton (2001) (shorter span).....	82
Figure 4-42. Time-dependent camber growth prediction vs. measured for bridge monitored by Gopalaratnam and Eatherton (2001) (longer span).....	82
Figure 4-43. Camber growth prediction vs. measured when using the AASHTO approach.....	83
Figure 4-44. Camber growth prediction vs. measured when using the Stalling approach with default ACI parameters.....	83
Figure 4-45. Camber prediction when using the Naaman approach with ACI creep equation	84
Figure 4-46. Predicted to measured camber with correction for sag in measurement line, overhang length, and actual concrete strength.....	87
Figure 4-47. Predicted to measured camber with correction for sag in measurement line, overhang length, and actual concrete strength for only Plant #2 girders.....	88
Figure 4-48. Predicted to measured camber with correction for sag in measurement line, overhang length, and design concrete strength for only Plant #2 girders.....	88
Figure 5-1. Girder details displaying the eccentricities and distances used in camber computations.....	93
Figure 5-2. Girder dimensions.....	94
Figure 5-3. Proposed spreadsheet page 1.....	104
Figure 5-4. Proposed spreadsheet page 2.....	105
Figure 5-5. Proposed spreadsheet page 3.....	106
Figure 5-6. Proposed spreadsheet page 4.....	107
Figure 5-7. Proposed spreadsheet page 5.....	108
Figure 5-8. Page heading in the spreadsheet.....	109
Figure 5-9. Prestressed girder definition.....	109
Figure 5-10. Haunch details.....	110
Figure 5-11. Slab details.....	110
Figure 5-12. Material properties.....	111

Figure 5-13. Strand profile and definition	112
Figure 5-14. Strand eccentricities	112
Figure 5-15. Input to account for debonded strands	113
Figure 5-16. Transformed section properties.....	114
Figure 5-17. Initial camber calculations	115
Figure 5-18. Loss estimation.....	116
Figure 5-19. Additional deflection.....	116
Figure 5-20. Time camber estimates (discrete time-step).....	117
Figure 5-21. Time camber estimates (time-step)	118
Figure 5-22. Sensitivity analysis.....	119
Figure 5-23. Comparison of Spreadsheet results vs PGSuper and Lusas for NU girder	121
Figure 5-24. Comparison of Spreadsheet results vs PGSuper and Lusas for Tx girder	122

List of Tables

Table 2-1: Previous research of camber calculation methods	5
Table 2-2: Comparison of camber prediction method by state.....	17
Table 3-1. Measured and predicted sag in string line	29
Table 3-2. Concrete mix design quantities	31
Table 3-3. Properties of field-tested girders	31
Table 3-4. Measured concrete compressive strength and modulus	31
Table 3-5. Camber measurement and prediction	34
Table 4-1. Factors affecting initial camber calculation	37
Table 4-2. Equations used in the initial camber prediction proposed by Tadros et al. 2001	40
Table 4-3. Equations used in the initial camber prediction proposed by PGSuper (Brice 2020)	42
Table 4-4. Comparison of experimental and predicted modulus of elasticity	49
Table 4-5. The values of the α and β constants.....	53
Table 4-6: Factors affecting long-term camber prediction	69

COPYRIGHT

Authors herein are responsible for the authenticity of their materials and for obtaining written permissions from publishers or individuals who own the copyright to any previously published or copyrighted material used herein.

DISCLAIMER

The opinions, findings, and conclusions expressed in this document are those of the investigators. They are not necessarily those of the Missouri Department of Transportation, U.S. Department of Transportation, or Federal Highway Administration. This information does not constitute a standard or specification.

ACKNOWLEDGMENTS

The authors would like to thank the Missouri Department of Transportation and the Missouri Center for Transportation Innovation for sponsoring this research. The authors would also like to thank the Missouri Department of Transportation Technical Advisory Committee for their assistance in the research.

ABSTRACT

The objective of this study was to develop accurate prestressed girder camber calculations and validate them with available data. The project team conducted a thorough literature review and analyzed recent girder camber research efforts in other states. The project collected existing data on 189 Missouri bridge girders. The project also collected field data and cylinder samples from four girders during fabrication. The camber prediction equations and parameters were evaluated and compared to the field data. The study found that the current prediction method under-predicted the initial camber measured in the field on average by about 23%. However, investigation also found that the field measurements may have had error due to sag in the measurement string line. The study found that the effect of the overhang (girder length past storage support locations) affects the camber. Temperature effects were found to be another source of camber error. The current camber calculations were modified to include the effect of the girder overhang and a continuous time-dependent prediction of camber. In addition, guidelines for camber measurement were developed. The modifications to the camber prediction reduced the underprediction of camber to less than 4% on average and decreased the average error from 35% to 20%. This yielded predictions that were in most cases within $\pm 25\%$ of the measured camber. The proposed method was implemented into a computer spreadsheet for easy calculation.

EXECUTIVE SUMMARY

The objective of this study was to develop accurate prestressed girder camber calculations and validate them with available data. Accurate bridge camber in prestressed concrete girders is a critical design component in the ride, appearance, maintenance requirements, slab placement, and overall life of a concrete bridge superstructure.

A literature review found several previous studies that have highlighted the difficulties in predicting initial and long-term camber. Even with improvements to equations, accuracy was at best in the $\pm 15\%$ range. The primary causes of camber error were concrete compressive strength, concrete modulus, temperature effects, creep and shrinkage parameters, support geometry, and camber measurement errors.

Data from 189 girders with initial camber and 33 girders with later camber measurements before hauling were analyzed to evaluate the accuracy of the camber calculation procedure. In addition, field measurements were conducted on four girders, including material characterization tests for concrete strength gain with time, modulus, and creep.

The current camber measurement showed an average under-prediction of the camber by about 23% with a RMSE of 0.81 in. and average error of 35%. The camber measurement method in two precast plants were compared. It was found that the self-weight of the string line used to measure camber caused a significant sag and led to larger than actual camber measurements.

A systematic look at the parameters affecting the accuracy of the initial and long-term camber predictions was undertaken. The parameters of overhang length, concrete modulus, concrete strength/age, temperatures, prestressing force, section properties, temperature during curing, concrete density, strand eccentricity, creep, shrinkage, humidity, and long-term analysis method were systematically investigated. The investigation found that the length of the overhang (distance past temporary supports) does affect camber. A change in overhang length from 0 ft. to 4 ft. can cause a change in camber of about 20% (average change based on girder data set). Analysis equations used in PGSuper can be used to include the effect of overhang in the initial camber. Concrete modulus equations from different sources only changed the camber prediction by about 4%. Using the measured compressive strength, decreases the trendline slope of the measured to predicted camber by 10%. Increased temperatures during curing can temporarily reduce prestress forces and reduce camber by about 12%. Daily temperature changes cause a thermal gradient in the girder and can increase camber by 25% with a 25 °F temperature change. The effect of temperature should be considered in the camber results. In order to mitigate the effect of temperature, camber can be measured at least 72 hours after form release, and in the morning (Tadros 2015). Other factors investigated did not significantly change the camber prediction. The project also found that procedures and tolerances for the measurement of camber and location of temporary supports at prestress girder plants are needed.

The main changes in the camber calculation equations compared to the current MoDOT method are:

- Incremental time-step approach. Rather than determining camber at transfer, 7 days, and 90 days, camber can thus be determined at any point in the life of the girder.
- Include effect of overhang length on camber.
- Additional options to include the effects of prestress loss due to elevated concrete temperatures during curing and daily temperature effects on camber.

The modifications to the camber calculation reduced the underprediction of camber to less than 4% on average (when sag in the string line measurement was accounted for) and decreased the RMSE from 0.81 in. to 0.30 in. and the average error from 35% to 20%. This yielded predictions that were in most cases within $\pm 25\%$ of the measured camber. The proposed method was implemented into a computer spreadsheet for easy calculation.

CHAPTER 1: INTRODUCTION

Accurate bridge camber in prestressed concrete girders is a critical design component in the ride, appearance, maintenance requirements, slab placement, and overall life of a concrete bridge superstructure. However, errors in the calculation of the prestressed girder camber may lead to difficulties during construction. Less than expected camber may increase the concrete needed to meet the deck slab bottom which causes additional weight to the superstructure. On the other hand, a higher-than-expected camber can result in difficulties in meeting planned deck grade. Differential camber is an issue with phased constructed bridges, as the girders from each phase can be fabricated and delivered at widely varying times, resulting in differences in camber. These cases cause undesirable sequences that may result in delays in the construction and increase the cost of material and labor. The motivation of this study was to improve the prestressed camber calculation and provide a validated calculation tool.

The study looked closely at possible contributors to the causes for error in camber, including concrete properties (e.g., strength, stiffness, creep), prestressing tendon relaxation, beam storage conditions, and camber measurement methods. Changes in some of these methods and conditions (such as the use of high-performance concretes) over the years have additionally led to more inaccuracies in the current camber calculations. This project evaluated the sources of error in camber calculation and measurement and developed a new calculation model validated with measured field data.

1.1 *Research Objectives and Methodology*

The main objective of this project was to develop accurate prestressed girder camber calculations and validate them with available data. To achieve this objective, specific objectives included:

- Evaluation of the existing camber calculation and measurement techniques. This was conducted through literature review and analyzing the recent girder camber research efforts in other states.
- Collection of existing data and gathering of additional data on Missouri prestressed concrete bridge girders.
- Evaluation of the camber data and comparison of calculated camber by different camber models.
- Development of an accurate calculation method considering time-dependent effects for camber.
- Validation of the calculation method with the existing and field data from Missouri bridges, as well as custom measurements on prestressed girders at a pre-casting plant.

1.2 *Organization of Report*

This report is organized as follows:

- Chapter 2 summarizes the previous research in camber calculation with a view to identify possible parameters for improved camber calculation. The chapter also reviews the main approaches to camber calculation.

- Chapter 3 describes the available field data from 189 girders with initial camber measurement, and 29 girders with later camber measurements before hauling. In addition, field testing was conducted for two bridge pours comprising four girders including material characterization tests for concrete strength gain with time, modulus, and creep.
- Chapter 4 describes the evaluation of the parameters that affect camber calculation. The parameters were considered in relation to the field data and evaluated to determine which changes improve camber calculation.
- Chapter 5 describes the proposed camber calculation method and camber measurement method. The chapter also details the guidelines for the use of the spreadsheet to calculate the camber.
- Chapter 6 provides the summary and conclusions for this study including recommendations and suggestions for practice and future research.

CHAPTER 2: BACKGROUND

Precast, pre-tensioned concrete beams (PPCBs) use prestressed steel to improve the flexural resistance of the beam. When prestressing steel is below the centroid of the beam, this causes an upward deflection that is counteracted by the self-weight of the member, resulting in a camber.

Accurate camber in prestressed concrete girders is a critical design component in the ride, appearance, maintenance requirements, slab placement, and overall life of a concrete superstructure bridge. The camber calculation helps to determine haunching requirements when the girder is placed, as well as slab deck requirements. Differential camber is an issue with phased constructed bridges, as the girders from each phase can be fabricated and delivered at widely varying times, resulting in differences in camber. However, there are some difficulties in accurately calculating this camber. Designers may have challenges with accurately predicting the variables employed in the design, such as concrete properties, prestress force, and temperature effects. During fabrication, there may be problems with the methods of camber measurement and storage conditions implemented with PPCBs.

Furthermore, PPCBs exhibit time-dependent structural responses due to the time-dependent characteristics of the constituent materials. Concrete used in prestressed members exhibits aging, creep, and shrinkage at normal service temperatures and environmental conditions. While conventional reinforcement does not exhibit measurable creep or relaxation at service temperatures, high-strength prestressing strands do exhibit relaxation loss. Furthermore, temperature changes can affect the camber. The long-term variation of camber with time also needs to be understood for Missouri bridges to allow for more accurate camber calculations.

The previous issues mentioned have led to variations in the calculated to measured camber by as much as 50% (Tadros et al. 2011). In order to understand variations in camber calculations, the previous studies and factors that affect camber need consideration.

2.1 *Previous Studies*

The estimation of camber and comparison with field data has been a topic in many previous studies. Table 2-1 gives an overview of some of the previous work and details of selected works are given in the following sections.

Table 2-1: Previous research of camber calculation methods

State (year)	Method	Conclusion
Alabama (Stallings et al. 2003)	Monitored five AASHTO BT-54 girders for Alabama’s HPC Showcase Bridge.	Existing analytical methods can lead to accurate expectations of HPC girder camber and prestress losses if the properties of the material used in the calculations are measured in girder construction.
Arkansas (Mohammedi and Hale 2018)	9 PPCB instruments and materials tested.	Underestimation of concrete elastic modulus and prestress losses. Suggest a modification to the long-term multiplier.
Idaho (Brown 1998)	Theoretical analysis of time-dependent camber.	Developed a time-dependent model for camber prediction.
Iowa (Honarvar et. al 2015)	Measured material properties, considered data for instant camber of 100 PPCBs, monitored long-term camber 66 PPCBs.	Recommended best practices for camber measurement and proposed new long-term multipliers.
Minnesota (O’Neill and French 2012)	Examined camber records of 1,000 PPCBs, measured material properties.	Found higher than design concrete strengths, and lower strand stress at release due to thermal effects and relaxation. Developed multipliers to predict long-term camber.
Mississippi (Tomley 2019)	Examined camber prediction practices of several states, evaluated historical material property data.	Suggested improvements to material property data and revised multipliers for camber prediction.

State (year)	Method	Conclusion
Missouri (Yang and Meyers 2005, Gopalaratnam and Eatherton 2001)	Evaluated prestress loss estimates in an HPC bridge. Monitored an extensively instrumented HPC bridge.	Compared prestress loss estimates and recommended procedure, evaluated prestress losses, creep and shrinkage, and temperature effects.
North Carolina (Rizkalla et al. 2011)	Evaluated material property data and other factors for camber prediction with field measurements and site visits.	Concrete strength, form deformations, debonding length, and temperature gradient affected camber prediction. Developed detailed and approximate method to predict camber.
Oklahoma (Jayaseela and BRUCE 2007)	Analytical investigation on parameters affecting long-term deflections and camber.	AASHTO time-step methods, NCHRP 496, and PCI Design Handbook method produced comparable results.
Texas (Byle et al. 1997, Bayrak et al. 2012)	Measured camber and prestress loss and compared predictions. Evaluated prestress loss prediction.	Analytical time-step program produced accurate results, proposed multipliers for hand calculations, developed new prestress loss prediction formulas.
Washington (Rosa et al. 2007)	Time-dependent computer analysis verified with measured camber.	Response is sensitive to prestress loss, elastic modulus, and creep coefficient. Applied adjustment factors for elastic modulus and creep coefficient.

2.1.1 Tadros (2011)

Tadros (2011) discussed camber variability and ways to improve the accuracy of camber predictions. The report includes detailed equations used to predict both long-term and initial camber. The equations from Tadros (2001) are one of the sets equations analyzed in this study and are presented in Appendix A. The initial camber equation includes the effect of storage conditions, debonded strands, and transfer length. Tadros et al. (2011) found that variability of initial camber can arise from the variability of the concrete modulus (E_{ci} values can vary by $\pm 22\%$), differences in the actual vs. design concrete strength at release, differential temperature, initial prestress, girder weight, and storage conditions. Additional factors found to have less influence

include the prestressing force and section (use of gross vs. transformed section properties), debonding length, and friction at girder ends. For the long-term camber, it was found that the AASHTO LRFD requirements including prestressing losses, and concrete modulus of elasticity, creep, and shrinkage prediction equations can be effectively used. A constant aging coefficient of 0.7 is applied to the prestress losses.

2.1.2 Tadros (2015)

A later work by Tadros reported that the causes of initial camber variability include the concrete modulus of elasticity (22% error), curing vs. ambient temperatures reducing prestressing force, location of lifting inserts and storage supports, and errors in the estimation of prestress force and girder self-weight. Tadros (2015) suggested allowing a girder to cool for 72 hours before measuring the camber to remove the effect of the strand detensioning due to curing temperatures and measuring the camber in the morning for a neutral thermal gradient. Even so, camber prediction may be accurate to only within $\pm 25\%$. Recommended tolerance levels were $\pm 1/2$ in. for a predicted camber < 1 in. and $\pm 50\%$ for predicted cambers > 1 in.

2.1.3 Gilbertson and Ahlborn (2004)

Gilbertson and Ahlborn (2004) looked at the inherent variability of the parameters used to estimate prestress losses. The study found that the parameters with major influence include the jacking stress (± 6 ksi), concrete compressive strength at release ($\pm 1,300$ psi), relative humidity ($\pm 9\%$), and strand eccentricity ($\pm 1/16$ in.). These parameters can cause a variation of the prestress loss on the order of 20% or more.

2.1.4 Nguyen et al. (2015)

Nguyen et al. (2015) investigated the impacts of variation in temperature on the camber before casting the deck. The paper presented an experimental work, which involved monitoring of the prestress girder camber and temperatures. The experiment work found that in two girders (lengths 172 ft. and 164 ft.) the temperature in the top flange may reach 100°F while the bottom is at 65°F. The temperature variation in one day caused a change in camber of 0.6 in. and 0.5 in. in the girders. The experimental data were used to generate validated theoretical camber caused by temperature variation. A new practical method was developed which allows the designer to predict the camber in a bridge girder caused by diurnal temperature variations. The possible variation in camber in 12 hours becomes:

$$\Delta_{camber} = \left(\frac{\alpha A_1}{h} \right) (T_{max} - T_{min}) \left(\frac{L^2}{8} \right) \quad 2-1$$

where:

T_{max} = maximum air temperature during the 24-hour period,

T_{min} = minimum air temperature during the 24-hour period,

α = coefficient of thermal conductivity $5.5 \times 10^{-6}/^\circ\text{F}$ ($9.9 \times 10^{-6}/^\circ\text{C}$),

A_1 = calibration factor, assumed to be 1.28,

L = length of the prestressed girder,

h = the girder height,

Δ_{camber} = camber variation due to temperature.

2.1.5 *Washington Study; Rosa et al. (2007)*

To improve the accuracy of camber prediction, (Rosa et al. 2007) developed a computer program to predict the camber as a time function. This program was compared with the measured camber from 146 girders, and the long-term camber calculations were compared with the measured values of 91 girders. The program was calibrated to minimize the error in the camber predictions.

Camber measurements made by the researchers using a self-leveling laser level were compared to those made by the precast yard using a tape measure (while lifting the girder measurement of the distance to the casting bed taken at ends and middle). The variation in the measurement methods was about 0.25 in.

The research recommended the AASHTO equations for predicting the modulus of elasticity and the creep coefficient of concrete multiplied by calibrated adjustment factors of 1.15 for modulus and 1.4 for the creep coefficient. These factors can be calculated based on local material testing. In addition, the prestress losses had to be considered when calculating the creep component of the camber. The report mentioned that the beam overhang effect due to temporary supports needs to be taken into account in the camber calculations.

In the set of 146 girders analyzed, the predicted camber using the previous standard WSDOT method was larger than the measured camber by an average of 0.42 in. with the error increasing in longer girders. The modified WSDOT method with the factors applied reduced the average error to 0.14 in. when using the design concrete strength and 0.03 in. when using the measured concrete strength.

2.1.6 North Carolina Study; Rizkalla et al. (2011)

Rizkalla et al. (2011) looked closely at factors related to girder production to improve camber predictions. The factors considered include concrete compressive strength at release (on average 25% higher than design), concrete compressive strength at 28 days (on average 45% higher than design), concrete elastic modulus (15% less than AASHTO predicted), variation of concrete properties within a girder, variation of prestress force with temperature (for 60°F temperature change during curing prestress force can reduce by 7%), the effect of thermal gradients, and debonding length.

The report proposed a detailed and approximate method in camber prediction. Correction factors for both methods used included: 1.25 for the design release compressive strength of concrete, 1.45 for the design 28 days compressive strength of concrete, and 0.85 for the concrete modulus of elasticity k_1 factor in the AASHTO LRFD model.

The proposed method uses AASHTO (2012) for calculating the prestress losses, concrete creep, and concrete shrinkage, which is the same as MoDOT specifications. The author recommended recognizing the temperature gradient effect on the camber measurement and found that the transfer length of the PPCB affected the camber of the PPCB. However, the method ignores the effect of the overhang on the camber.

The original NCDOT method over-estimated the camber of the girders by an average of 52%, while the proposed approximate method reduced this to 16% and the detailed method to 6%.

2.1.7 Minnesota Study; French and O'Neill (2012)

French and O'Neill (2012) looked at historical data from 1,067 girders and found cambers at release and erection were 74% and 83.5% of the predicted values. They developed a computer program that evaluated the influence of time-dependent effects such as solar radiation, relative humidity, concrete creep, shrinkage, length of cure, and storage conditions.

French and O'Neill (2012) recommended a correction factor to the concrete properties, 1.15 for the release design compressive strength of concrete, and recommended the AASHTO 2010 equation for concrete modulus. Thermal effects caused a strand relaxation of approximately 3%. The correction increased the accuracy of the release camber to 99% but did not reduce the scatter.

For long-term camber, they found that solar radiation can change the camber as much as 15% during the course of a day. In addition, the ACI 209R-92 models for calculating concrete creep and shrinkage provided the best long-term results. The influence of temperature and relative humidity on the creep and shrinkage were considered to predict the time-dependent camber. Storage conditions were found to be important and recommended limits (e.g., at least 2 ft. but no more than 8 ft. for certain girder shapes) to limit variability. Finally, a simple multiplier approach was proposed to calculate the long-term camber that multiplied the release camber by different factors (1.65 to 2.05) based on the girder age at erection. The proposed modifications were expected to reduce camber variability to $\pm 15\%$.

2.1.8 Iowa Study; Honarvar et al. (2015)

To minimize the potential sources of errors between the designed and measured camber, Honarvar et al. (2015) conducted a study that looked closely at concrete material properties and factors

affecting release camber for 100 girders and long-term camber in 66 girders. The current Iowa method was found to over-predict camber in long bulb-tee girders 75% of the time, and under-predicted in shorter girders.

They evaluated the factors that affect the release camber and found the impact of sacrificial strands (2.6%), transfer length (1.5%), prestress losses (11.3%), and transformed vs. gross moment of inertia (2.9%). For release camber, they recommended using AASHTO (2010) for concrete modulus, increasing the concrete release strength (40% to 10%), the gross moment of inertia, and including prestress losses.

Furthermore, the effects of concrete creep and shrinkage, overhang and prestress force, and the temperature were considered. They found that the AASHTO (2010) creep and shrinkage models gave the best estimates but still showed large errors. They proposed their own equations for creep and shrinkage. In instrumented girders, they found that long-term camber varied as much as 0.75 in. in 24 hours due to thermal effects. Sophisticated analytical models including all the parameters mentioned were able to predict the long-term camber within $\pm 15\%$. They proposed a set of multipliers to improve camber predictions based on the amount of camber ($<$ or $>$ 1.5 in.), assumed temperature difference (15°F), and overhang length ($L/30$).

2.1.9 Alabama Study; Stallings et al. (2003)

The over-estimation of camber and prestress losses for high-performance prestressed bridge girders motivated Stallings et al. (2003) to improve the camber calculations. In this research, camber and strains from prestressing transfer to bridge completion were measured for five AASHTO BT-54 girders for Alabama's HPC Showcase Bridge. In addition, the camber of 31

girders was measured at an average concrete age of 200 days. Sample cylinders for creep, shrinkage, and modulus of elasticity tests were cast and match-cured during girder production. Modified properties using the ACI 209R-92 models for creep, and shrinkage were used to calculate the camber and prestress losses up to the construction time of the deck. The field measurements displayed good agreement with values calculated with measured material properties.

2.1.10 Arkansas Study; Mohammedi and Hale (2018), Feedle (2017)

A more recent study in Arkansas also aimed to improve the camber prediction accuracy. The measured cambers were less than the design cambers due to concrete compressive strengths that were 26% to 80% higher than the design strength, and the concrete elasticity modulus that were 20% to 50% higher than the design modulus. The researchers proposed a k_1 correction factor of 1.0 to 1.2 in the AASHTO (2014) equation for concrete modulus based on the aggregate source and concrete compressive strength. The long-term camber multiplier was modified from 2.45 to 1.4. These modifications decrease the variation between the calculated and measured camber.

2.1.11 Idaho Study; Brown (1998)

Brown (1998) analyzed the current models for calculating the time-dependent camber of prestressed concrete girders. A time-dependent model for predicting the camber was proposed as well as a simple formula for estimating the camber at erection. The camber prediction of both approaches was compared to the provided data by girder manufacturers in Idaho. Finally, the author provided relevant approaches for predicting the camber in Idaho.

2.1.12 Mississippi Study; Tomley (2019)

This research aimed to improve the camber prediction since MDOT experienced over- prediction of the prestressed girders camber on several projects. To reach this goal, the author examined camber prediction practices of several states and evaluated historical material property data. After that, newly revised multipliers for long-term camber prediction were proposed with some improvements to material property data.

2.1.13 Oklahoma Study; Jayaseelan and Russell (2007)

This study aimed to investigate the relevant literature about the prediction of prestress losses. In addition, the research investigated the variation in concrete material properties. Recommendations were made to ODOT and OTA for a more accurate calculation of prestress losses, camber, and deflection. These recommendations are as follows:

- Addition of top prestressing strands in prestressed concrete girders to decrease the long-term prestress losses and camber by about 69%,
- Addition of mild steel to increase the concrete beam stiffness and lower the long-term camber by about 17.4%,
- Using the AASHTO Time-Step approach to calculate the losses and camber in prestressed concrete bridge girder.

2.1.14 Summary of Previous Literature

Several previous studies have highlighted the difficulties in predicting initial and long-term camber. Even with improvements to equations, accuracy was still not better than $\pm 15\%$. Most of

the previous studies highlighted an over-prediction of camber, while a few noted an under-prediction in shorter girders. The primary causes of camber calculation error were:

- Concrete compressive strength (on the order of 22% higher at release),
- Concrete modulus (many studies recommended the AASHTO 2010 equation for modulus with k_1 factors from 0.85 to 1.2),
- Temperature (differences in ambient and curing temperatures causing reduction of prestress force at release, and daily temperature variations causing as much as 0.75 in. change in camber),
- Creep and shrinkage parameters (most studies recommend use of AASHTO creep and shrinkage models but some (Honarvar et al. 2015, Stallings et al. 2003) used modification factors),
- Storage locations (overhang length in storage affects the girder camber and most studies recommend including the effect),
- Variability in initial prestress and girder self-weight.

2.2 *Camber Prediction Overview*

The prediction of camber requires the estimation of the initial camber and long-term camber. The initial camber is the summation of upward deflection caused by the prestressing strands and the downward deflection caused by the girder's weight. Long-term camber considers the time-dependent factors that influence the camber such as creep and prestress losses.

The initial camber and deflection resulting from loads and the prestressing force and losses are calculated based on the structural analysis theorems. The long-term camber can be calculated using

three basic approaches with varying levels of computational difficulty: the multiplier method, refined approach, and the incremental time-step analysis approach.

2.2.1 Multiplier Method

In the multiplier method, the instantaneous camber is calculated, and the long-term camber is multiplied by set multipliers. This method is primarily based on the PCI multiplier method. For example, in Iowa, the instantaneous camber is calculated using the program CONSPAN. The initial camber is multiplied by a multiplication factor (0.85 if $f'_c < 6\text{ksi}$) and the final camber by another factor (1.85 if initial camber $< 1.5\text{ in.}$). This is the simplest camber calculation and is used in many states, but is based on set multipliers and may not be able to accommodate differences in beam conditions.

2.2.2 Refined/Approximate Method

The refined or approximate method calculates individual components of prestress losses and creep separately at discrete points in time. The method is primarily based on the refined methods in the AASHTO-LRFD and PCI Bridge design manual and is currently used by MoDOT. MoDOT suggests calculating the camber and deflections at four different times, which are the time of release strands, 7 days after prestress transfer, 90 days after prestress transfer, and after the slab is cast. The calculation of the camber at the defined time points are based on time-dependent properties. Details of the current MoDOT equations to calculate camber are given in Appendix A.

2.2.3 Incremental Time-Step Approach

Incremental time-step analysis can be used for the determination of prestressed girder deflection and camber over time. These kinds of calculations are made practical by using a computer program, for example, a spreadsheet. Compared to the discrete approach, this method can give camber at any time point.

Aging, creep, shrinkage, relaxation, and prestress losses are all time-dependent phenomenon that affects the deflection history of a prestressed member. All of these phenomena are nonlinear in nature and have a coupled effect on the behavior of the member. All of these time-dependent effects are also more significant in the early ages compared to later ages, and hence influence camber prediction accuracies during construction of the bridge superstructure (e.g., deck slab placement). Typically, lump-sum estimates of deflection often used while predicting camber do not systematically account for the coupling or the nonlinear nature of these deflection contributions. An incremental time-step approach, even though somewhat cumbersome, provides a more realistic and accurate estimate of the contribution of these coupled nonlinear effects. This approach is based on Naaman (2012) and the details of the method are given in Appendix A.

2.2.4 Camber Prediction Methods in Other States

Most states use one of the previously described generic methods to predict camber. Table 2-2 gives a summary of the methods used by some states.

Table 2-2: Comparison of camber prediction method by state

State (year)	Method of predicting camber	Type of moment of inertia
Alabama	Refined method	Considers the gross moment of inertia.

State (year)	Method of predicting camber	Type of moment of inertia
Arkansas	Multiplier	Considers the gross moment of inertia.
Minnesota	Multiplier	Considers the gross moment of inertia. Long-term 1.4 times initial.
Idaho	Multiplier	Considers the gross moment of inertia. 1.65 times self-weight induced; 1.55 times prestress induced
Illinois	Multiplier	Considers the gross moment of inertia.
Iowa	Multiplier	Considers the transformed moment of inertia. Initial camber times 0.85, long term times 1.65.
Kansas	Refined method	Considers the gross moment of inertia.
Mississippi	Design program (CONSPAN, PSBeam, or In-house)	Considers the gross moment of inertia.
Missouri	Refined method	Considers the transformed moment of inertia.
North Carolina	Refined method	Considers the gross moment of inertia.
Oklahoma	Multiplier	Considers the gross moment of inertia. Considers the non-composite for loads applied before the slab is hardened. After that, the composite properties of the girder shall be considered.
Texas	Time-dependent computer analysis (PG super)	Considers the gross moment of inertia.
Washington	Time-dependent computer analysis (PG super)	Considers the gross moment of inertia.
Wisconsin	Multiplier	Considers the gross moment of inertia. Long-term 1.4 times initial.

2.3 *Camber Measurement*

In addition to the prediction of camber, the accurate measurement of camber is also critical. Honarvar (2015) found release camber error and variability stemmed from bed deflections, inconsistent beam depth, and bed friction and proposed a measurement method to reduce these influences. They found that different measurement methods from the researchers (rotary laser

level) and precasters (tape measure to bed) gave an average error of 19% and as much as 89%. They recommend the use of a rotary laser level with several measurement locations and accounting for bed deflections. French and O'Neill (2012) recommended a string line procedure using 80-lb. fishing line. They highlighted that it is important to keep the self-weight of the string line as low as possible to reduce sag in the measurement line.

The amount of sag in a string line can be calculated from simple structural analysis principles. The sag is:

$$sag = \frac{wL^2}{8H} \quad 2-2$$

where:

w = the self-weight of the string line (lb./ft.),

L = the length of the line (ft.),

H = the horizontal pull force (lb.).

As can be seen in the equation, the self-weight of the string line is directly related to the sag in the line. The choice of the lightest weight possible string would produce the best measurement. Also, the sag is inversely proportional to the horizontal pull force. Consistent pulling forces are required for consistent camber measurements.

CHAPTER 3: MISSOURI BRIDGE CAMBER FIELD DATA

Data from 189 girders with initial camber and 33 girders with later camber measurements before hauling was analyzed to improve prediction of camber on prestressed girders in Missouri. In addition, field testing was conducted on four girders including material characterization tests for concrete strength gain with time, modulus, and creep.

3.1 Girder Properties

Field data from bridge girders was mostly available on NU shape girders commonly used in Missouri. Figure 3-1 and Figure 3-2 give the distributions of the number of bridges with the girder types in the study compared to the Missouri prestressed bridge inventory.

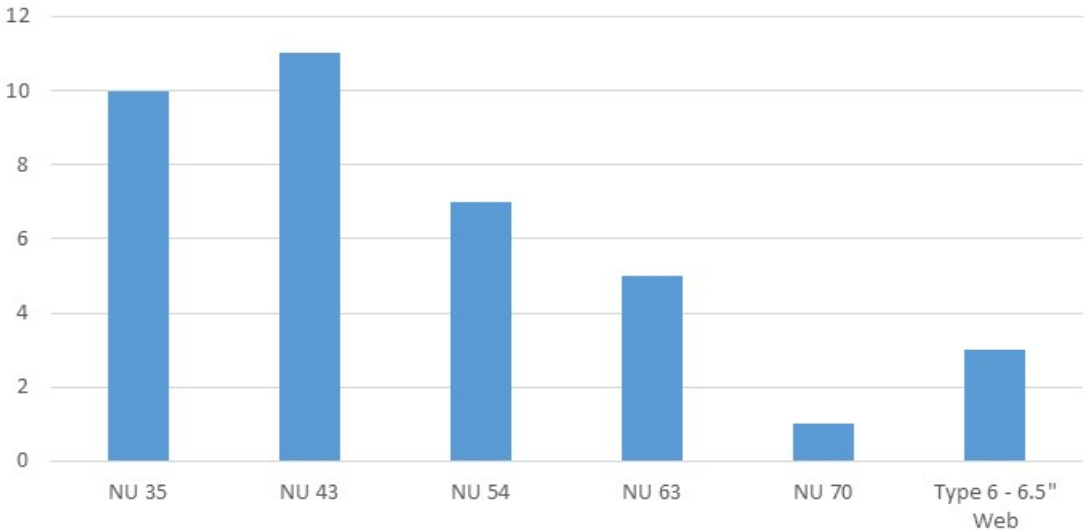
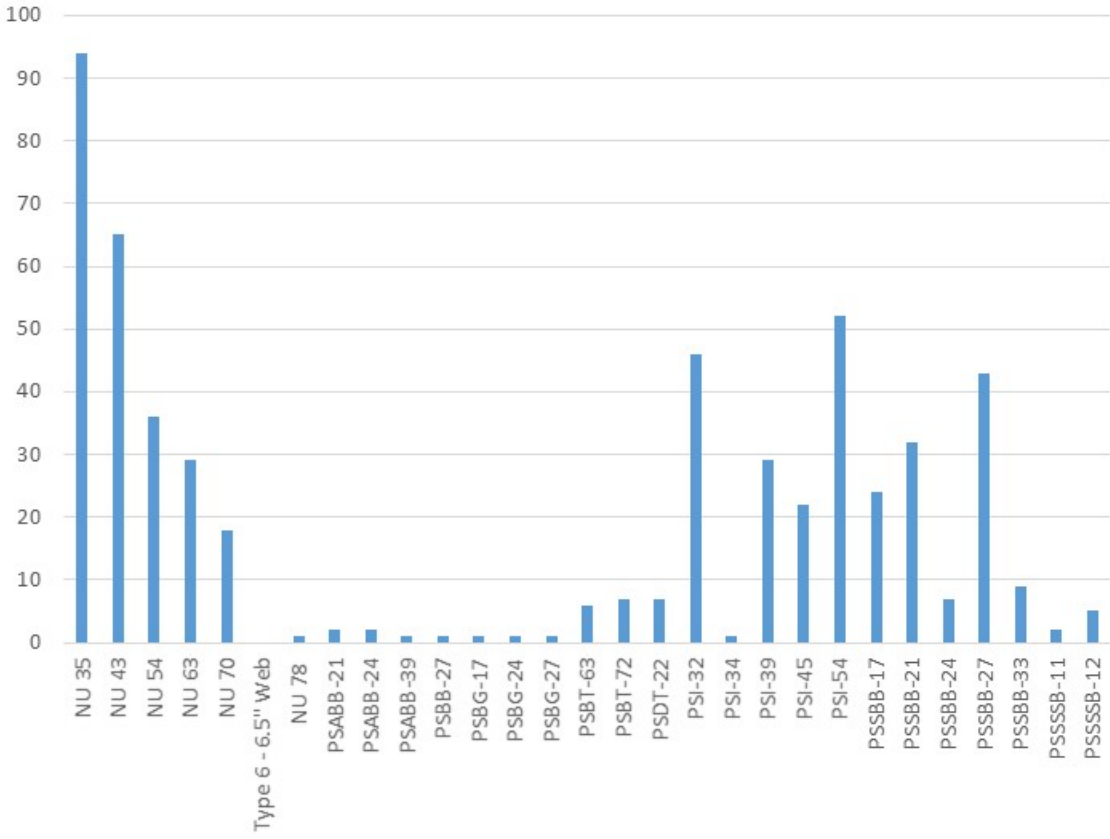


Figure 3-1. Number of bridges in study for each girder type



PSSBB – Prestressed Concrete Spread Box Beam

PSABB – Prestressed Concrete Adjacent Box Beam

PSI – Prestressed Concrete I-Girders

PSNU – Prestressed Concrete Nebraska Girders

PSDT – Prestressed Concrete Double-Tee Girders

PSBT – Prestressed Concrete Bulb-Tee Girders

PSSSSB – Prestressed Concrete Spread Solid Slab Beam

PSBG – Prestressed Concrete Box Girders (now PSABB or PSSBB)

Figure 3-2. Inventory of Missouri bridges based on girder type

Figure 3-3 gives the distribution of the length of the girders in the analysis database. The average length of the girders was 99 ft. The average length of NU girders in the Missouri inventory was 74 ft. Although the study database is, in general, longer than the inventory average, the distribution is thought to match well enough to give a basis for the evaluation of the camber calculation method.

Most of the field measurements came from the two major precast plants in Missouri. Sixty-eight girders were from precast Plant #1, and 115 girders were from precast Plant #2.

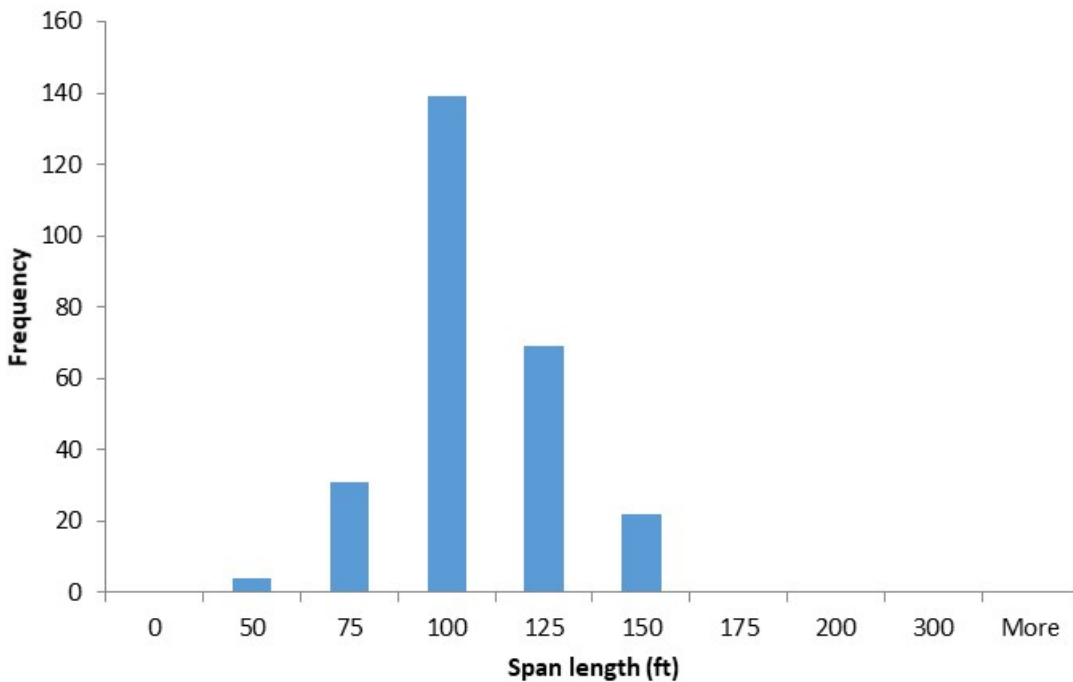


Figure 3-3. Distribution of girder length in the study database

3.2 *Camber Measurements and Predictions*

Camber field measurements were provided by MoDOT as collected by the precasters. At precast Plant #1, the general method to measure camber was to string a taut mason’s line along a form

seam line on the beam, as shown in Figure 3-4, directly after the beam was placed on temporary supports. The location of the supports varied from 20 in. to the depth of the girder. At precast Plant #2, a Kevlar braided string was hooked to an extended piece of prestressing steel and strung along the bottom of the beam to the other side while the beam was suspended by the lifting inserts. The plant tried to use the same technicians to pull the string to a similar level for each girder.



Figure 3-4. Seam line in beam for precast Plant #1

A comparison was made between the field measurements and the predicted cambers listed on the bridge plans. The predicted 7-day camber using the current MoDOT procedures is generally lower than the field measured camber in the bridge plans by about 25%. It is noted that the predicted camber is at 7 days, and the measured camber usually occurs on the day the strands are cut (usually

1 to 2 days after pouring the concrete). Although this is an important difference, the comparison here is made simply to evaluate given data. Camber at transfer is calculated in Figure 3-7. When the measured camber is compared to the 90-day camber listed on the bridge plans (Figure 3-6), the measured camber is generally less than that at 90 days. This agrees with the precaster's observations that the camber measured at transfer is between the 7-day and 90-day predicted cambers.

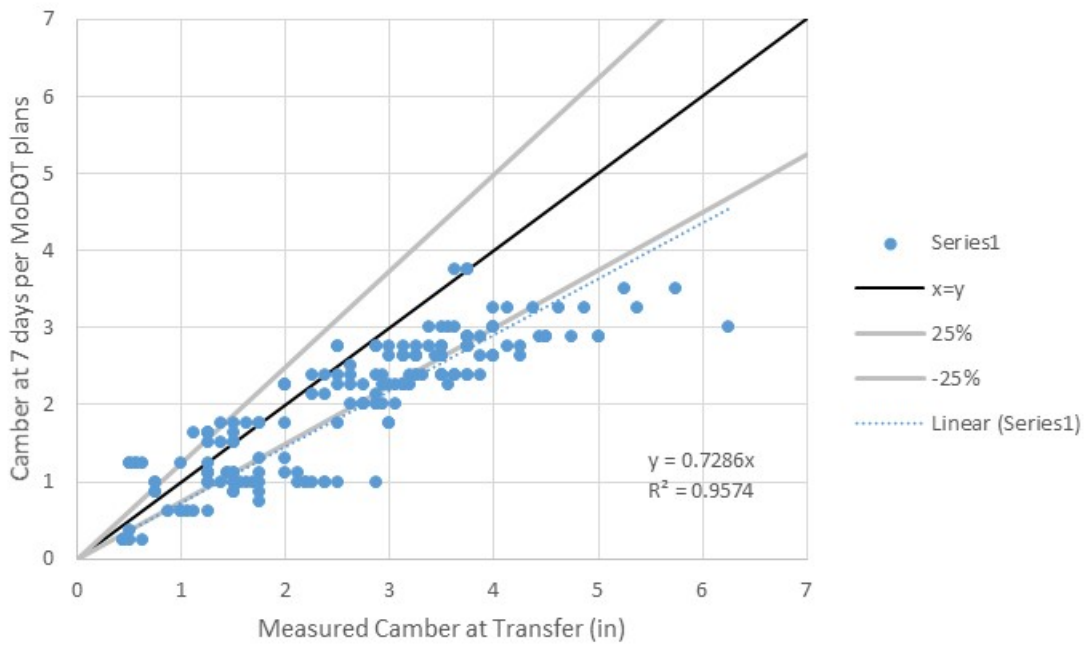


Figure 3-5. Comparison of camber at 7 days on bridge plans and measured camber

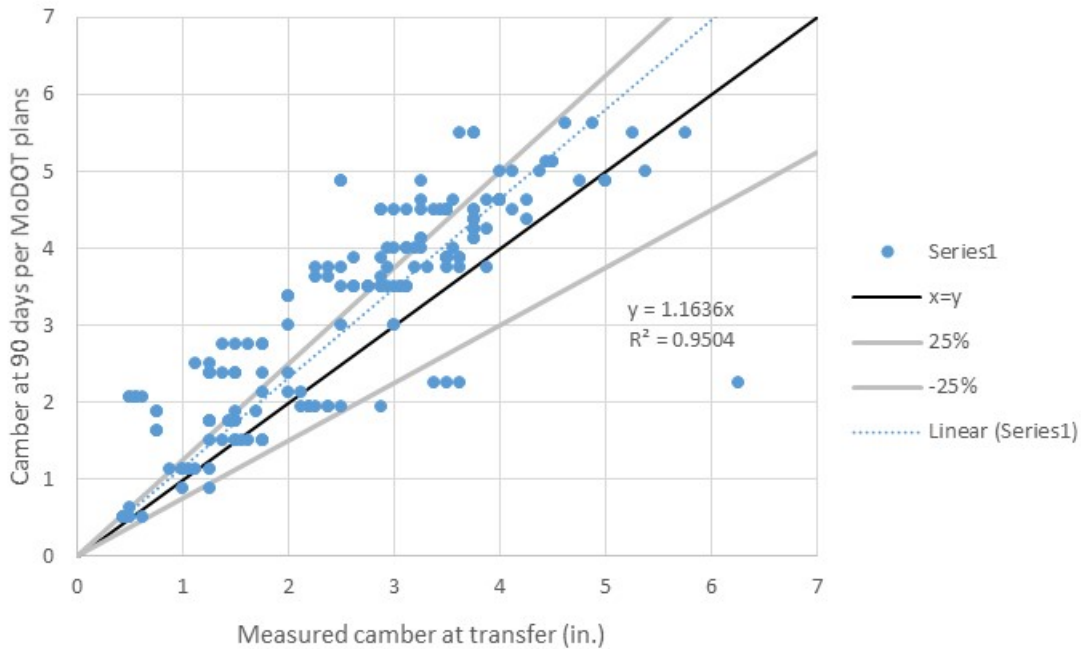


Figure 3-6. Comparison of camber at 90 days on bridge plans and measured camber

A spreadsheet was created to compute the initial camber at transfer for all the selected girders in this study. The spreadsheet follows the current MoDOT camber equations as listed in Appendix A. As can be seen in Figure 3-7, the analysis using the spreadsheet developed in this study gives a similar result to the camber at 7 days listed on the bridge plans (Figure 3-5). In addition, the measured camber is higher than the predicted camber with an average absolute error of 35%, or a RMSE (root mean square error) of 0.81 in. This means that due to errors in the prediction equation, or errors in the measurement method, the camber is underpredicted by about 23% (trendline slope = 0.77).

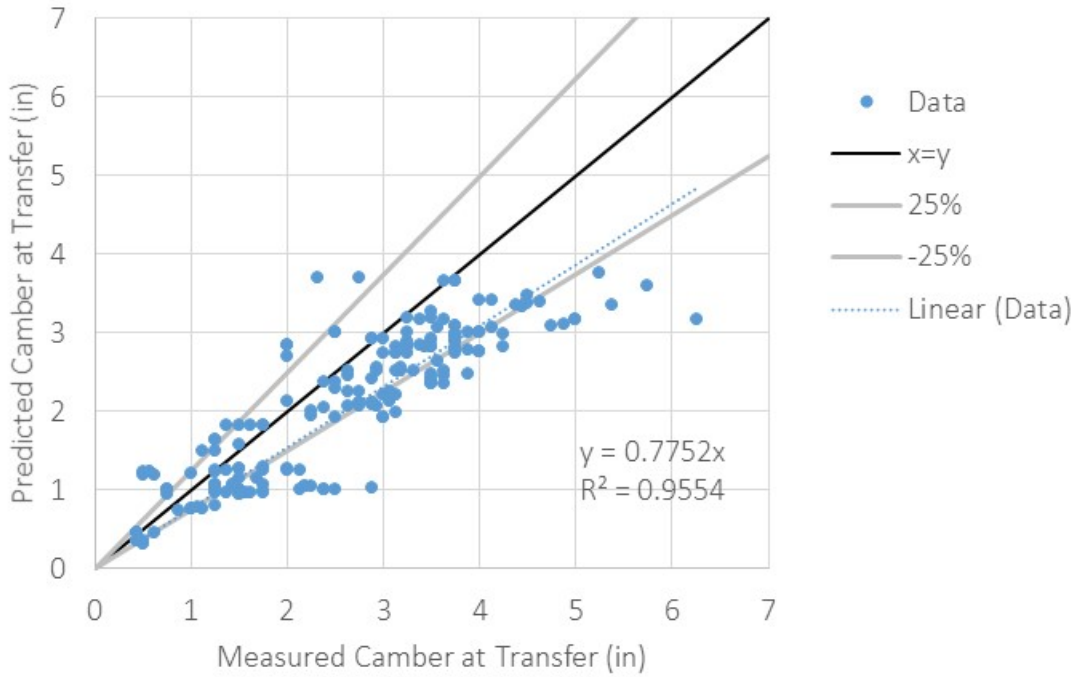


Figure 3-7. Camber prediction at transfer using current MoDOT method

3.2.1 Camber Measurement Method

Figure 3-8 shows the subset of girders from precast Plant #1, while Figure 3-9 shows the subset from precast Plant #2. While both plants show a similar amount of under-predicting the camber at transfer, precast Plant #2 shows less variability ($r^2 = 0.973$) in the data. This is likely due to the measurement method using a Kevlar string that is pulled tight by the same technicians.

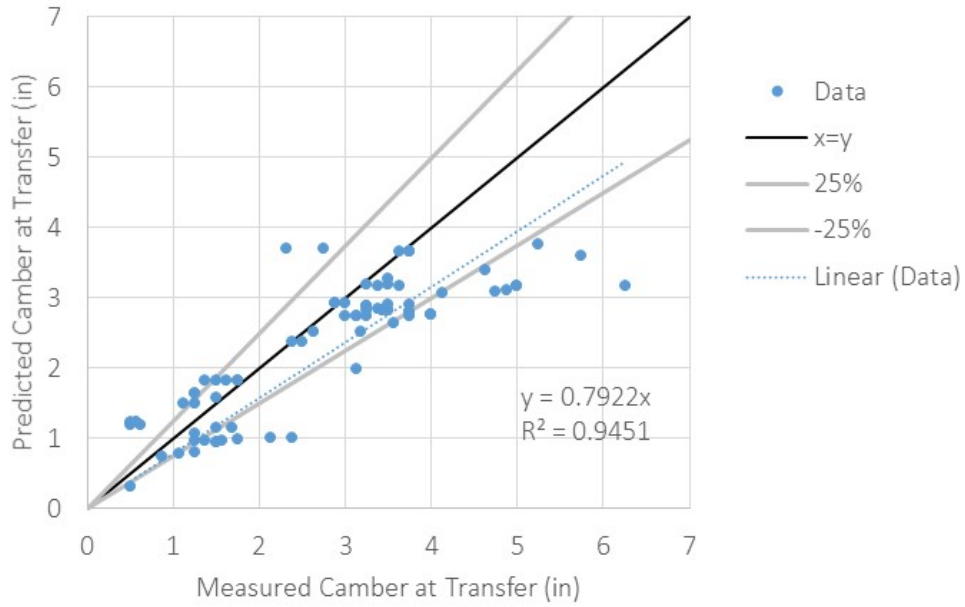


Figure 3-8. Comparison of predicted and measured camber from precast Plant #1

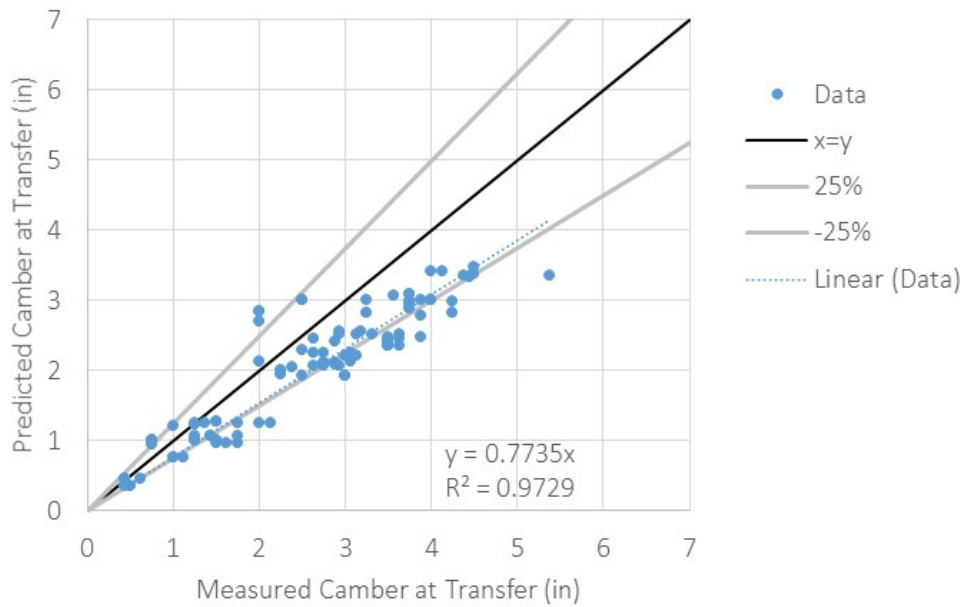


Figure 3-9. Comparison of predicted and measured camber from precast Plant #2

One possible reason for the overall under-prediction of camber is error in camber measurement is due to sag in the string line used to measure camber, or inconsistency with the pulling force. Equation 2-2 is a theoretical equation used to predict the sag in the line. It shows that the sag is related to the weight of the string line, length of the line, and the pulling force.

In order to verify the sag, an experiment was conducted. Two types of string lines were evaluated. A 1.7 mm braided Kevlar line used by Plant #2 which weighs 0.0016 lb./ft., and an 80-lb. test braided fishing line which weighs 0.00013 lb./ft. (similar to the line used in French and O'Neill (2012)). Each line was stretched over a distance of 100 ft. and different weights hung vertically from the ends of the line to create the pulling force. The sag in the line was measured with a rotary laser level with an accuracy of 0.05 in. The results in Table 3-1 show that the sag in the Kevlar line was quite high, as much as 1 in. with a strong pull force of 30 lbs. However, due to the lighter self-weight of the line, the braided fishing line only had a sag of about 0.05 in. under a similar level of force. Furthermore, the measured and predicted sag was accurate to about 0.2 in. for the Kevlar and 0.01 in. for the fishing line, indicating that the equation used to predict the sag is accurate.

The Kevlar string used by Plant #2 weighs 0.0016 lb./ft. Assuming a pull force of 35 lbs., the predicted sag in a 100 ft. line would be 0.68 in. using Equation 2-2. If a correction for sag is applied to all of Plant #2 girders, then the result in Figure 3-10 is obtained. The slope of the trendline increased by 25% and resulted in the average camber measurement only 4% less than the predicted value. This result showed that the sag error may be significant and the possible cause for the under-predicted camber.

For Plant #1, the type of line used for camber measurements was less consistent. Based on conversation with plant personnel, the type is like a mason’s line, which would have a similar weight to the Kevlar line.

It is recommended that future string line measurements use the lightest weight line that will withstand the pull force and abrasion along the concrete. Furthermore, a method for consistent pulling force (perhaps by use of a scale to measure the level of force) would increase the consistency of the camber measurement.

Table 3-1. Measured and predicted sag in string line

1.7 mm braided Kevlar			
Weight (lb.)	Measured sag (in.)	Predicted sag (in.)	Error (in.)
17	1.65	1.42	0.23
29	1.05	0.83	0.22
35	0.95	0.69	0.26
44	0.7	0.55	0.15
80 lb. braided fishing line			
Weight (lb.)	Measured sag (in.)	Predicted sag (in.)	Error (in.)
13	0.15	0.15	0.00
26.8	0.05	0.07	-0.02

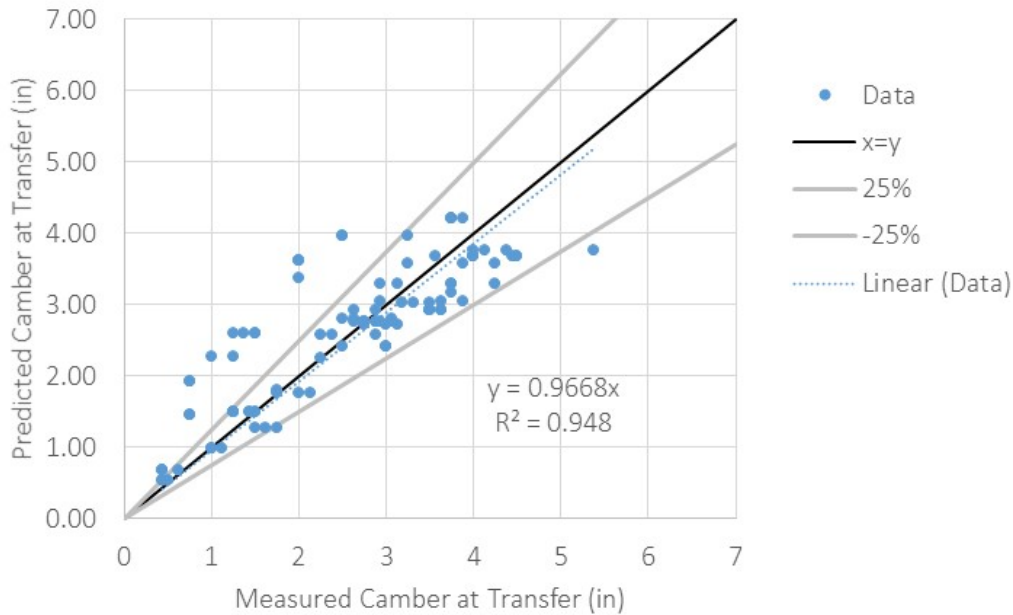


Figure 3-10. Comparison of predicted and measured camber from precast Plant #2 correcting for the line sag

3.3 *Field Measured Cambers*

In Plant #1, four girders were monitored for the construction of two bridges. The concrete mix design is given in Table 3-2, and the properties of the girders are shown in Table 3-3. Bridge #1 was cast on 4/27/2021, and the strands cut on 4/29/2021, two days after casting. Bridge #2 was cast on 5/4/2021, and the strands cut on 5/5/2021, one day after casting. For Bridge #2, the initial break of the cylinders in the morning of the prestress release (cutdown) was low, so the strands were cut at noon after the concrete strength had increased. The average of three cylinder tests for the measured concrete compressive strength and elastic modulus for 4x8 cylinders taken from the bridges are given in Table 3-4.

Table 3-2. Concrete mix design quantities

Material	Design quantity (per yd³)
Coarse aggregate (E limestone)	1,490 lbs.
Sand (Missouri River)	1,195 lbs.
Cement type III	850 lbs.
Air entrainer (Daravair 1400)	41.44 oz.
AdvaCast 585	96.05 oz.
Water	4,596.6 oz.

Two additional cylinders from Bridge #2 were tested for creep under sustained compressive load following ASTM C512. The cylinders were placed under a compressive load of 31,000 lbs. (2,468 psi) as shown in Figure 3-11. The 28-day compressive strength for this concrete batch is about 124,000 lbs. (9,870 psi). The results, shown in Figure 3-12, show a similar behavior to both the AASHTO and ACI equations for predicting creep strains and to previous concrete testing by Gopalaratnam and Eatherton (2001). Overall, based on these two cylinders, the ACI equation seems to be the most accurate at predicting the creep behavior. However, more data from additional testing would be needed to confirm the trend.

Table 3-3. Properties of field-tested girders

Bridge	Bridge #1	Bridge #2
Section type	NU 54	NU 63
Height (in.)	53.16	63.00
Area (in. ²)	743.88	801.72
Neutral axis depth (in.)	23.71	28.14
Moment of inertia (in. ⁴)	297512	451,306
Cl to Cl bearing pad length (ft.)	125.50	141.25
End - end length (ft.)	126.42	142.13

Table 3-4. Measured concrete compressive strength and modulus

Bridge #1 (pour date: 4/17/2021, release date: 4/29/2021)		
Concrete age	Ultimate strength (ksi)	Modulus of elasticity (ksi)
2	7,755	5,213
8	8,507	5,095
21	9,576	5,407
30	9,707	5,889
91	9,406	5,619

Bridge #2 (pour date: 5/4/2021, release date 5/5/2021)		
Concrete age	Ultimate strength (ksi)	Modulus of elasticity (ksi)
1	7,306	4,686
14	8,919	5,329
90	10,885	5,776



Figure 3-11. Concrete creep test setup

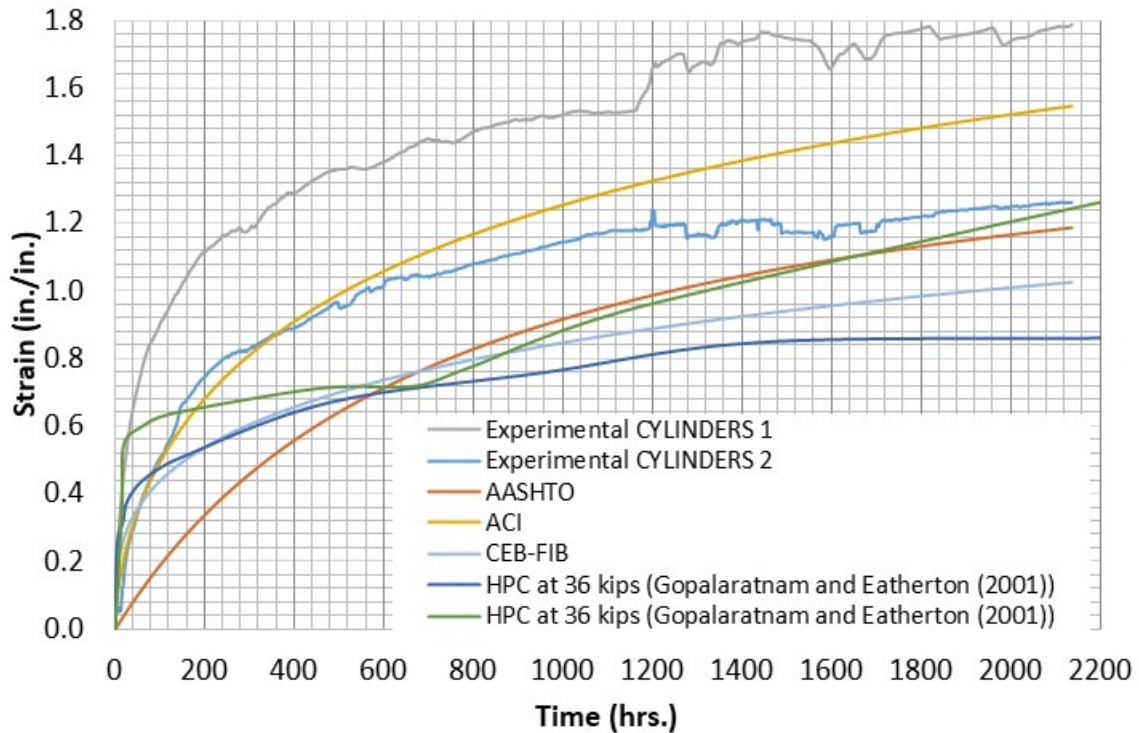


Figure 3-12. Creep testing results

3.3.1 Field Camber

Camber was also measured by the research team. A 30-lb. fishing line was used to measure the camber. First, reference lines were drawn at both ends and the middle of the girder using the string line pulled to about 20 lbs. force before the strands were cut. Then, the strands were cut, and the girder moved off the bed and placed on temporary wooden supports. The string line was then matched with pre-drawn reference line at both ends of the girder and pulled taut. The camber was measured at the difference in the pre-drawn reference line at the middle of the girder and the location of the string line after strands were cut. This procedure allowed the researchers to remove the error resulting from the line sag. The camber growth for these girders was monitored over time (see Table 3-5).

Table 3-5. Camber measurement and prediction

Bridge	Girder ID	Date	Concrete age (days)	Field camber (in.)	Predicted camber at release (in.)		
					MoDOT procedure		ACI
					Discrete	Time-step	Time-step
1	IB001	4/29/21	2	2.75	3.406	3.406	3.39
1	IB002	4/29/21	2	2.3125	3.406	3.406	3.39
1	IB001	5/4/21	7	3.25	4.056	4.048	3.66
1	IB002	5/4/21	7	2.875	4.056	4.048	3.66
1	IB001	5/14/21	17	3.75	4.608	4.604	3.87
1	IB002	5/14/21	17	3.125	4.608	4.604	3.87
2	IB001	5/5/21	1	3.25	2.997	2.997	2.99
2	IB002	5/5/21	1	3.5	2.997	2.997	2.99
2	IB001	5/14/21	10	4.125	3.726	3.717	3.2
2	IB002	5/14/21	10	4.375	3.726	3.717	3.2

A comparison shows Bridge #1 with over-predicted camber and Bridge #2 with under-predicted (see Figure 3-14 and Figure 3-13). The measured camber for Bridge #1 girders at transfer was (2.75 in. and 2.3125 in.) on average 26% lower than the calculated camber using existing MoDOT procedures (3.406 in.). However, when considering overhang effect and the measured concrete strength, the predicted initial camber became 3.36 in.

On the other hand, the measured camber at transfer for Bridge #2 girders was 3.25 in. and 3.5 in., on average 12% higher than the predicted initial camber (2.997 in.). However, when considering overhang effect and the measured strength the predicted camber was 3.33 in. The measured values are within -2% and 5% of the predicted value at the time of transfer. At the time of 10 days, the measured camber was 4.125 in. and 4.375 in., on average 14% higher than predicted (3.73 in.) using the original MoDOT procedures, and about 2% higher if considering the effect of overhang and measured release strength.

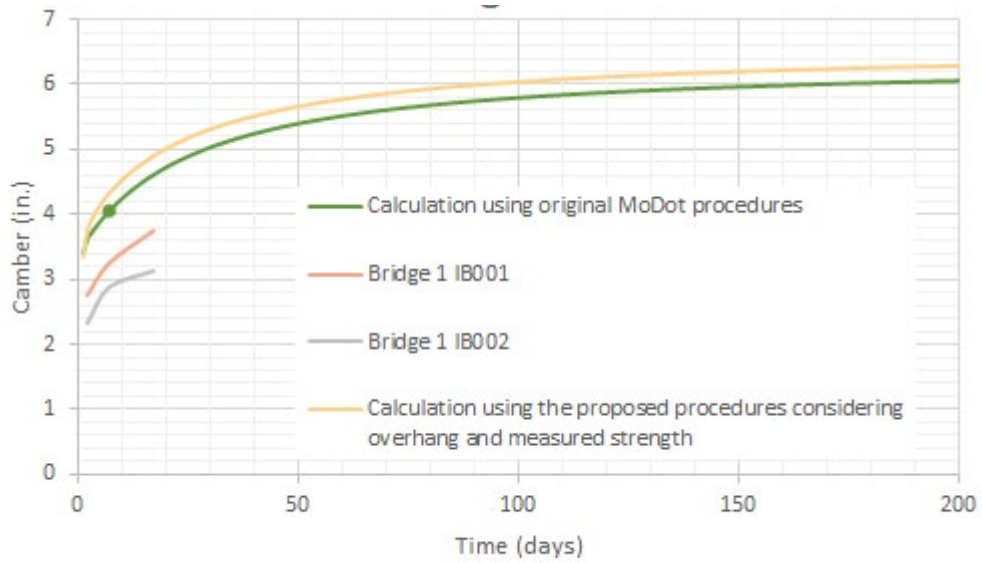


Figure 3-13. Measured vs. calculated camber for Bridge #1 girders

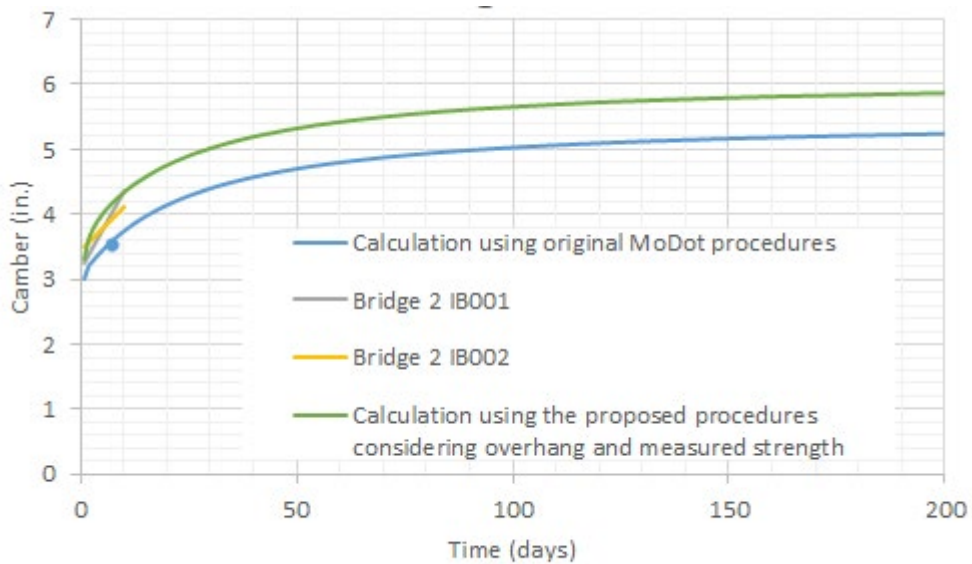


Figure 3-14. Measured vs. calculated camber for Bridge #2 girders

3.4 *Summary*

Data from 189 girders with initial camber and 33 girders with later camber measurements before hauling were obtained. In addition, field testing was conducted on four girders, including material characterization tests for concrete strength gain with time, modulus, and creep.

The girders selected for this study were found to be reasonably representative of the inventory of NU girders in Missouri. However, the current camber measurement showed an under-prediction of the camber by about 23%. The camber measurement method in the two plants was compared. It was found that the self-weight of the string line used to measure camber was causing a significant sag and leading to larger than actual camber measurements. Field measurements were made on four girders from two separate pours and cylinder strength, modulus, and creep data taken. The field cambers showed an over-prediction of camber for one set of girders, while the other was well-predicted.

CHAPTER 4: CAMBER CALCULATION – A PARAMETRIC ANALYSIS OF RELATIVE SENSITIVITY

To enhance the calculation of the initial camber for PPCBs, the parameters that influence the camber need to be investigated. Factors that are used to determine the initial camber and that influence the accuracy of calculation include the concrete stiffness modulus, concrete strength, the prestress force, prestress losses, overhang length, and temperature. The factors are summarized in Table 4-1. Details of each factor are given in Sections 4.1 to 4.7.

Table 4-1. Factors affecting initial camber calculation

Factor	Details	% Effect on camber*
Concrete compressive strength	The compressive strength varies with time, so the time of camber calculation is important. Also, the aggregate strength, the ratio between the aggregate and cement paste, and the type of cement affect the camber.	Increasing the compressive strength (f'_c) by 10% leads to a decrease in the initial camber calculation by about 4%.
Concrete modulus	The concrete stiffness (modulus) is directly related to the concrete strength and varies with time. It is important that prestress loss and early age detection computations include explicit modeling of the time-dependent nature of the elastic modulus of concrete.	Increasing the concrete stiffness (E_c) by 10% leads to a decrease in the initial camber calculation by about 8%.
Prestress force	Prestress force is affected by many factors like the jacking force, strands' temperature variations, and prestress losses.	Decreasing the initial prestress force by 5% causes about a 10% decrease in the initial camber.
Initial losses	Initial prestress losses mainly consist of seating, elastic shortening, and relaxation after the preliminary	The overestimation of the initial prestress losses leads to a decrease in the camber; decreasing the initial losses by

Factor	Details	% Effect on camber*
	tensioning to the bonding time of the concrete.	10% causes about a 1% increase in the initial camber.
Support conditions	The location of supports in the storage area affects the field camber measurement.	Placing the storage supports at distance equal to the girder height from the end of the girder leads to an increase in the initial camber values by about 14%.
Using gross properties of the beam	The gross properties are calculated based on concrete only, ignoring the reinforcement and the prestressing strands. MoDOT suggests using the transformed properties of the beam in the camber calculations.	Change in camber less than 2% if gross used instead of transformed.
Temperature	Nguyen et al. (2015) investigated the influences of temperature variation on the girder camber.	Temperature variation of 20°F results in an increase in the camber measurement by about 23%.
Concrete age/strength at strand release	This time affects the initial camber as well as the final camber calculations.	The variation in the initial strength and concrete age at release affects the camber measurements, so the camber calculation should be revised after measuring the compressive strength at the time of release.
Concrete density	The concrete density affects the dead load deflection.	Decreasing the concrete density by 5% results in an increase in the camber measurement by about 3%.

* Effect of each factor on camber determined through incremental time-step analysis. Change in camber based on average change in suite of 189 girders in study.

4.1 *Effect of Overhang*

After releasing the pretensioned strands, the prestressed concrete girders are typically transferred from the precasting bed to the storage area, where they are placed on temporary supports. Usually,

these temporary supports are timber or concrete blocks positioned beneath the girder. Typically, the blocking supports are placed within one girder depth from the girders' ends, but their locations are random. The field observations saw that the locations of the supports from the girders' ends were between 20 in. and 50 in.

The overhang will cause a change in the initial camber and a change in the camber growth throughout the time of storage. The overhang length alters the moment diagram due to the self-weight of the girder (as seen in Figure 4-1). The change in the moment diagram alters the stress distribution of the girder and affects initial camber deflection and long-term deflections.

Tadros et al. (2011) recommended the overhang effect to be considered in the calculation of the camber. He proposed a calculation method which considers that the prestressed girder is located on temporary supports at the storage yard that is a few feet into the span from the girder's ends. In addition, this method includes the effect of debonding strands and transfer length. The current MoDOT equations are the same, except it ignores the effect of the overhang and the transfer length. The equation used in this method is listed below in Table 4-2.

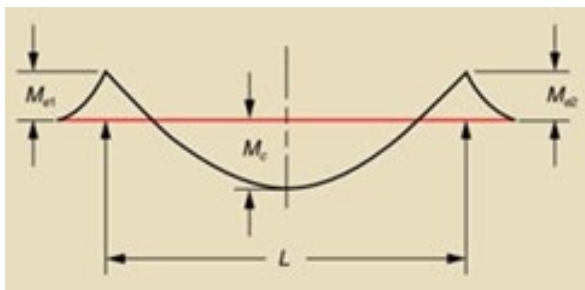


Figure 4-1. Bending moment diagram due to girder's weight (Tadros et al. 2001)

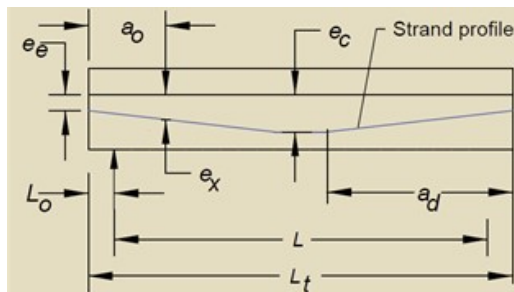


Figure 4-2. Optimum strand arrangement used in Tadros method (Tadros et al. 2001)

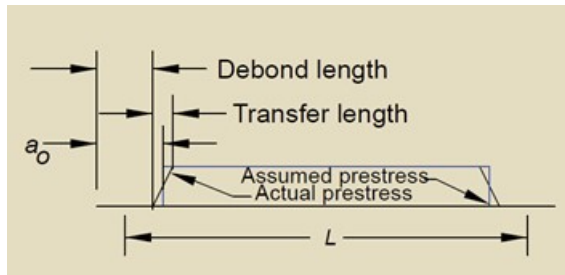


Figure 4-3. Debond and transfer length (Tadros et al. 2001)

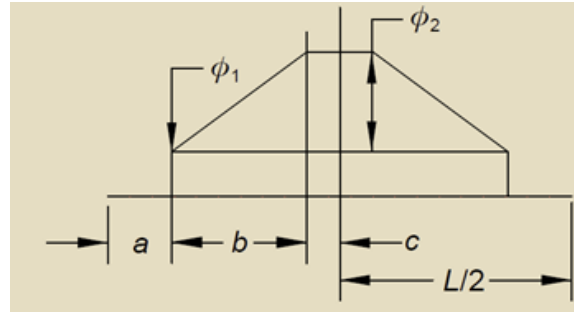


Figure 4-4. The curvature distribution due to the initial prestress (Tadros et al. 2001)

Table 4-2. Equations used in the initial camber prediction proposed by Tadros et al. 2001

Factor	Equation
Δ_{ic}	$\Delta_{ic} = \Delta_d + \Delta_s$
Δ_d	$\Delta_d = \frac{5L^2}{48E_{ci}I_{ti}} (0.1M_{e1} + M_c + 0.1M_{e2})$
Δ_s	$\Delta_s = \frac{\phi_1}{2} (b + c)(2a + b + c) + \frac{\phi_2}{6} (3ab + 2b^2 + 6ac + 3c^2)$
	$\phi_1 = \frac{P_i e_x}{E_{ci} I_{ti}} \quad \phi_2 = \frac{P_i (e_c + e_x)}{E_{ci} I_{ti}}$
a	$a = a_0 - L_0, \quad L_0 = \frac{L_t - L}{2}$
b	$b = a_d - a_0$
c	$c = \frac{L}{2} - a - b$
e_x	$e_x = e_e + \frac{a_0}{a_d} (e - e_e)$

where:

Δ_{ic} = initial camber,

Δ_d = deflection caused by the dead load of the girder,

Δ_s = camber caused by the straight and harped strands,

M_{e1} = moment at left support, negative if overhang exists, zero if overhang ignored,

M_{e2} = moment at right support, negative if overhang exists, zero if overhang ignored,

M_c = midspan moment,

L = girder length between supports,
 L_o = overhang length,
 L_t = total member length,
 E_{ci} = initial concrete modulus,
 I_{ti} = moment of inertia of precast concrete transformed section at time of prestress release,
 a = distance between the support and the assumed start of prestress in girder,
 b = distance between start of ϕ_1 and start of ϕ_2 ,
 a_o = modified debond length = (actual debond length + transfer length/2),
 a_d = distance from member end to hold-down point,
 c = distance from the start of curvature to the midspan,
 e_x = eccentricity of strand group at the point of debonding,
 ϕ_1 = curvature due to straight strands,
 ϕ_2 = curvature due to harped strands.

The equations are theoretically sound; however, the camber given in the calculation is the deflection from the support to the middle of the girder. An additional term would need to be added to include the deflection from the end of the girder to the support. This term is considered when using PGSuper software (Brice 2020), used by WsDOT and TxDOT for calculating the prestressed girder camber, and considers the overhang effect. Equation 4-1 shows the equation used for calculating the initial camber. In this method, the self-weight deflection is divided into two components as seen in Figure 4-5. In addition, Figure 4-6 and Figure 4-7 illustrate the eccentricities and the dimension used in this method. The PGSuper method and the Tadros (2011) equations are equivalent, the only difference is the reference point (end vs. support) for the deflection.

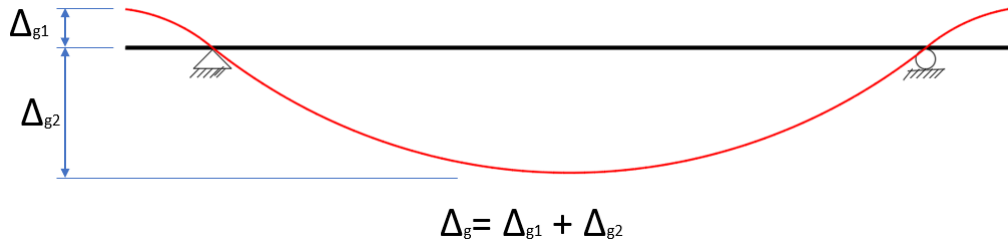


Figure 4-5. Girder self-weight deflection during lifting

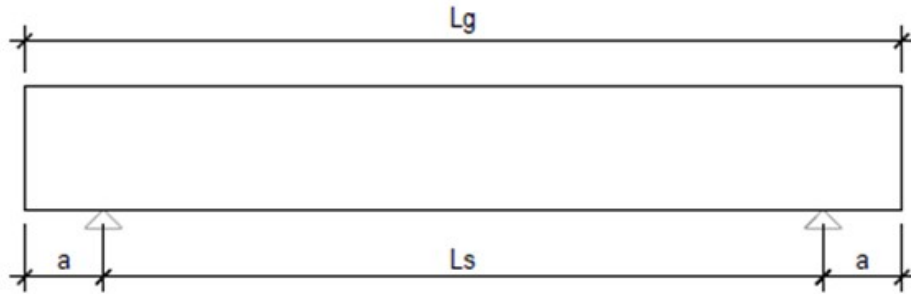


Figure 4-6. Girder dimensions (Brice 2020)

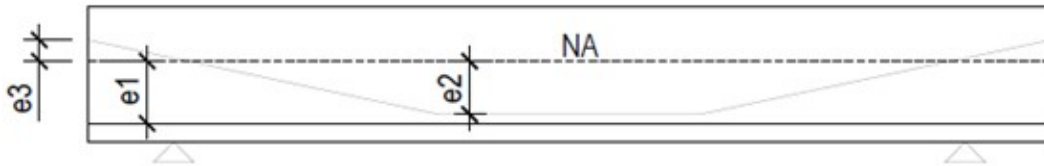


Figure 4-7. Strand eccentricities (Brice 2020)

Table 4-3. Equations used in the initial camber prediction proposed by PGSuper (Brice 2020)

Factor	Equation
Δ_{ic}	$\Delta_{ic} = \Delta_{g1} - \Delta_{g2} + \Delta_{SS} + \Delta_{HS}$
Δ_{g1}	$\Delta_{g1} = \frac{w_g \cdot a}{24E_{ci}I_x} [3a^2(a + 2L_s) - L_s^3]$
Δ_{g2}	$\Delta_{g2} = \frac{5w_g L_s^4}{384E_{ci}I_x} - \frac{w_g a^2 L_s^2}{16E_{ci}I_x}$
Δ_{SS}	$\Delta_{SS} = \frac{P_s e_1 L^2}{8E_{ci}I_x}$

$$\Delta_{HS} = \frac{b(3 - 4b^2)NL^3}{24E_{ci}I_x} + \frac{P_h e_1 L^2}{8E_{ci}I_x}$$

$$N = \frac{P_h(e_2 + e_3)}{bL}$$

where:

Δ_{ic} = initial camber,

Δ_{g1} = deflection from support to end of girder,

Δ_{g2} = deflection from support to center of girder,

Δ_{HS} = deflection due to harped strands,

Δ_{SS} = deflection due to straight strands,

w_g = self-weight of girder (weight per unit length),

L_s = girder length between supports,

E_{ci} = initial concrete modulus,

I_x = moment of inertia of precast concrete transformed section at time of prestress release,

a = length of overhang,

b = length between harped points (in.),

P_s = total prestressing force of straight strand group just prior to transfer with initial relaxation losses (kips),

P_h = total prestressing force of harped strand group just prior to transfer with initial relaxation losses (kips),

e_x = eccentricity of strand group at the point of debonding – see Figure 4-7.

To investigate the effect of overhang on the camber, an analysis was done using both the Tadros (2011) equations and the equations in PGSuper on a set of prestressed girders constructed in Missouri. With an assumed overhang distance equal to the girder depth, the analysis showed an insignificant change happened in the camber estimated compared to the current MoDOT procedure (Figure 4-9) using the Tadros (2011) equations. This is because the Tadros equations calculate the deflection from the support to the center of the beam, which ignores the deflection in the overhang.

However, using the equations in PGSuper, which calculate the deflection from the end of the girder to the center, a significant change happened in the camber calculation as shown in (Figure 4-9). The trend line slope is 14% higher than the original MoDOT analysis.

For precast Plant #2, camber was measured while the girder was lifted in the air by the lifting inserts. Figure 4-10 shows the calculated camber considering the overhang length equal to the distance of the lifting device from the girder end. That gives a trend line slope about 5.4% higher than the original MoDOT trend line slope.

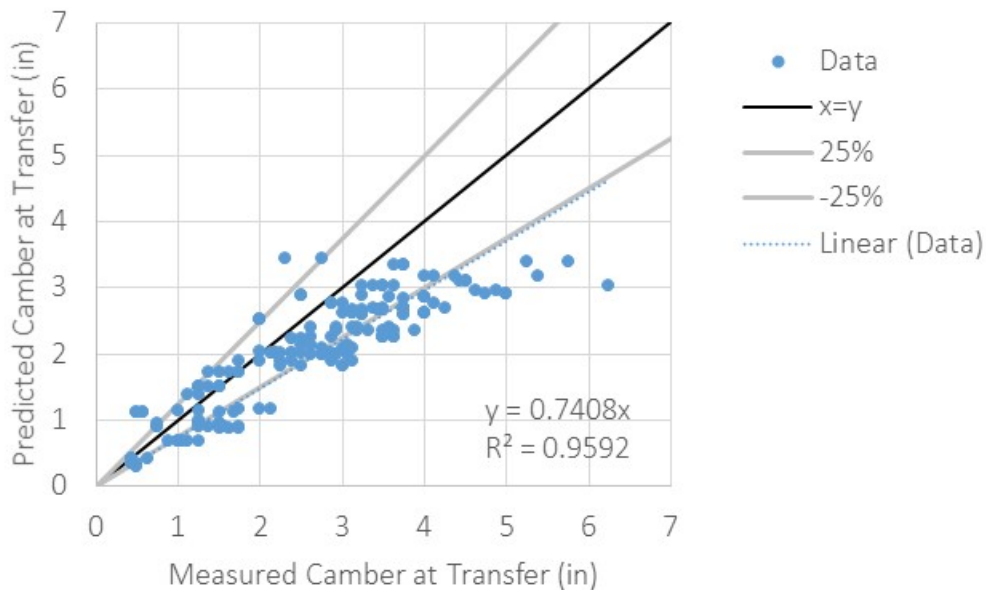


Figure 4-8. Camber including overhang length equal to girder depth per Tadros (2011)

A sensitivity analysis was done to examine the effect of the overhang length on the camber prediction. A change in the overhang length from 0 to 4 ft. caused on average a 20.22% change in the camber for the 189 girders in this study (Figure 4-11).

The results show that the overhang length has a significant effect on the camber, and is included in the proposed procedure. The research team recommends that the equations used in PGSuper to include the effect of the overhang be used. Furthermore, it is recommended that the location of temporary supports be more consistent, perhaps under location of lifting loops.

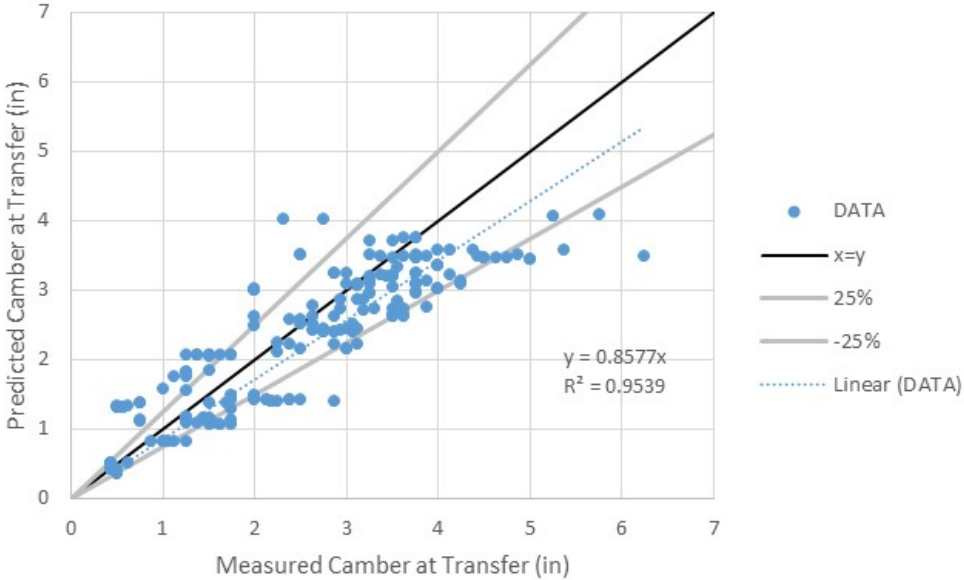


Figure 4-9. Camber including overhang length equal to girder depth per PGSuper method

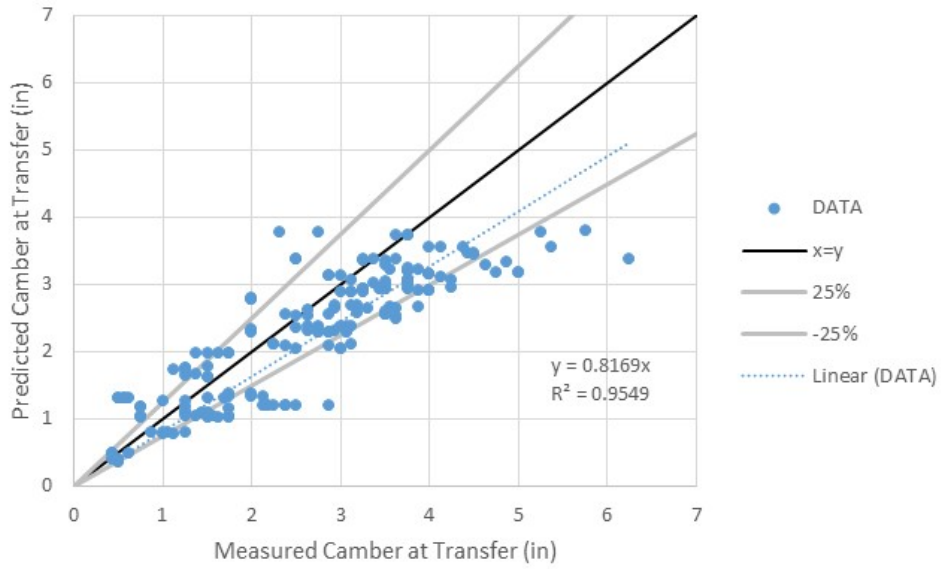


Figure 4-10. Camber including overhang length equal to lifting location per PGSuper method

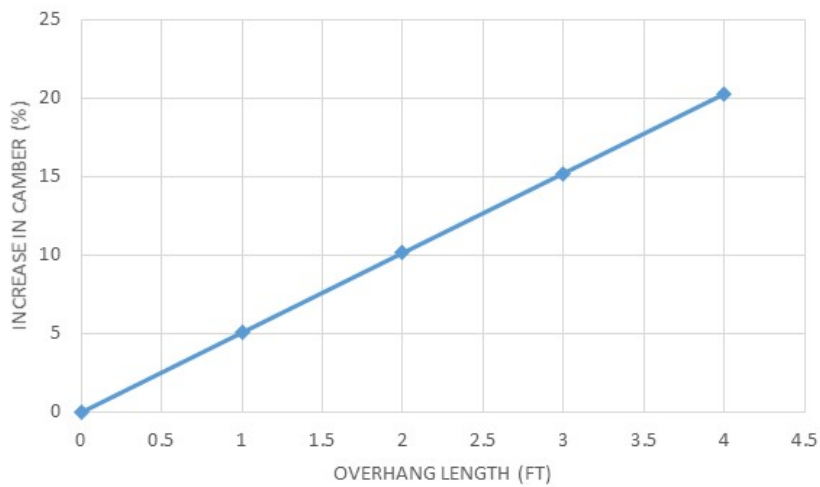


Figure 4-11. Sensitivity of overhang length on camber per PGSuper method

4.2 *Effect of Concrete Modulus of Elasticity*

Modulus is related to compressive strength, but the relationship varies based on the source of aggregate and inherent variability. The previous studies found the modulus was a significant contributor to the accuracy of the camber prediction. Most studies suggested the AASHTO (2010) equation but used different k_1 factor depending on their aggregate source.

There are several methods used to predict the modulus of elasticity discussed in this section. The equation currently used by MoDOT is noted in the AASHTO LRFD (2010) Article 5.4.2.4 employed for normal-weight concrete. The AASHTO equation is as follows:

$$E_c(t) = 33000k_1\gamma^{1.5}\sqrt{f'_c(t)} \quad (\text{ksi}) \quad 4-1$$

where:

$E_c(t)$ = the time modulus of elasticity,

k_1 = correction factor,

γ = the concrete unit weight,

$f'_c(t)$ = the time compressive modulus.

However, ACI Committee 363 suggests a different formula for high-strength concrete which is typically used in prestressed girders. The ACI equation is as follows:

$$E_c(t) = \left(\frac{\gamma}{0.145}\right)^{1.5} (1000 + 1265\sqrt{f'_c(t)}) \quad (\text{ksi}) \quad 4-2$$

The ACI-363 and ASHTO LRFD equations do not consider material properties other than the compressive strength and unit weight of concrete. Tadros et al. (2003) proposed a formula that considered the influence of the coarse aggregate and is shown as follows:

$$E_c(t) = 33000k_1k_2\left(0.14 + \frac{f'_c(t)}{1000}\right)^{1.5}\sqrt{f'_c(t)} \quad (ksi) \quad 4-3$$

where:

k_1 and k_2 are correction factors for local materials.

The formula recommended by the fib Model Code 1990 (MC1990) is only proportional to the concrete compressive strength. Both equations recommended by Tadros and fib are independent of the concrete unit weight. The fib formula is as follows:

$$E_c(t) = 21500\alpha_E\left(\frac{f'_c(t)}{10}\right)^{\frac{1}{3}} \quad (MPa) \quad 4-4$$

where:

α_E = aggregate correction coefficient,

$f'_c(t)$ = concrete compressive strength (MPa).

Table 4-4 shows the comparison of the experimental and predicted modulus using the three methods for the concrete cylinders tested in this study. All three methods provide a reasonable prediction of the modulus with an error less than 10%, however the ACI method for high strength concrete was slightly better than the other two with an average error of 3%.

Table 4-4. Comparison of experimental and predicted modulus of elasticity

Bridge #1 (pour date: 4/17/2021, transfer date: 4/29/2021)								
Concrete age	Ultimate compressive strength (ksi)	Experimental modulus of elasticity (ksi)	Modulus of elasticity (ksi) AASHTO		Modulus of elasticity (ksi) ACI		Modulus of elasticity (ksi) fib	
			Predicted	Error (%)	Predicted	Error (%)	Predicted	Error (%)
2	7,755	5,213	5,220	0.12	4,902	-5.96	5,453	4.60
8	8,507	5,095	5,508	8.11	5,083	-0.23	5,624	10.38
21	9,576	5,407	5,907	9.26	5,327	-1.48	5,850	8.20
30	9,707	5,889	5,956	1.14	5,356	-9.05	5,877	-0.20
91	9,406	5,619	5,845	4.01	5,289	-5.88	5,815	3.49
Bridge #2 (pour date: 5/4/2021, cutdown date 5/5/2021)								
1	7,306	4,686	5,043	7.61	4,790	2.21	5,345	14.06
14	8,919	5,329	5,663	6.27	5,179	-2.83	5,713	7.20
90	10,885	5,776	6,381	10.47	5,608	-2.92	6,105	5.70
			Average error	5.9		-3.3		6.7

The modulus of elasticity has a strong effect on the initial camber. Changing k_1 in the AASHTO equation from 0.7 to 1.2 changes camber prediction by about 33% to -15% on average for the suite of 189 bridge girders.

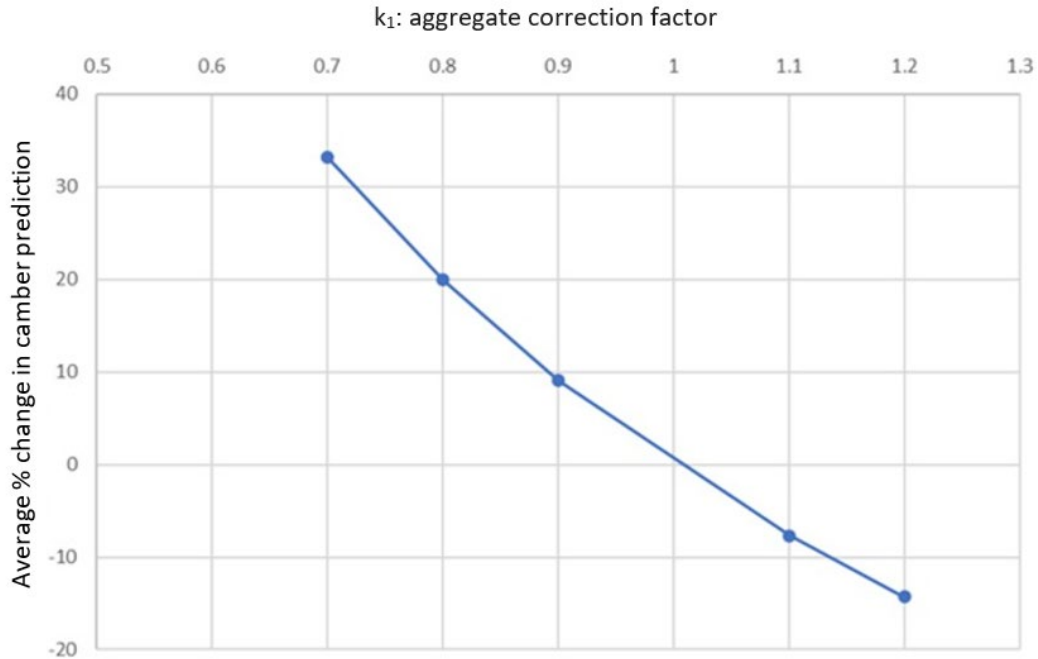


Figure 4-12. Effect of k_1 modulus factor on camber prediction

Figure 4-13 and Figure 4-14 show the predicted camber vs. the field camber measurements using the AASHTO and ACI modulus of elasticity. The slope of the trend line using the ACI equation is higher than the AASHTO equation by about 4%, though the variability is about the same. On the other hand, the fib equation (Figure 4-15) gives results with a trend slope lower than the AASHTO by about 6% (see figure 19).

Based on the analysis, ACI 363 may give more accurate results unless a k_1 correction factor is used with the AASHTO formula. However, the difference in the two results is less than 4%.

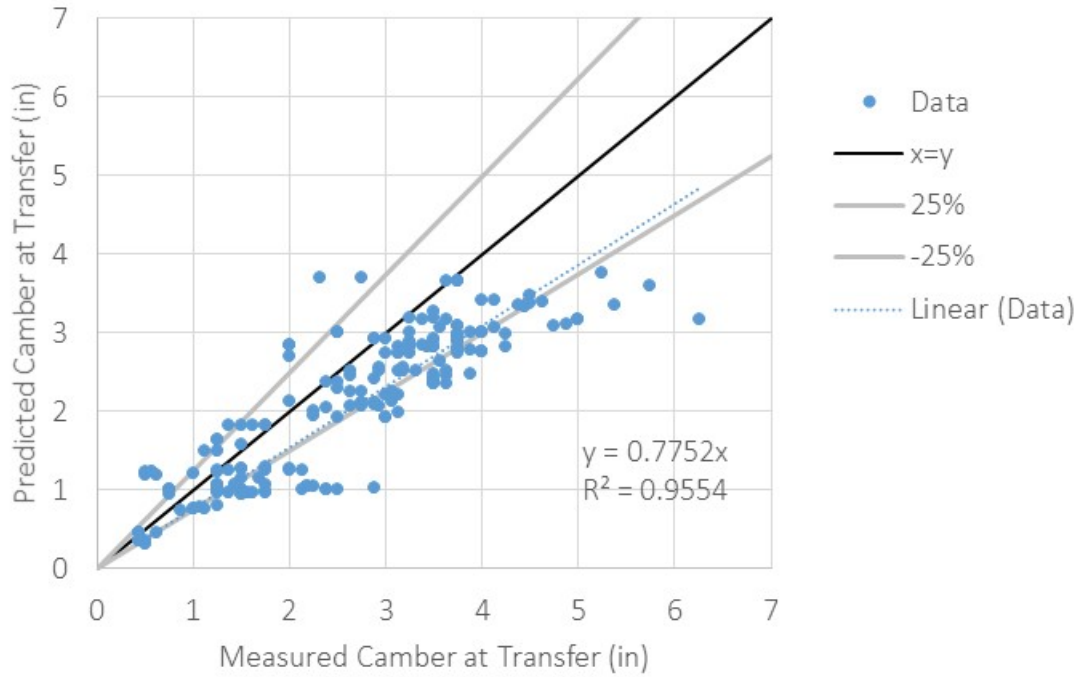


Figure 4-13. Camber using AASHTO (2010) equation for concrete modulus

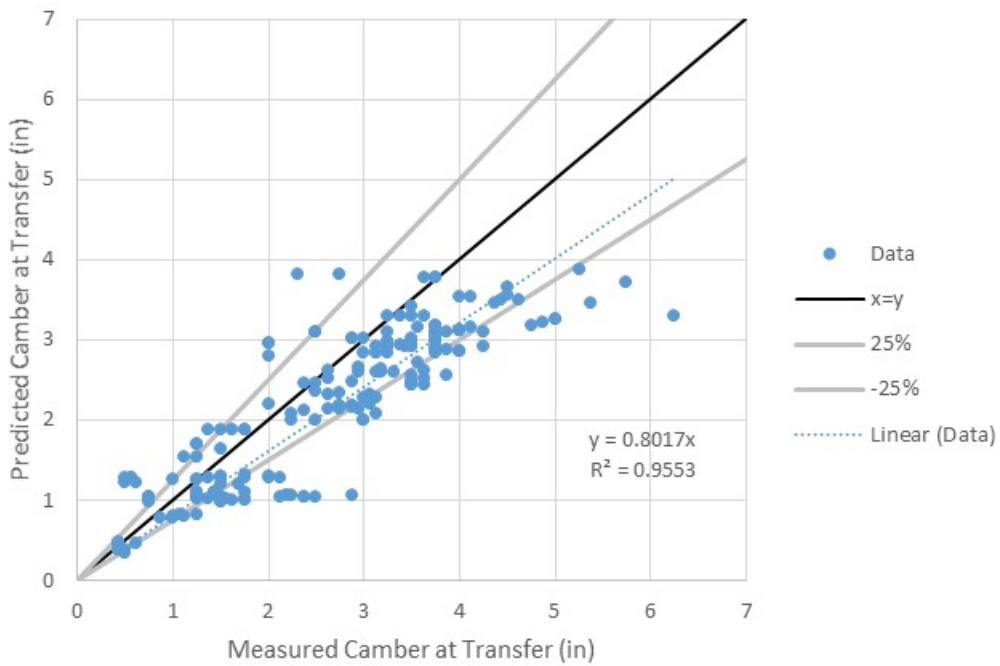


Figure 4-14. Camber using ACI 363 equation for concrete modulus

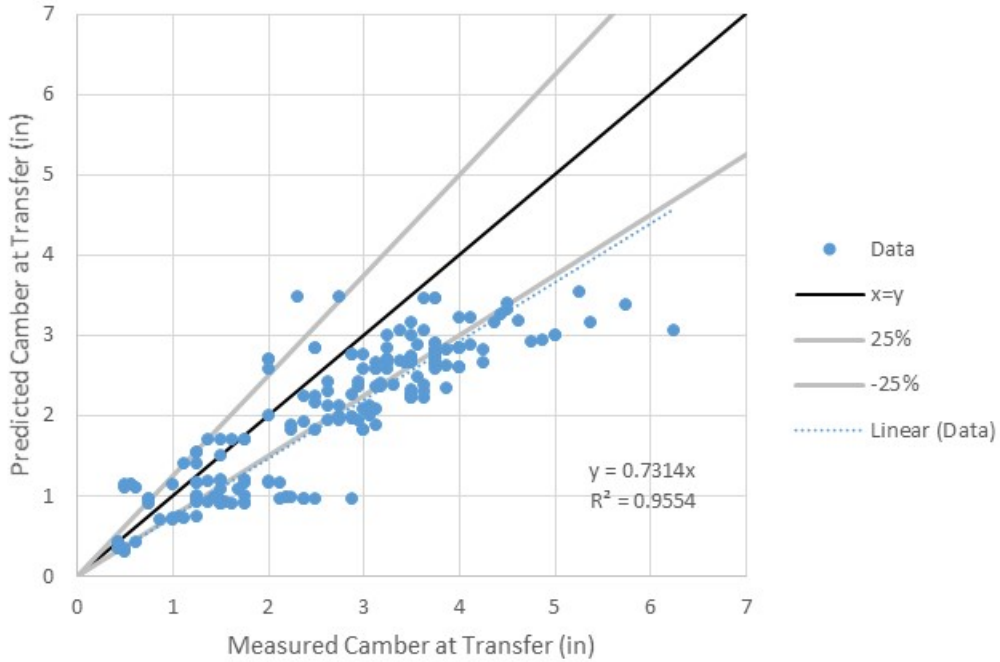


Figure 4-15. Camber using CEB-FIP Model Code 1990 equation for concrete modulus

4.3 *Effect of Concrete Age/Strength at Prestress Transfer*

The effect of the concrete compressive strength at the time of prestress transfer was also a major factor cited in previous literature. The main effect of the compressive strength in the initial camber is that the strength is directly proportional to the modulus of elasticity of concrete. Usually, the fabricator uses a greater strength mix design to get the expected initial strengths at release at concrete age 1 day. However, when looking through the field data, the average concrete ages at release were 2 ± 1.25 days (Figure 4-16).

Concrete strength varies with age. The American Concrete Institute (ACI 209R-92) uses a well-established time function for early-age strength, ($f'_c(t)$, t less than 28 days) as well as early age

stiffness (elastic modulus, $E_c(t)$). Equation 4-6 gives the variation of concrete compressive strength with time which is applicable for high and normal reinforced concrete.

$$f'_c(t) = \frac{t}{\alpha + \beta t} (f'_c)_{28} \quad 4-5$$

where:

$(f'_c)_{28}$ = the concrete compressive strength at 28 days,

t = concrete age (days),

α and β = factors given in Table 4-5.

Table 4-5. The values of the α and β constants

Type of curing	Cement type	α	β
Moist	I	4.0	0.85
	III	2.3	0.92
Steam	I	1.0	0.95
	III	.70	0.98

An analysis was done to compare the measured strength with the ACI formula on a set of bridges that have the same compressive strength at 28 days ($(f'_c)_{28} = 8 \text{ ksi}$). Figure 4-17 shows that all the bridges had compressive strength higher than expected. The average initial compressive strength was $8.58 \pm 1.17 \text{ ksi}$, which is about 32% higher than the design strength (6.5 ksi).

The field measured concrete cylinder strengths from the two test bridges are compared to the prediction equations from ACI using the 28-day measured strength of 9,700 psi in Figure 4-18. The measured strengths show a slower increase in strength than the steam cured specimens, but a faster increase than the moist cured specimens. The use of an α and β factor between that of the moist and steam cured specimens ($\alpha=1.4$, $\beta=0.95$) yields a better match to the measured time variation of concrete compressive strengths (Figure 4-19). However, this is a small number of

cylinder tests, and it is recommended to use the published values in ACI 209R-92 unless more comprehensive data is obtained.

In the analysis of the 189 bridge girders, using the measured initial compressive strength decreases the trend line slope (0.6957) compared to using the design compressive strength the slope (0.7752), by about 10% (see Figure 4-20), however, the variability is about the same. Because it is not possible to know the compressive strength before the concrete is cast, it is recommended that the design compressive strength continue to be used in the camber prediction. If after casting, the camber measurement is found to be out of tolerance, an analysis with the measured compressive strength may be used.

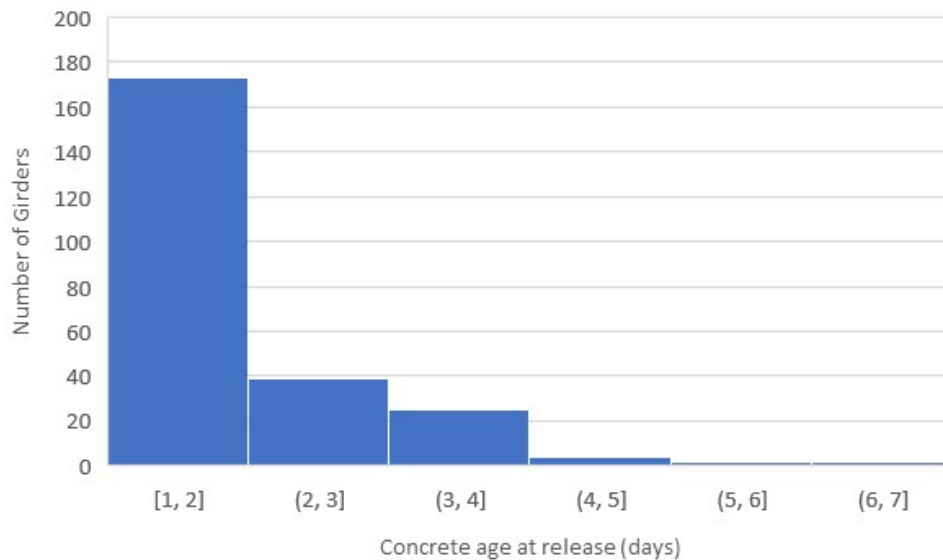


Figure 4-16. Concrete age at release for the available field data

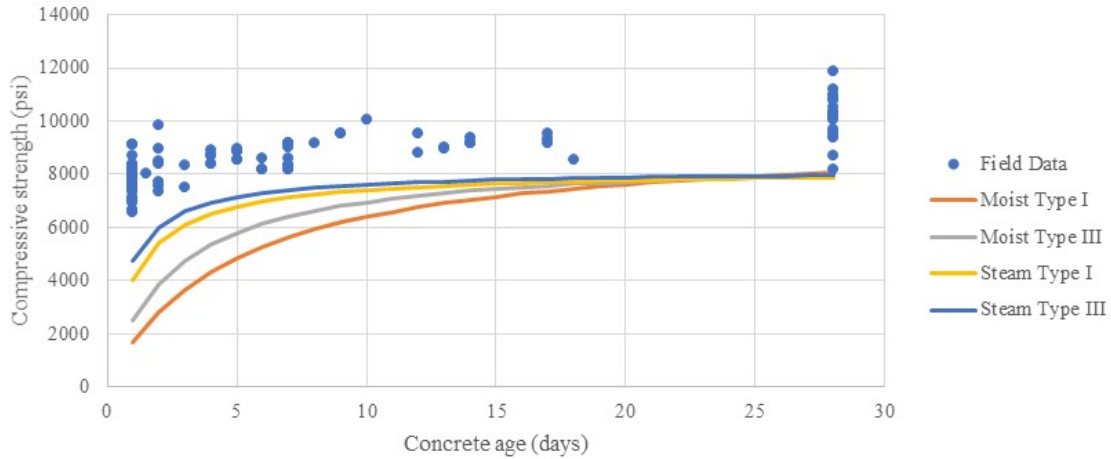


Figure 4-17. Reported cylinder strengths vs ACI predictions using design compressive strength

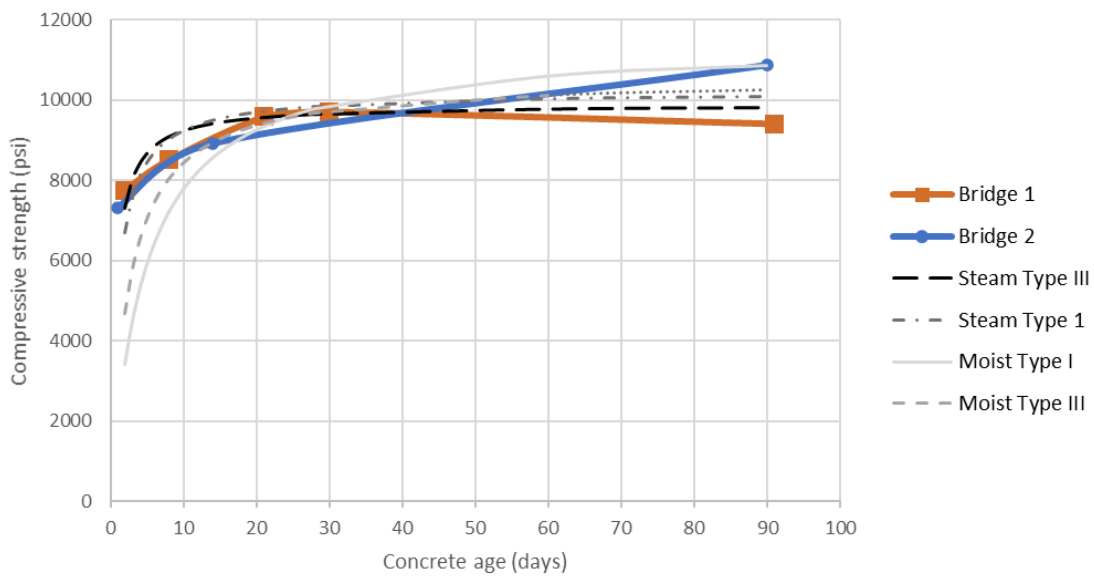


Figure 4-18. Field measured compressive strength of concrete vs. the expected compressive strength using ACI 209R-92 formula

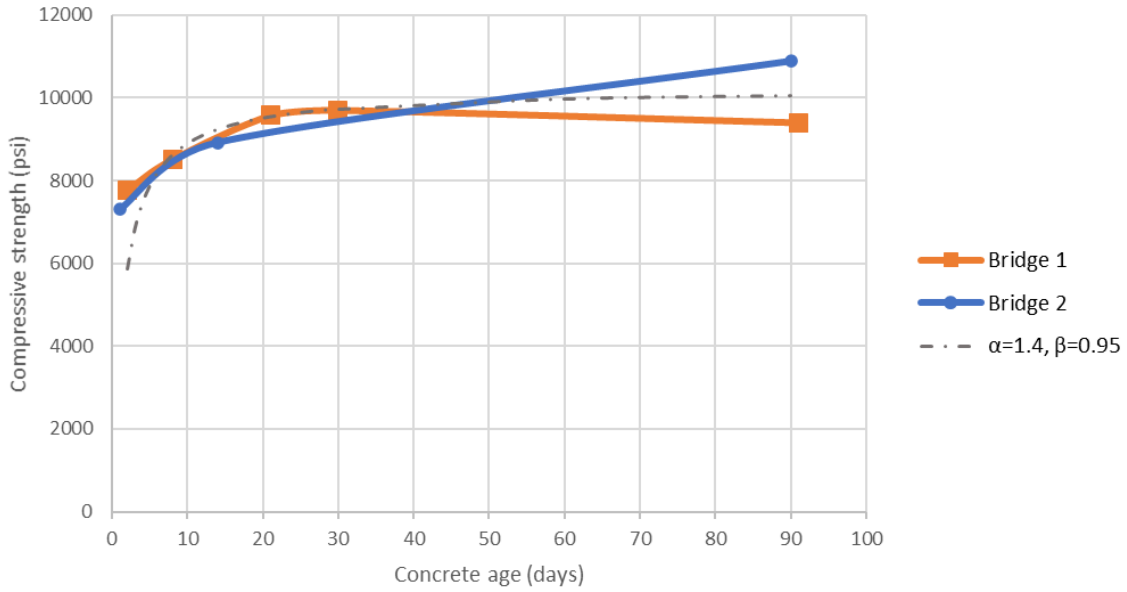


Figure 4-19. Field measured compressive strength of concrete vs. the expected compressive strength modified ACI 209R-92 formula

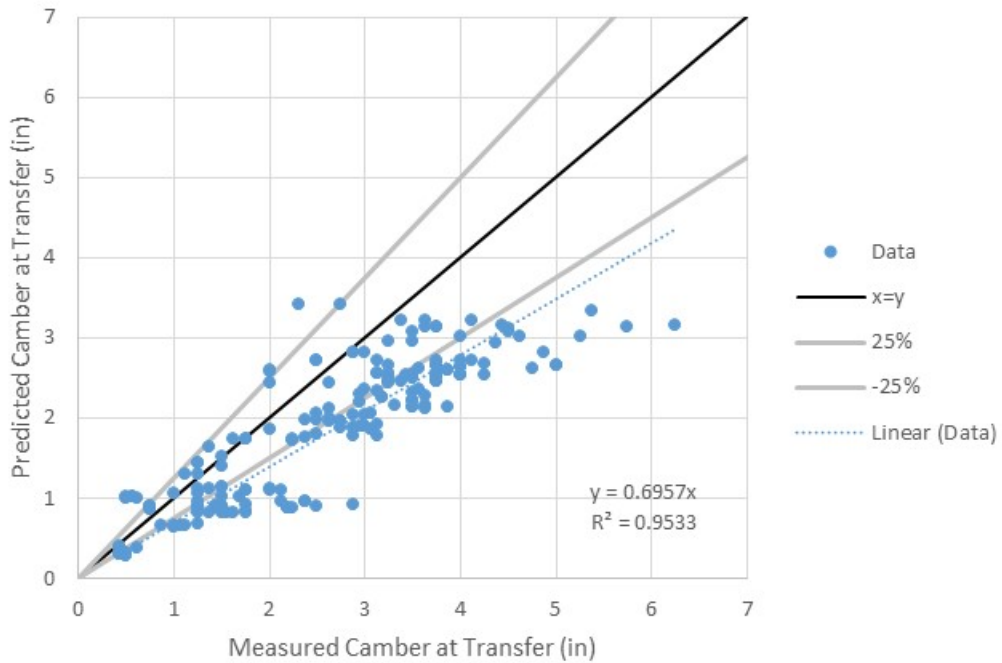


Figure 4-20. Predicted camber using the measured initial concrete strength

4.4 *Effect of Temperature*

Thermal camber due to daily temperature variations has been another cited cause for camber variability in previous research. Several researchers have evaluated the temperature gradients and their impacts on the prestressed girder camber. For example, Nguyen et al. (2015) investigated the influences of temperature variation on the girder camber. A practical method was developed which allows the designer to predict the camber in the prestressed girder caused by the variation in temperature. The model is as follows:

$$\Delta_T = \left(\frac{\alpha A_1}{h}\right) (T_{max} - T_{min}) \left(\frac{1 - \cos\left[\frac{t-t_0}{24} 2\pi\right]}{2}\right) \left(\frac{L^2}{8}\right) \quad 4-6$$

where:

t_0 = reference time for counting the thermal camber during that day,

T_{max} = maximum air temperature during a period of 24 hours,

T_{min} = minimum air temperature during a period of 24 hours,

α = coefficient of thermal conductivity $5.5 \times 10^{-6}/^\circ\text{F}$ ($9.9 \times 10^{-6}/^\circ\text{C}$),

A_1 = calibration factor,

L = length of the prestressed girder (in.),

h = the girder height (in.),

Δ_T = camber variation due to temperature.

Figure 4-21 shows the predicted camber vs. the measured camber for the studied bridges assuming a 20°F temperature change. This temperature change is the average change in Missouri in the summer months. The trend line slope about 23% higher than the current MoDOT camber calculation.

In another analysis, the actual temperature variation on the day of prestress transfer was used. The trend line slope is about 25% higher than the current calculation. (see Figure 4-22).

The results show that the daily temperature variation does impact the camber. Therefore, it is recommended that camber measurements occur in the morning to avoid significant temperature variation, or that the analysis take into account the variation in temperature. However, for the case of initial camber, the increased internal temperature due to the concrete curing will also alter the results, see Section 4.7.

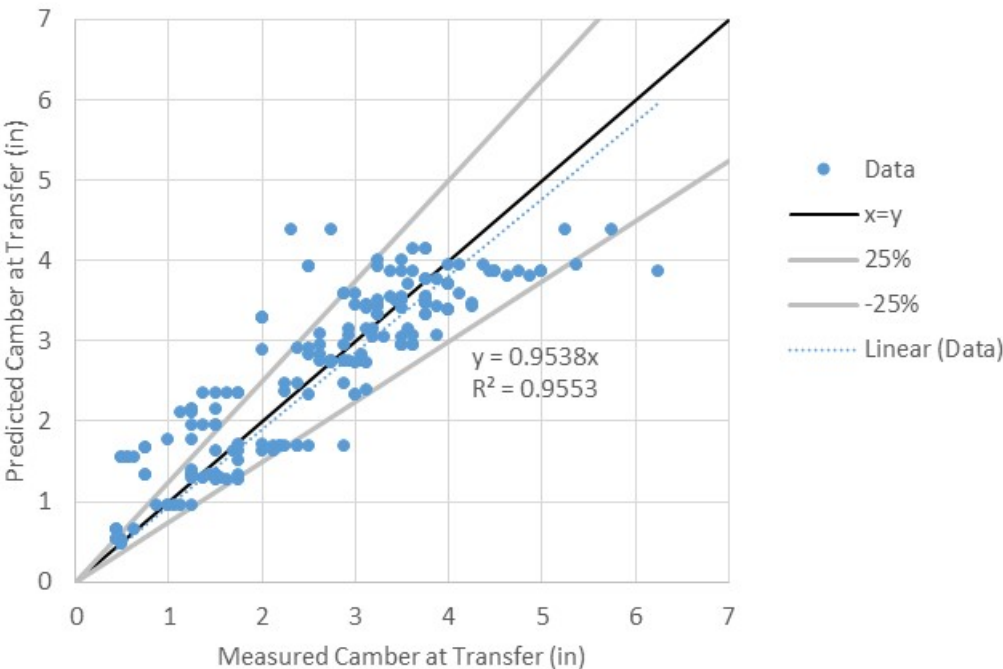


Figure 4-21. Predicted camber considering 20°F temperature variation

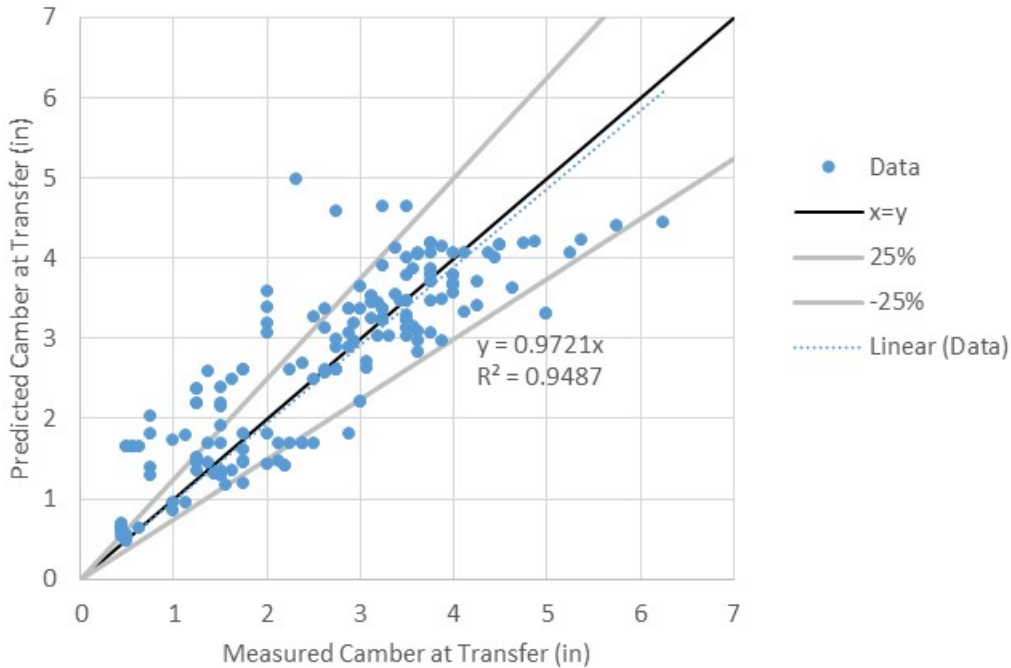


Figure 4-22. Predicted camber considering actual daily temperature variation

4.5 *Effect of Prestressing Force*

Prestress losses and elastic shortening losses will reduce the initial prestressing force and result in less camber. The total prestress losses, in general, can be determined by considering the individual components. The prestress losses are divided into instantaneous losses and long-term losses. The instantaneous losses are due to anchorage set, friction, and elastic shortening. The long-term prestress losses are due to concrete creep, concrete shrinkage, and steel relaxation after transfer.

$$\Delta f_{pTL} = \Delta f_{pES} + \Delta f_{pSR} + \Delta f_{pCR} + \Delta f_{pR} \quad 4-7$$

where:

Δf_{pTL} = total prestress loss,

Δf_{pES} = elastic shortening loss,

Δf_{pSR} = shrinkage loss,

Δf_{pCR} = creep loss,

Δf_{pR} = relaxation loss after prestress transfer.

4.5.1 Elastic Shortening

According to AASHTO, the elastic shortening losses can be calculated using Equation 4-9. This equation may be used at the various loading conditions for each section along the beam. Tadros et al. (2003) concluded that the suggested approach of predicting the relaxation prestress losses provides acceptable agreement with the measured value. The total elastic shortening gain or loss may be calculated as the sum of the effects of prestressing and external loads.

$$\Delta f_{pES} = \frac{E_p}{E_{ct}} * f_{cgp} \quad 4-8$$

where:

f_{cgp} = the concrete stress at the center of gravity of prestressing tendons due to the prestressing force immediately after transfer and the self-weight of the member at the section of the maximum moment (ksi),

E_p = modulus of elasticity of prestressing steel (ksi),

E_{ct} = modulus of elasticity of concrete at transfer or time of load application (ksi).

4.5.2 Relaxation Losses

The loss in tensile stress in a prestressing tendon over time maintained at a sustained strain and constant temperature is referred to as relaxation loss. Relaxation loss is negligible for initial stress levels of less than 55% of the yield stress of the prestressing tendon, f_{py} . For higher levels of initial prestress often used, relaxation loss, Δf_{pR} , is given by the following equation:

$$\Delta f_{pR} = f_{pi} \frac{\log(t)}{K} \left(\frac{f_{pi}}{f_{py}} - 0.55 \right) \quad 4-9$$

where:

f_{pi} = the initial prestress stress,

K = 10 for stress-relieved strands, and 45 for low-relaxation strands.

Figure 4-25 shows the predicted camber vs. the measured camber for the studied bridges when decreasing the initial prestress force by 5%. The trend line slope for it is lower than the current MoDOT calculation trend line slope by about 8.5%. That gives evidence that the prestress force has a significant effect on the camber calculation.

Another sensitivity analysis was done to know the effect of the jacking force on the camber prediction. This analysis was motivated by research, done by Gilbertson and Ahlborn (2004), which mentioned that the jacking force may have a variation (± 6 ksi). When increasing the jacking force by 6 ksi, the trend line slope (0.8049) is higher than the existing MoDOT calculation trend line slope (0.7752) by about 4% (see Figure 4-23). However, when decreasing the jacking force by 6 ksi, the trend line slope (0.7209) is lower than the existing MoDOT calculation trend line slope (0.7752) by about 7% (see Figure 4-24).

Although the results do show that prestressing force affects camber, the actual prestress force would be difficult to determine. It is recommended current methods for the determination of prestress force continue to be used.

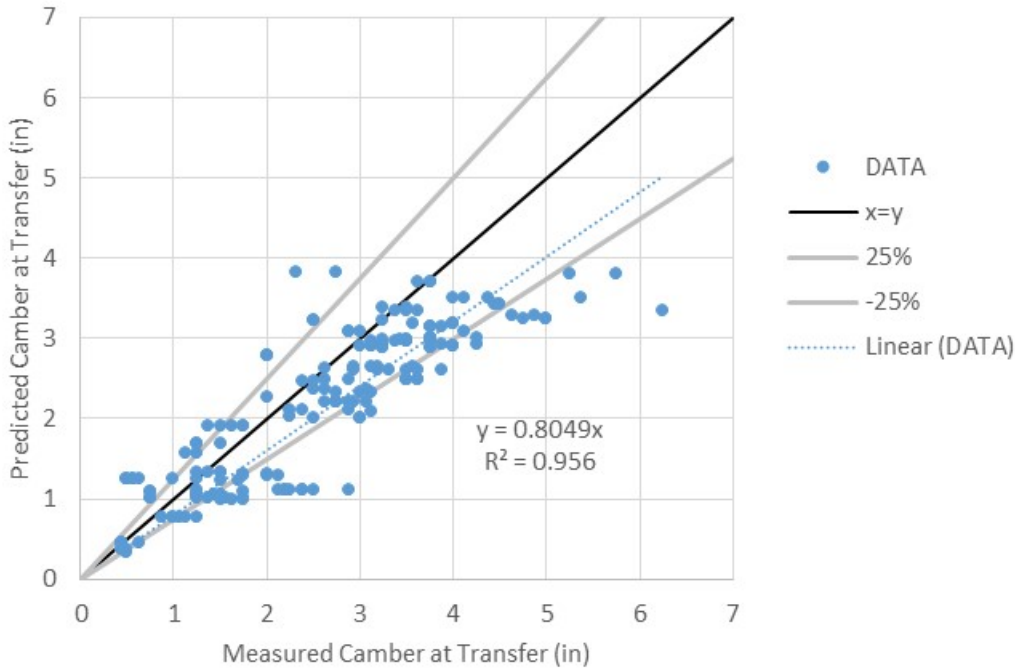


Figure 4-23. Predicted camber when increasing the jacking force by 6 ksi

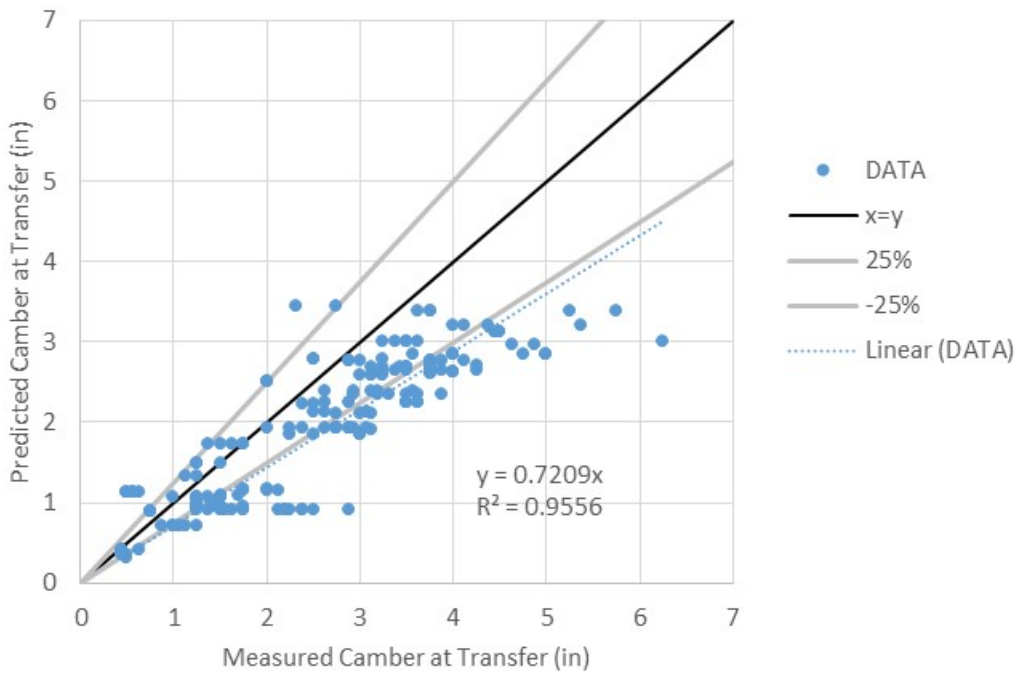


Figure 4-24. Predicted camber when decreasing the jacking force by 6 ksi

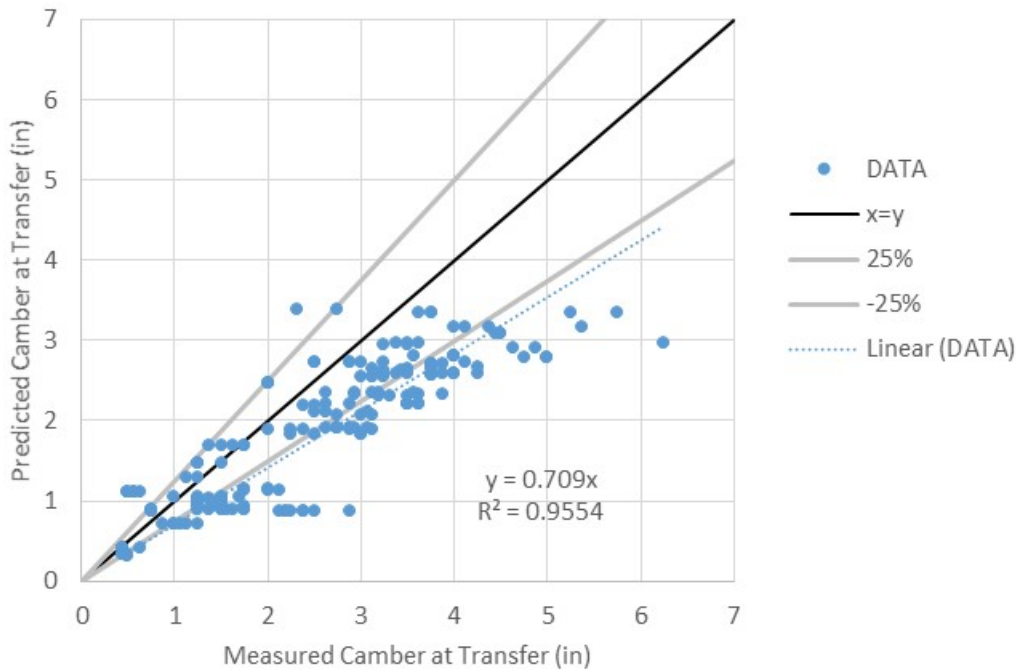


Figure 4-25. Predicted camber when decreasing the initial prestress force by 5%

4.6 *Transformed vs. Gross Section Properties*

For the calculation of camber, either transformed or gross section properties can be used. Tadros et al. (2003) recommended that transformed properties be used, however, the elastic shortening losses should not be considered. The current MoDOT method also uses transformed section properties for camber calculations.

An analysis was done to evaluate the difference in the camber prediction when using gross and transformed properties. As shown in Figure 4-26 and Figure 4-27, the results are similar for both analyses (trend line slope of 0.7752 for transformed and 0.7611 for gross properties). This result is similar to Honarvar et al. (2015) who found only a 2% difference in camber due to the choice of section properties. Due to the small change in camber results, it is recommended that the transformed properties continue to be used.

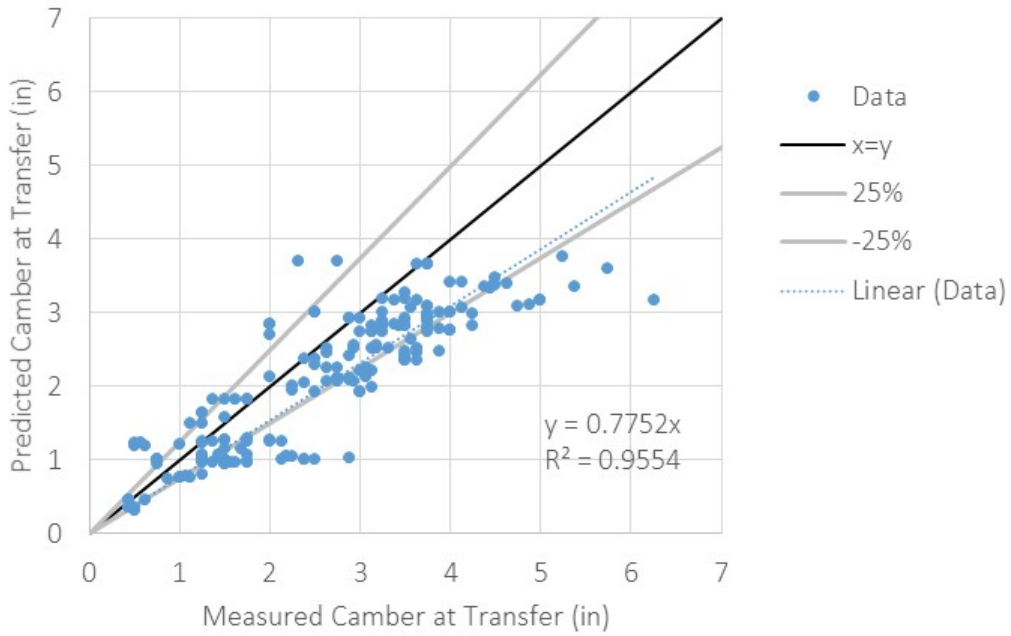


Figure 4-26. Predicted camber using transformed properties

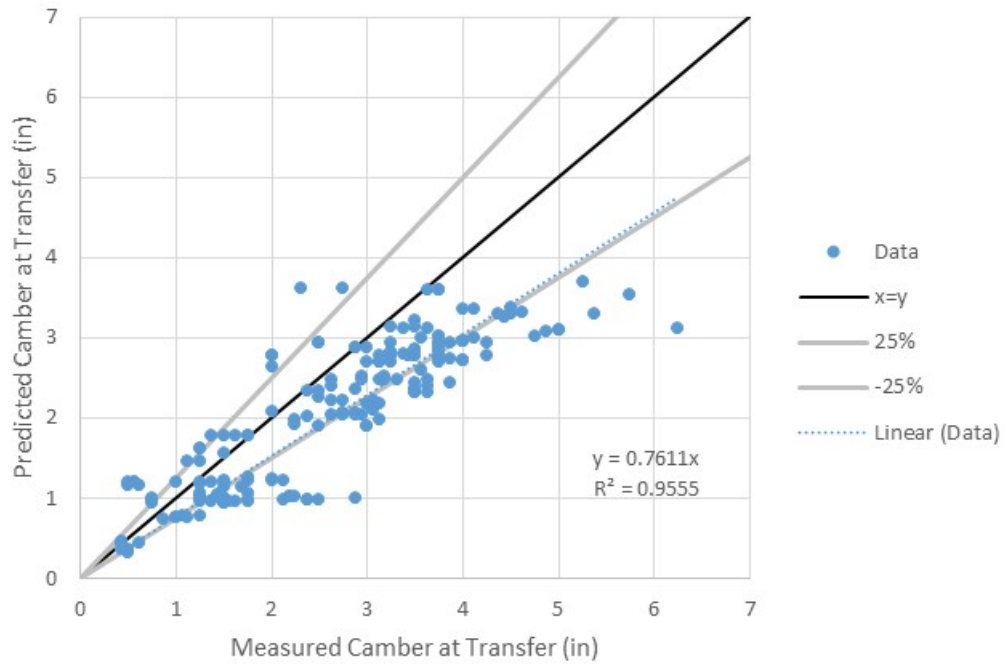


Figure 4-27. Predicted camber using gross properties

4.7 *Temperature Due to Concrete Curing*

The increased temperature of the concrete during curing reduces the prestressing force because thermal increase causes the strands to relax. As a result, the girder camber is affected by these losses.

In order to explain this behavior, a study by Roller and Russell (2003) concluded that there are losses in the prestressing force caused by the increased temperature of the concrete. The influence of temperature impacts can be calculated according to the following:

$$\Delta f_p = E_p \mu_p \Delta T \quad 4-10$$

where:

μ_p = the thermal expansion coefficient of steel cable (8×10^{-6} strain / F),

ΔT = the estimated change in temperature (assumed to be 60°F for increase in curing temperature),

E_p = elastic modulus of prestressing steel (ksi),

Δf_p = change in prestressing force.

An analysis was done to evaluate the difference in the camber prediction when considering increased curing temperature by 60°F (see Figure 4-28). The trend line slope is lower than the current MoDOT calculation trend line slope by about 12%. It is recommended that this effect is considered in initial camber, or that the initial camber is measured 72 hours after form removal so that the temperature in the concrete can cool (Tadros, 2015).

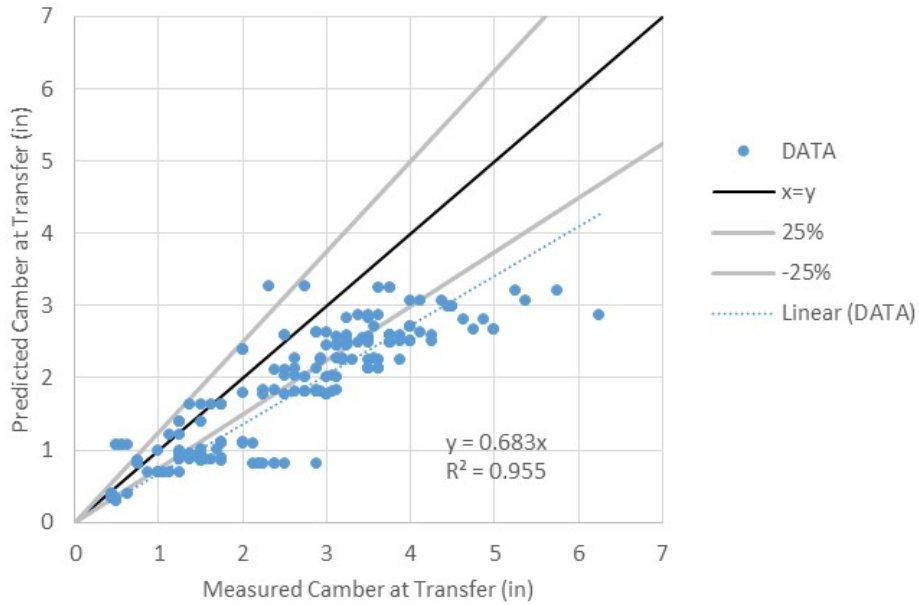


Figure 4-28. Predicted camber including prestress reduction due to increased concrete temperature at curing

4.8 *Effect of Concrete Density*

The concrete density is related to the girder's self-weight which affects the deflection caused by the dead load. An analysis was done to evaluate the difference in the camber prediction when decreasing the concrete density by 5% (see Figure 4-29). The analysis showed that the trend line slope is higher than the current MoDOT calculation trend line slope by about 3%. Therefore, the effect of concrete density does not have a significant effect on girder camber.

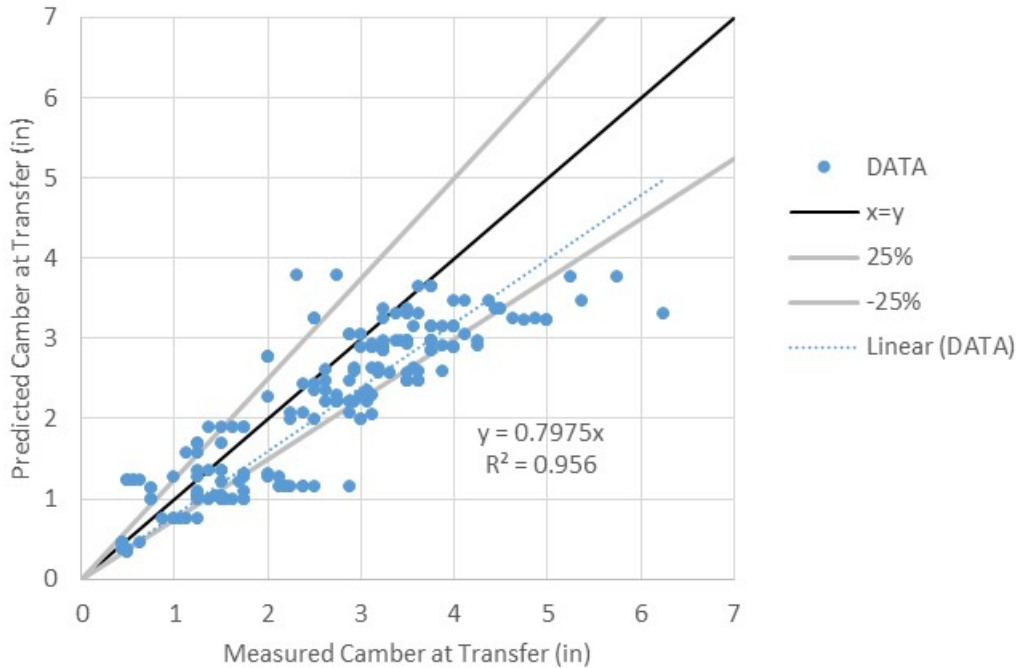


Figure 4-29. Predicted camber when decreasing the concrete density by 5%

4.9 *Strand Eccentricity*

A sensitivity analysis was completed to establish the impact of the strand eccentricity on the camber calculation. This analysis was motivated by research, done by Gilbertson and Ahlborn (2004), who observed that the strand eccentricity may have a variation ($\pm 1/16$ in.). When considering strand eccentricity by $+1/16$ in., the trend line slope is lower than the current MoDOT calculation trend line slope by about 1.5% (see Figure 4-30). When considering strand eccentricity by $-1/16$ in., the trend line slope is higher than the current MoDOT calculation trend line slope by about 1.6% (see Figure 4-31). The strand eccentricity does not have a significant impact on camber.

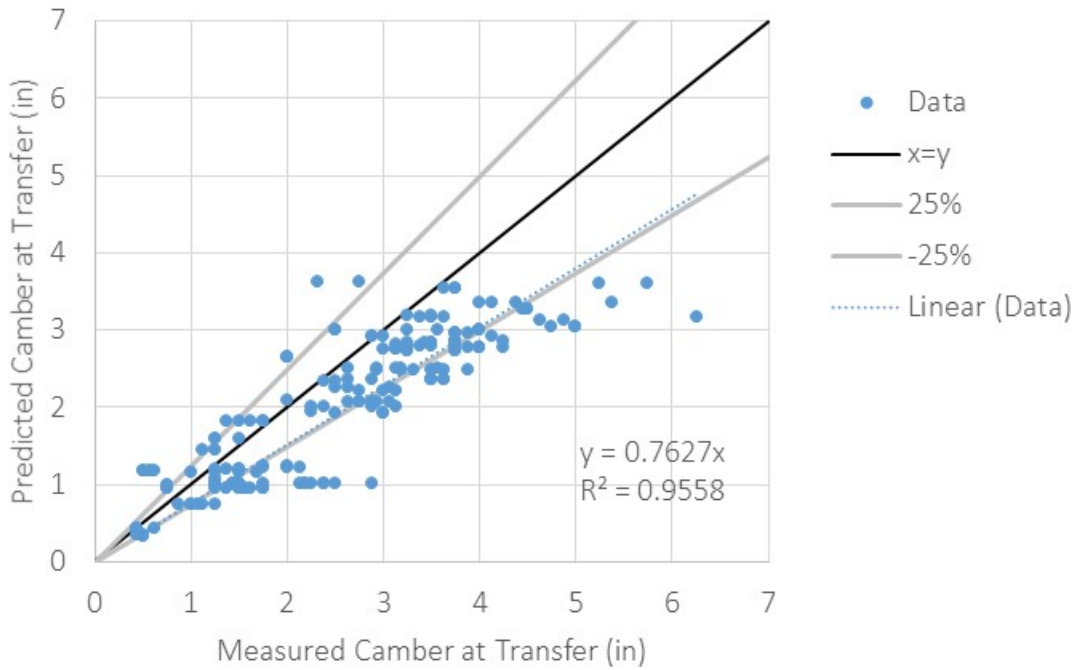


Figure 4-30. Predicted camber when considering strand eccentricity of (+1/16 in.)

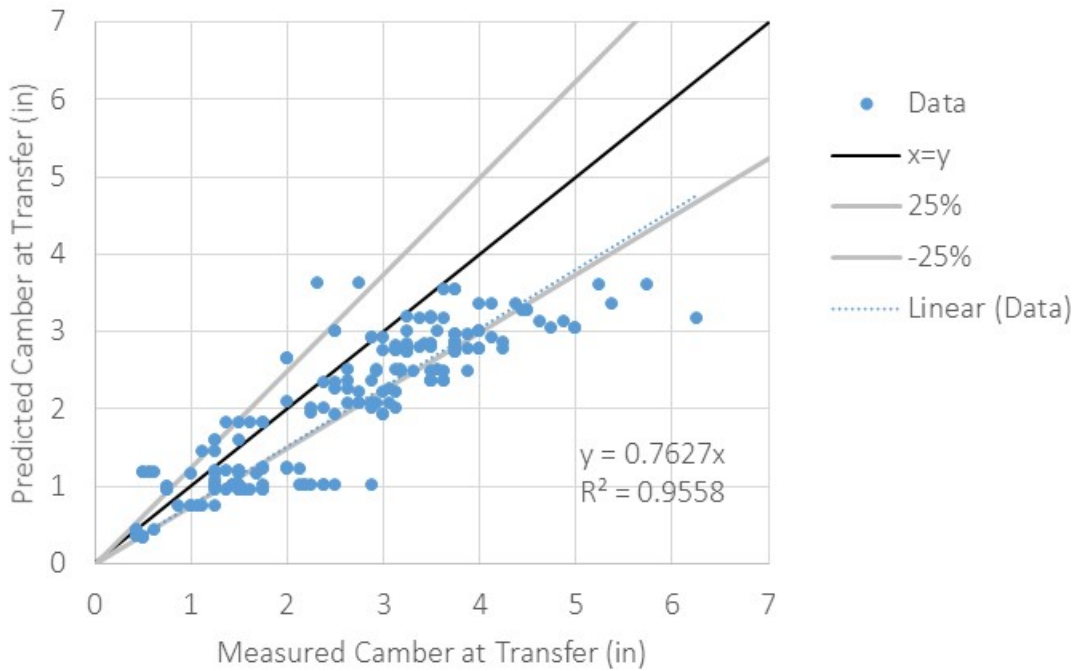


Figure 4-31. Predicted camber when considering strand eccentricity of (-1/16 in.)

4.10 Effect of Creep

The long-term camber of bridge girders includes the effects of creep and shrinkage in the concrete.

The factors are summarized in Table 4-6.

Table 4-6: Factors affecting long-term camber prediction

Concrete creep	Time-dependent strain due to sustained stress is attributed to the creep of concrete. The concrete creep is more significant in the long-term losses of the prestress force.	Increasing the creep coefficient has an insignificant effect on the initial camber calculations. That if the creep coefficient (C_u) is increased by 10%, the long-term camber at one year will be increased by about 4%.
Concrete shrinkage	Shrinkage is defined as volume decrease in concrete with time. The concrete shrinkage influences the long-term losses of the prestress force.	The shrinkage strain has an insignificant effect on the initial camber calculation. Increasing the shrinkage strain (ϵ_{sh}) by 100% results in decreasing the long-term camber at one year by about 6%.

4.10.1 Effect of Concrete Creep

Concrete creep is an important property that affects long-term camber growth. Several existing methods already exist to predict creep in concrete and their equations are presented in the next sections.

4.10.1.1 AASHTO LRFD 5.4.2.3.2 (2012)

$$\Psi(t, t_i) = 1.9k_s k_{hc} k_f k_{td} t_i^{-0.118} \quad 4-11$$

$$k_s = 1.45 - 0.13(v/s) \geq 1.0 \quad 4-12$$

$$k_{hc} = 1.56 - 0.008H \quad 4-13$$

$$k_f = 5/(1 + f'_{ci}) \quad 4-14$$

$$k_{td} = t / \left(\frac{12(100 - 4f'_{ci})}{f'_{ci} + 20} + t \right) \quad 4-15$$

where:

- Ψ = creep coefficient from time t_i to time t ,
- H = 70, average annual ambient relative humidity,
- t = maturity of concrete (day), defined as age of concrete between time of loading for creep calculations, or end of curing for shrinkage calculations, and time being considered for analysis of creep or shrinkage effects,
- t_i = age of concrete when a load is initially applied, (days) Use 0.75 days for camber design,
- v/s = volume-to-surface area ratio, (in.),
- f'_{ci} = initial girder concrete compressive strength, (ksi),
- K_s = factor for the effect of the volume-to-surface ratio of the component,
- K_f = factor for the effect of the concrete strength,
- K_{hc} = humidity factor for creep,
- K_{td} = time development factor.

4.10.1.2 ACI Committee 209 (1997)

$$C_c(t - t_i) = \frac{(t-t_i)^{0.6}}{10+(t-t_i)^{0.6}} C_{CU} K_{CH} K_{CS} K_{CA} \quad 4-16$$

where:

- t = maturity of concrete (day), defined as age of concrete between time of loading for creep calculations, or end of curing for shrinkage calculations, and time being considered for analysis of creep or shrinkage effects,
- t_i = age of concrete when a load is initially applied, (days). Use 0.75 days for camber design,
- $C_c(t - t_i)$ = creep coefficient,
- C_{CU} = nominal ultimate creep coefficient (2.35),
- K_{CH} = ambient relative humidity factor = $1.27 - 0.67h$,

$$K_{CS} = \text{volume-to-surface ratio factor} = \frac{2}{3} \cdot \left(1 + 1.13e^{\left(-0.54\left(\frac{v}{s}\right)\right)} \right),$$

$$K_{CA} = \text{age application of load factor} = 1.13t_i^{-0.094}.$$

4.10.1.3 fib Model Code 2010 (MC2010)

$$\varphi(t, t_i) = \varphi_0 \cdot \beta_c(t - t_i) \quad 4-17$$

$$\varphi_0 = \phi_{RH} \beta(f_{cm}) \beta(t_i) \quad 4-18$$

$$\phi_{RH} = 1 - \frac{1 - RH/RH_0}{0.46 \left(\frac{h}{h_0}\right)^{1/3}} \quad 4-19$$

$$\beta(f_{cm}) = \frac{5.3}{\left(\frac{f_{cm}}{f_{cm0}}\right)^{0.5}} \quad 4-20$$

$$\beta(t_i) = \frac{1}{0.1 + \left(\frac{t_{i,eff}}{t_1}\right)^{0.2}} \quad 4-21$$

$$t_{i,eff} = t_i \left(\frac{9}{2 + \left(\frac{t_i}{t_1}\right)^{1.2}} + 1 \right)^\alpha \geq 0.5 \quad 4-22$$

$$\beta_c(t - t_i) = \left(\frac{\frac{t-t_i}{t_1}}{\beta_H + \frac{t-t_i}{t_1}} \right)^{0.3} \quad 4-23$$

$$\beta_H = 150 \left(1 + \left(1.2 \frac{RH}{RH_0} \right)^{1.8} \right) \frac{h}{h_0} + 250 \leq 1500 \quad 4-24$$

where:

$\varphi(t, t_i)$ = creep coefficient,

ϕ_{RH} = relative humidity factor,

RH = the relative humidity of the ambient environment in %,

f_{cm} = the 28 days mean compressive strength of concrete in MPa,

$\beta(f_{cm})$ = concrete strength factor,

$\beta(t_i)$ = concrete age at loading factor,

h_0 = the notional size of the member in mm where: $h_0 = 2A_c/u$,

A_c = the cross-sectional area,

u = the perimeter of the member in contact with the atmosphere,

$\beta_c(t - t_i)$ = coefficient to describe the development of creep with time after loading,

β_H = coefficient depending on the relative humidity (RH in %) and the notional member size,

$t_{i,eff}$ = the temperature adjusted age of concrete at loading in days, note: $\alpha=-1$ for cement class S; $\alpha=0$ for cement class N; $\alpha=1$ for cement class R.

In order to calculate the change in deflection using the creep coefficient the following equation is used:

$$\Delta_{CR} = (\Delta_{SS-j} + \Delta_{HS-j} + \Delta_g) * \text{creep coefficient} + (\Delta_{SS-i} + \Delta_{HS-i})0.7 * \text{creep coefficient} \quad 4-25$$

where:

Δ_g = deflection due to self-weight of girder (in.),

Δ_{SS-j} = initial camber due to prestressing straight strands (in.),

Δ_{HS-j} = initial camber due to prestressing harped strands (in.),

Δ_{SS-i} = camber due to prestressing straight strands using the prestress losses (in.),

Δ_{HS-i} = camber due to prestressing harped strands using the prestress losses (in.).

The 0.7 factor is the aging coefficient recommended in Tadros (2011). A comparison of the results from different models is completed for the concrete cylinders tested in this investigation (see Figure 4-32). The ACI creep model provides closer results to the creep obtained from the cylinders tested. The model was about 26.64% lower than the average cylinder result at 7 days and 1.31% higher at 90 days. The difference using AASHTO was about 66% lower at 7 days and 22% lower at 90 days. On the other hand, the difference using fib Model Code 2010 (MC2010) was about 41% lower at 7 days and 33% lower at 90 days. However, when comparing to the cylinders that were tested by Gopalaratnam and Eatherton (2001), the fib Model Code 2010 (MC2010) gives the most accurate results with the lowest error (about 11%).

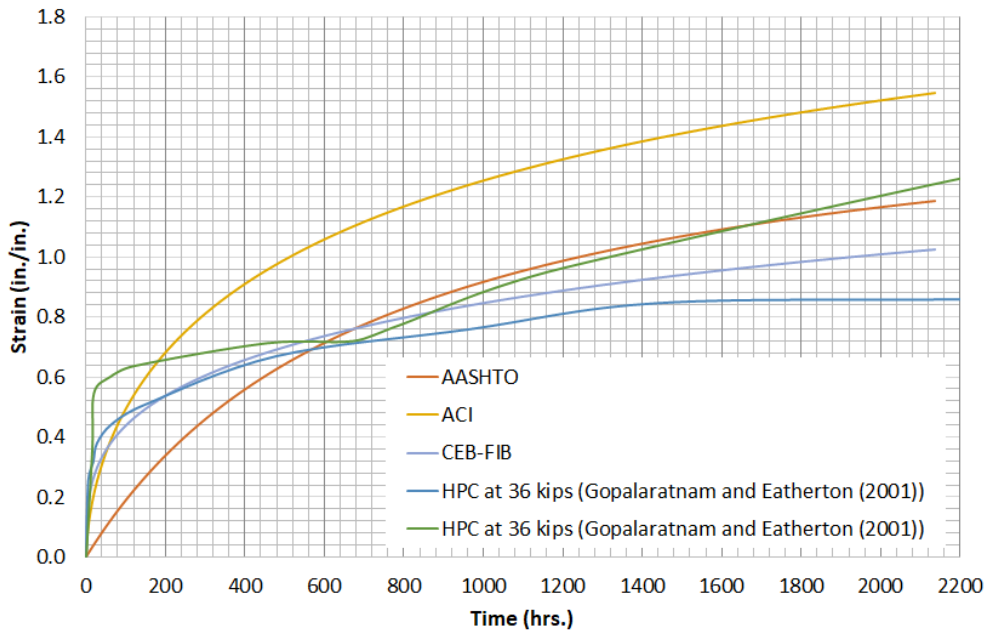
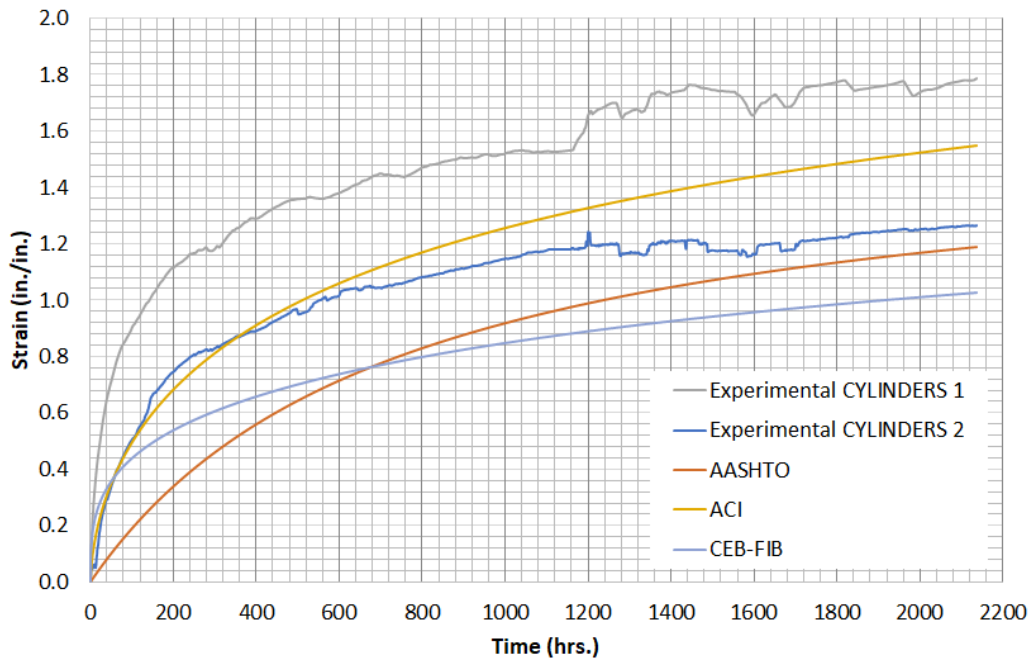


Figure 4-32. Comparison of the different creep models with the tested concrete cylinders

A sensitivity analysis was done to understand the effect of concrete creep on the long-term camber calculation as shown in Figure 4-33. Multiplying the AASHTO creep coefficient by a factor ranged

from 1.1 to 1.5 changes 90-day camber prediction by about 4% to 18%, on average for the suite of 189 bridge girders.

An analysis of the current MoDOT camber calculation compared to the measured camber growth for 33 girders with a later camber measurement before hauling is presented in Figure 4-34. The current analysis under-predicted the camber growth by about 12%. Another analysis was done using the current MoDOT calculation method to evaluate the difference in the long-term camber prediction when increasing the creep coefficient by 20% (see Figure 4-35). The trend line slope is higher than the current MoDOT calculation trend line slope by about 5.5%. It appears that changing the creep coefficient causes a significant change in the long-term camber calculations.

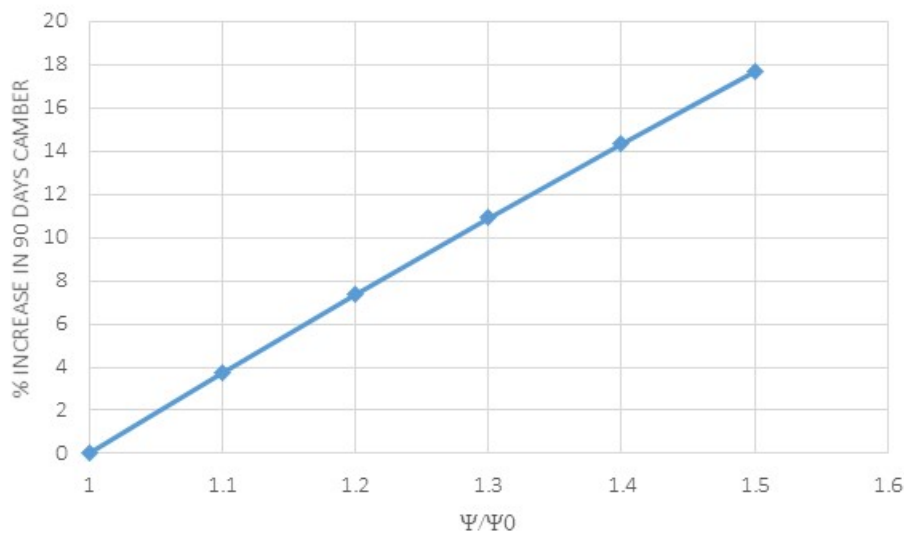


Figure 4-33. Change in 90-day camber due to the creep coefficient

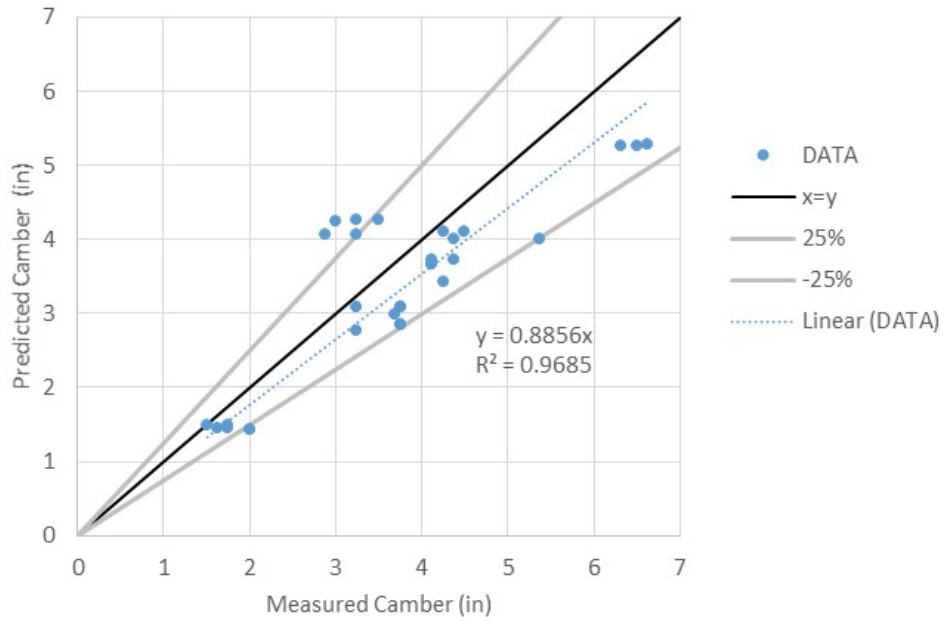


Figure 4-34. Camber prediction at later time using the current MoDOT method

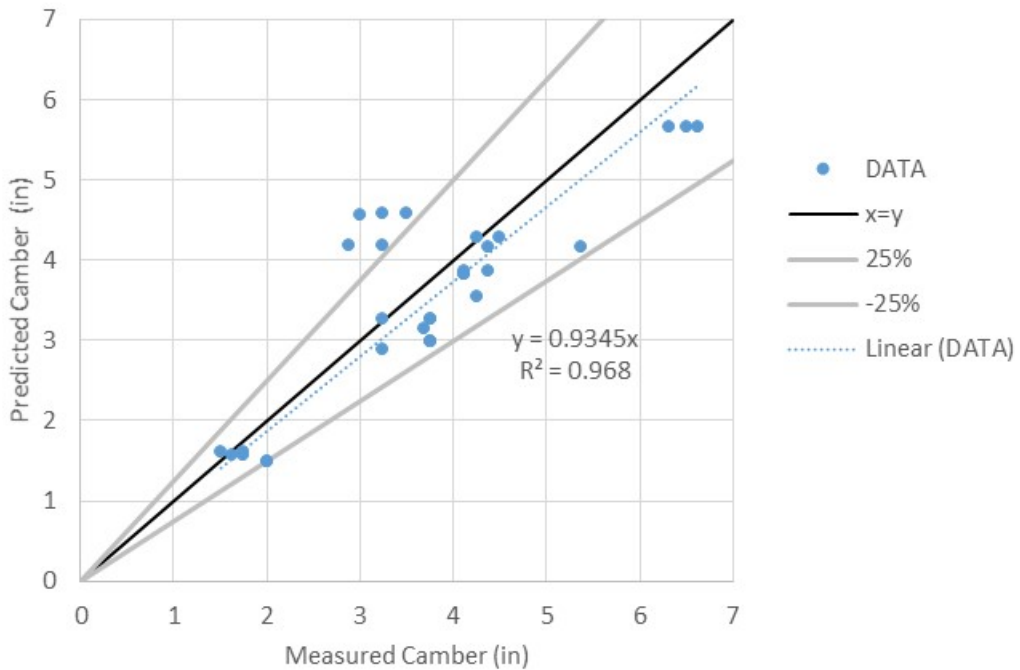


Figure 4-35. Camber prediction at later time when increasing the creep coefficient by 20%

4.11 *Effect of Concrete Shrinkage*

Drying shrinkage is the contraction in the concrete in time caused by moisture loss from drying concrete. A sensitivity analysis was completed to study the influence of concrete shrinkage on the long-term camber calculation (Figure 4-36). Changing ($\varepsilon/\varepsilon_0$) from 1.2 to 2 changes 90-day camber prediction by about 1% to 6%.

An analysis was done to evaluate the difference in the camber prediction when increasing the shrinkage strain by 50% (see Figure 4-37). The trend line slope is lower than the current MoDOT calculation trend line slope by about 1.4%. It appears that changing the shrinkage causes an insignificant change in the long-term camber calculations.

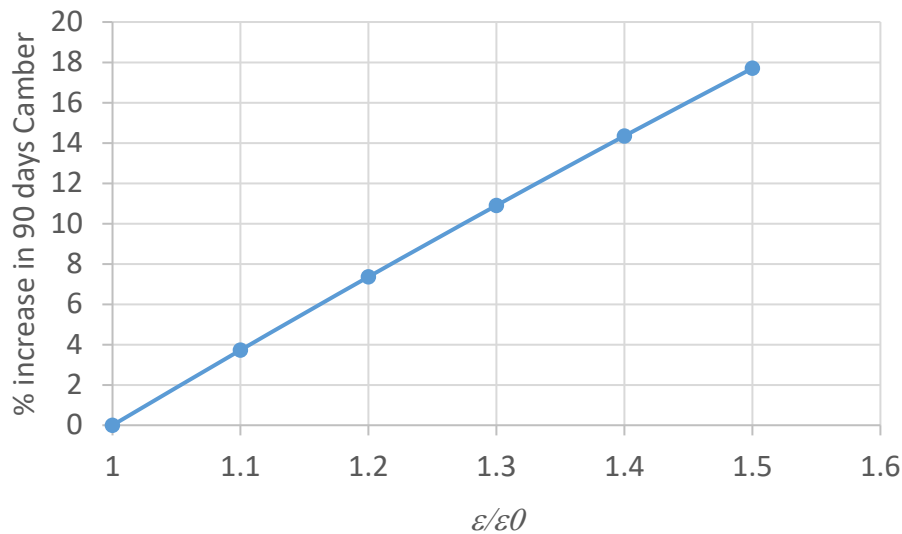


Figure 4-36. Change in 90-day camber due to shrinkage strain

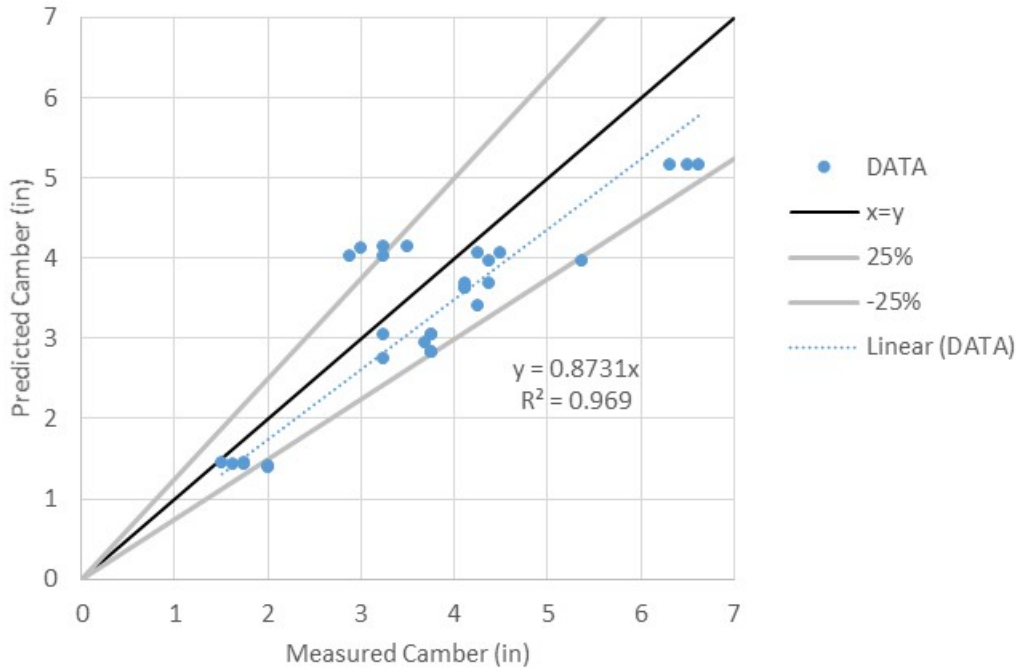


Figure 4-37. Camber prediction at later times when increasing the shrinkage strain by 50%

4.12 *Effect of Humidity*

Relative humidity plays an important role in the creep of concrete. The current MoDOT calculation considers the relative humidity of 70%. However, it changes from day to day throughout the year. To understand the significance of this factor, a sensitivity analysis was done by considering the relative humidity as 50% (see Figure 4-38). The trend line slope is higher than the existing MoDOT calculation trend line slope by about 3.4%. It appears that changing the relative humidity causes a minor change in the long-term camber calculations.

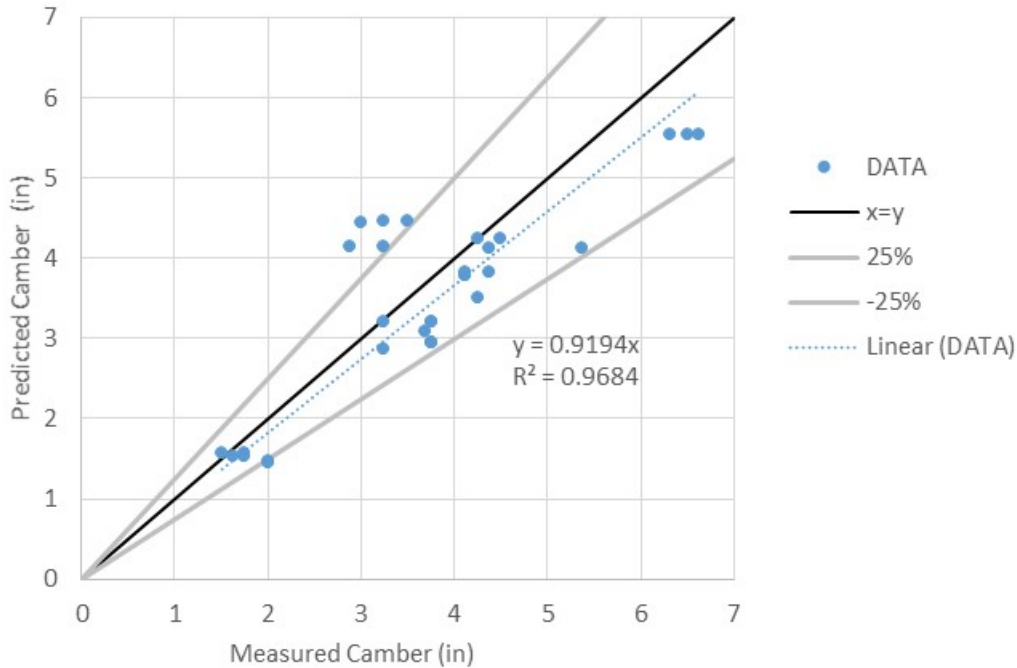


Figure 4-38. Camber prediction at later times when using relative humidity as 50%

4.13 *Effect of the Long-Term Prediction Method*

This section presents a comparison between three existing techniques for predicting the long-term camber. These methods are the AASHTO discrete time-step approach (currently used by MoDOT), approximate time-step approach by Stallings et al. (2003) using the ACI Committee 209 (1997) creep equations, and the Naaman (2012) approach using the ACI Committee 209 (1997) creep equations.

Figure 4-39 and Figure 4-40 show a comparison of the approaches for the two bridges that were monitored. For the Bridge #1, the camber growth after 200 days is about 2.68 in. using AASHTO discrete time-step approach. The Naaman approach (1.15 in.) is about 57% lower, and the Stalling approach (3.6 in.) is about 35% higher. For Bridge #2, the camber growth is about 2.62 in using

AASHTO. The Naaman approach (0.96 in.) is about 63% lower, and the Stalling approach (2.06 in.) is about 21% lower.

The measured camber growth for both bridges is compared to the predictions. The Bridge #1 girder cambers at 17 days are about 38% higher than the Naaman approach, and about 40% lower than the AASHTO approach; however, the Bridge #2 camber growth after 10 days was only 25% lower than the AASHTO approach.

Figure 4-41 and Figure 4-42 show this comparison on the two bridges that were monitored by Gopalaratnam and Eatherton (2001). For the shorter span, the camber growth after 40 days is about 0.17 in. using AASHTO, about 70% higher than the measured value (0.1 in.), which is 30% lower than it is using the Naaman approach (0.132 in.). For the longer span, the measured camber growth is about 0.55, which is about 22% lower than using AASHTO (0.67 in.), and about 10% higher than it is using the Naaman approach (0.5 in.).

Another analysis was done to evaluate the difference in the camber growth prediction when using different approaches for the suite of bridge girders in this study (see Figure 4-43 to Figure 4-45). The AASHTO approach and Naaman method show underprediction of the camber with trendline slopes of 0.89 and 0.78. The Stalling method showed over-prediction with a trendline slope of 1.0692. Given that there is still possible error in the camber measurement as described in Section 3.2.1, and better prediction for the bridges with field measurement in this study, it is recommended that the AASHTO discrete time- step approach continue to be used for the prediction of long-term camber.

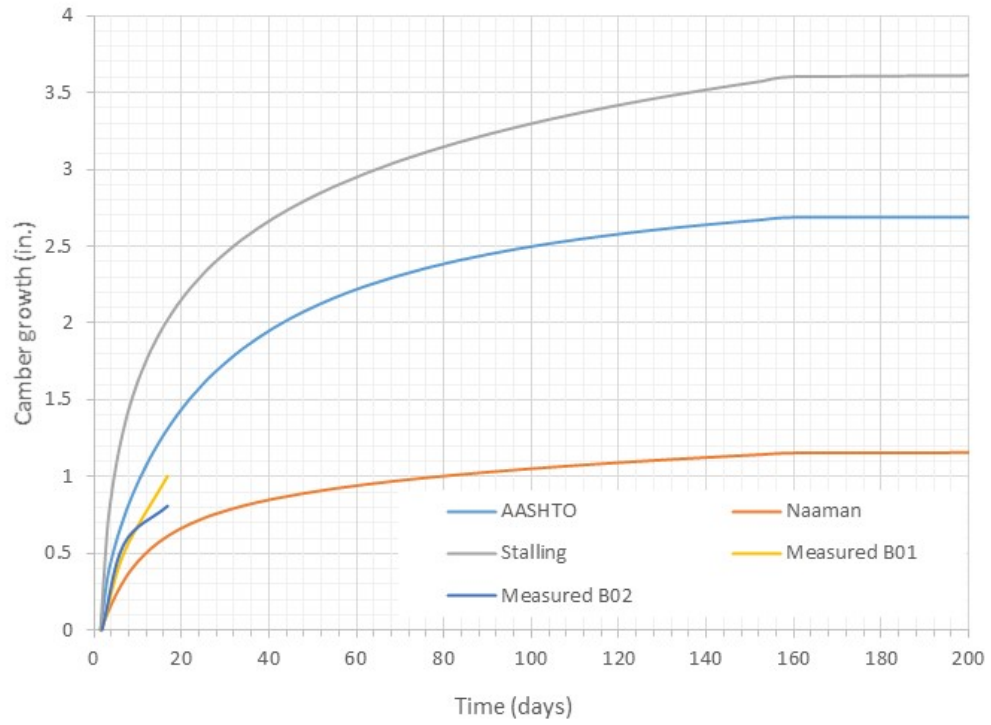


Figure 4-39. Time-dependent camber growth prediction vs. measured for Bridge #1

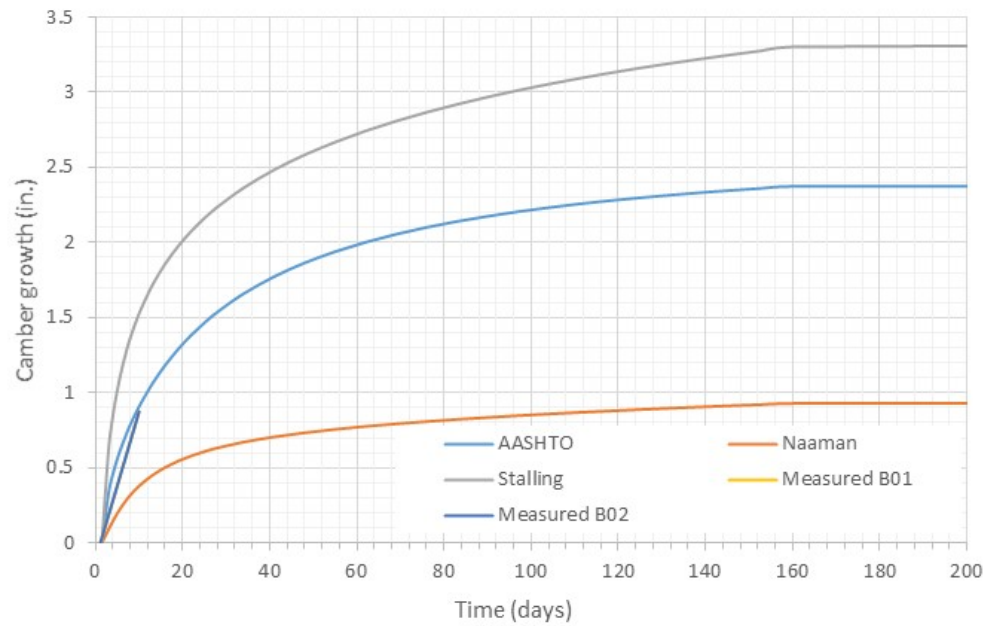


Figure 4-40. Time-dependent camber growth prediction vs. measured for Bridge #2

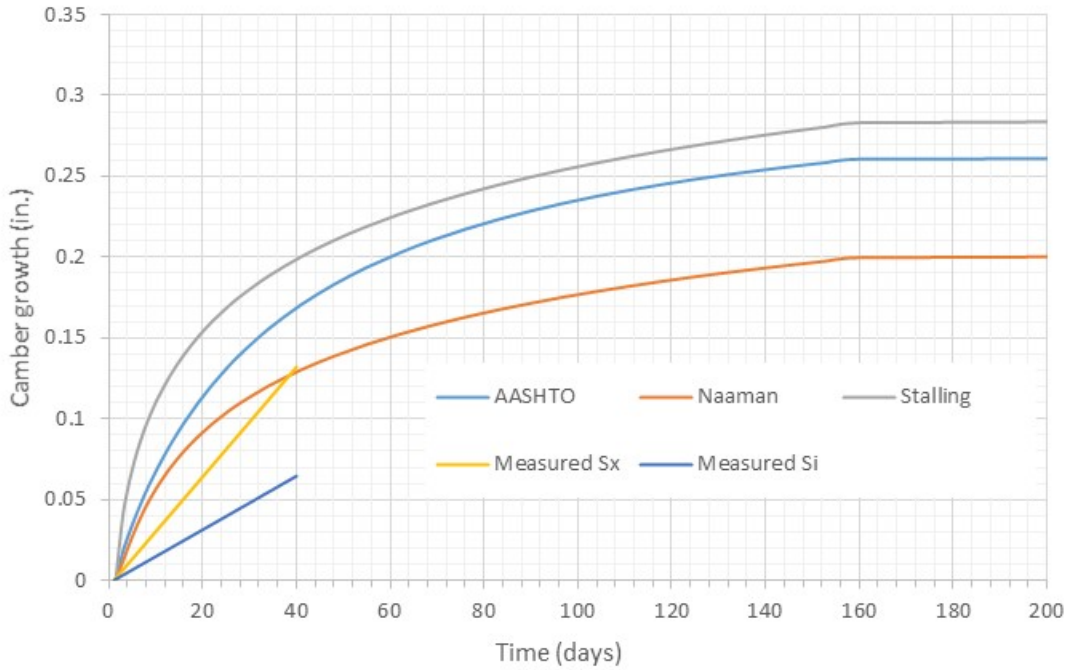


Figure 4-41. Time-dependent camber growth prediction vs. measured for bridge monitored by Gopalaratnam and Eatherton (2001) (shorter span)

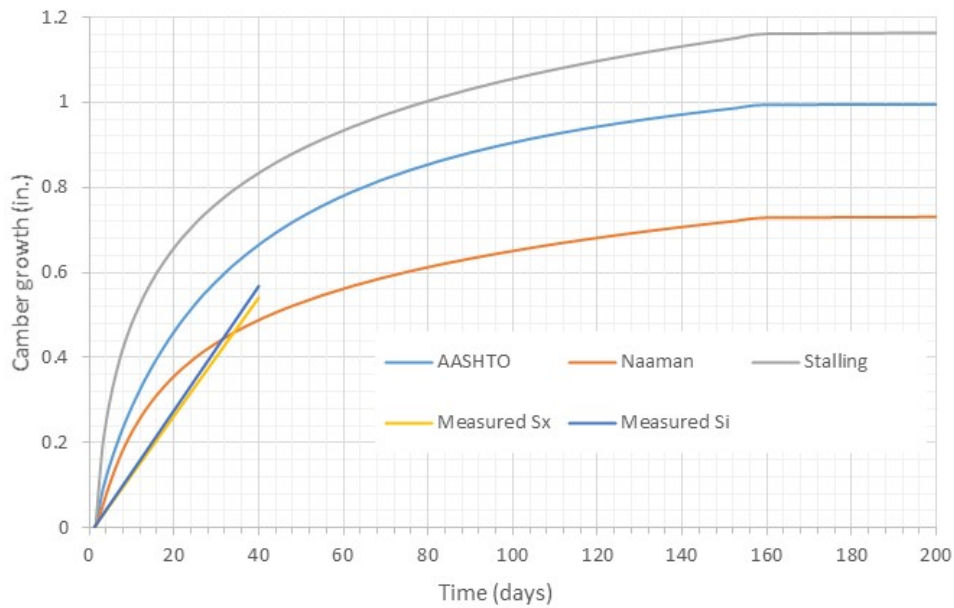


Figure 4-42. Time-dependent camber growth prediction vs. measured for bridge monitored by Gopalaratnam and Eatherton (2001) (longer span)

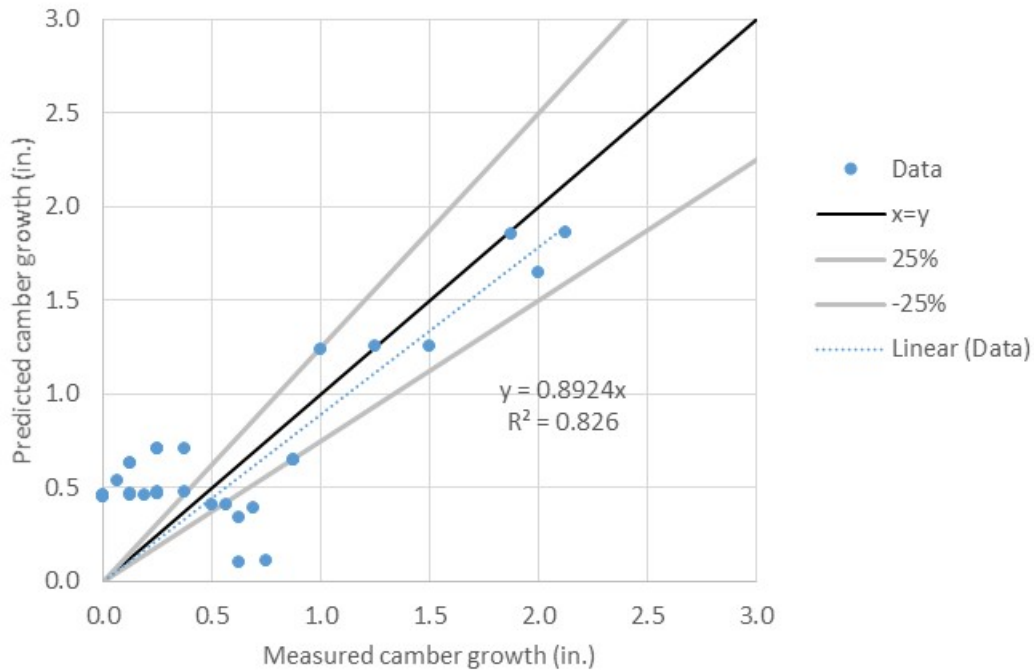


Figure 4-43. Camber growth prediction vs. measured when using the AASHTO approach

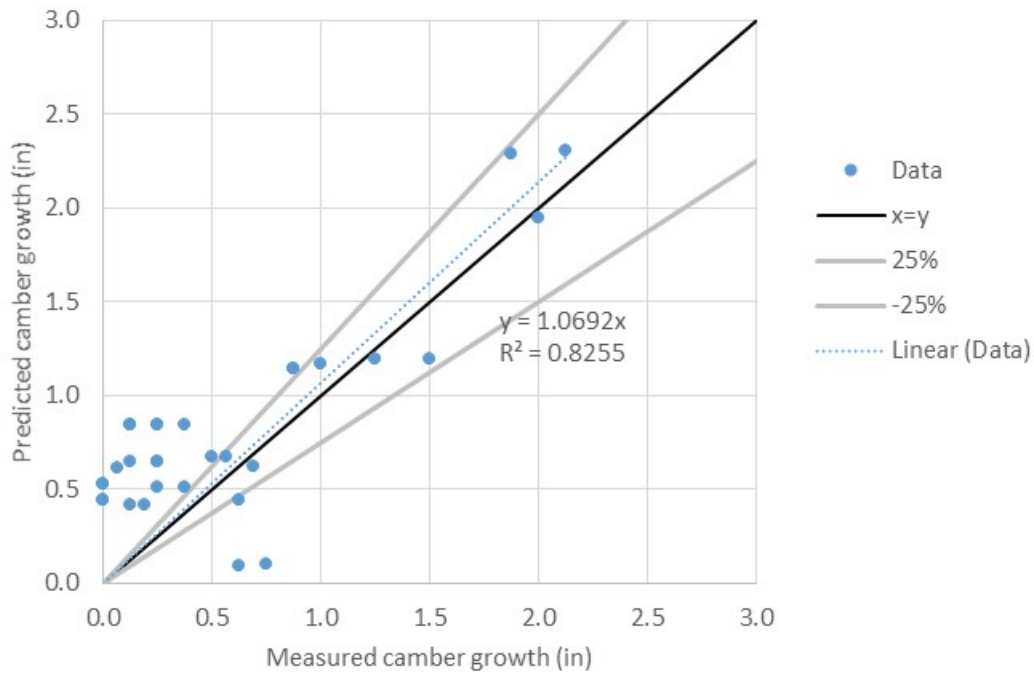


Figure 4-44. Camber growth prediction vs. measured when using the Stalling approach with default ACI parameters

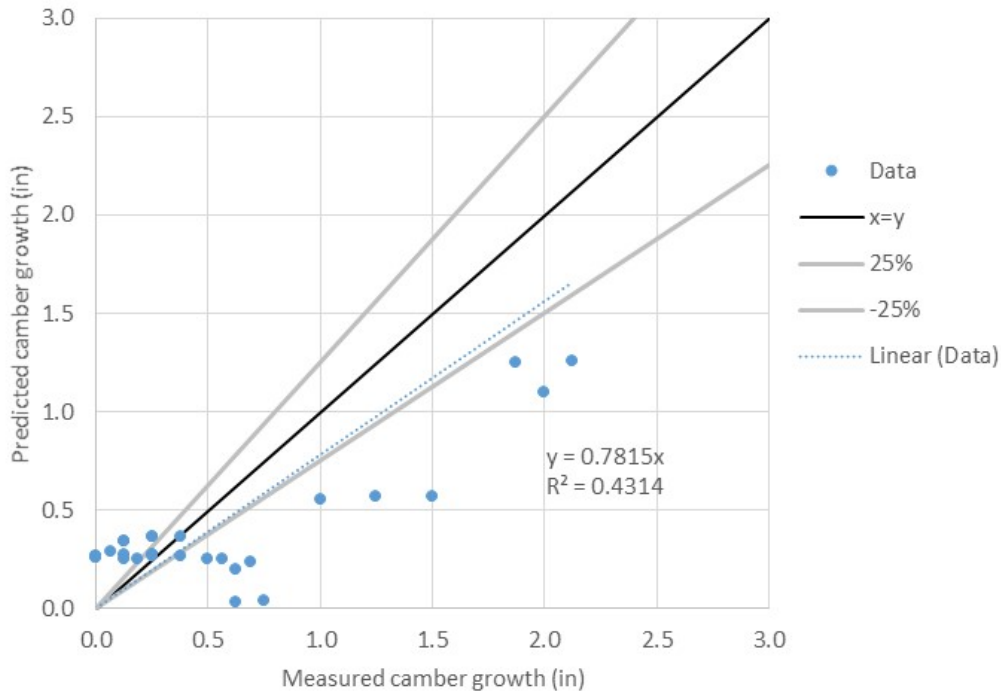


Figure 4-45. Camber prediction when using the Naaman approach with ACI creep equation

4.14 *Conclusions and Recommendations*

A systematic investigation at the parameters affecting the accuracy of the initial and long-term camber predictions was undertaken. The following conclusions are made based on the analyses:

- An evaluation of the current MoDOT camber prediction method found that the current method under predicts the initial camber by about 23%.
- The method of camber measurement is critical to the accuracy of the camber measurement. The current heavy Kevlar string line used by Plant #2 produced a line sag of 0.56 in. under a 45 lb. pull force for a 100 ft. girder. If the camber measurement is corrected for possible sag in the string line, then the under-prediction of initial camber using the current MoDOT method is reduced to 4%.

- Consistency of the camber measurement is also important. Plant #2 had a more consistent measurement method and less variability than Plant #1.
- The length of the overhang (distance past temporary supports) affects camber. A change in overhang length from 0 ft. to 4 ft. can cause an average change in camber of about 20% for the girder data set. Analysis equations in PGSuper can be used to include the effect of overhang in the initial camber. In addition, the location of temporary supports should be specified and be consistent to ensure improved camber predictions.
- Actual concrete strength at transfer often exceeds the design concrete strength at transfer. The average initial compressive strength of the field bridges was 8.58 ± 1.17 ksi, about 32% higher than the design strength (6.5 ksi).
- The increased compressive strength affects the modulus of the concrete and thereby the calculated camber. Using the measured compressive strength, the trendline slope of the measured to predicted camber decreases by 10%.
- Equations used to calculate concrete modulus from concrete compressive strength were evaluated. Using the AASHTO LRFD 5.4.2.3.2 (2012) equations vs. the ACI Committee 209 (1997) changed the camber by only 4%.
- Both elevated temperatures during curing and daily temperature changes affect camber. Increased temperatures during curing can temporarily reduce prestress forces and reduce camber by about 12%. Daily temperature changes cause a thermal gradient in the girder and can increase camber by 25% with a 25 °F temperature change.

- Variability in initial prestress force, concrete density, type of section property used (gross vs. transformed) and strand eccentricity results in a change of camber of less than approximately 5%.
- The current AASHTO discrete time-step approach can predict the long-term camber.

Based on the analysis of camber prediction methods and comparison to Missouri bridge data the following recommendations are made:

- Procedures and tolerances for the measurement of camber at prestress girder plants are needed.
- The length of the overhang (distance past temporary supports) needs to be included in the camber analysis. The equation used in PGSuper to account for actual overhang used in the precast storage yard is recommended for camber predictions.
- While concrete compressive strength (and related modulus) affects camber, it is not possible to predict the actual strength beforehand. Therefore, design initial concrete strength can still be used.
- The effect of temperature should be considered in the camber predictions. In order to mitigate the effect of temperature, camber can be measured at least 72 hours after form release, and in the morning (Tadros 2015).
- Other factors affect camber to a lesser degree (initial prestress force, concrete density, type of section property used (gross vs. transformed) and strand eccentricity) and need not be modified in predicting camber.

Using the correction for sag using the Kevlar string line with a pull force of 25 lbs., including the overhang length equal to the location of the lifting loops, and using measured concrete strength at release, the comparison of the measured to predicted camber is shown in Figure 4-46. The camber is under-predicted by only 10% on average. If only girders from Plant #2 are considered, then the variability of the data is also reduced with most predictions within 25% error. Use of the design initial concrete strength (which is lower than the actual strength and thereby increases the predicted camber) yields a predicted camber on average only 4% less than the measured camber.

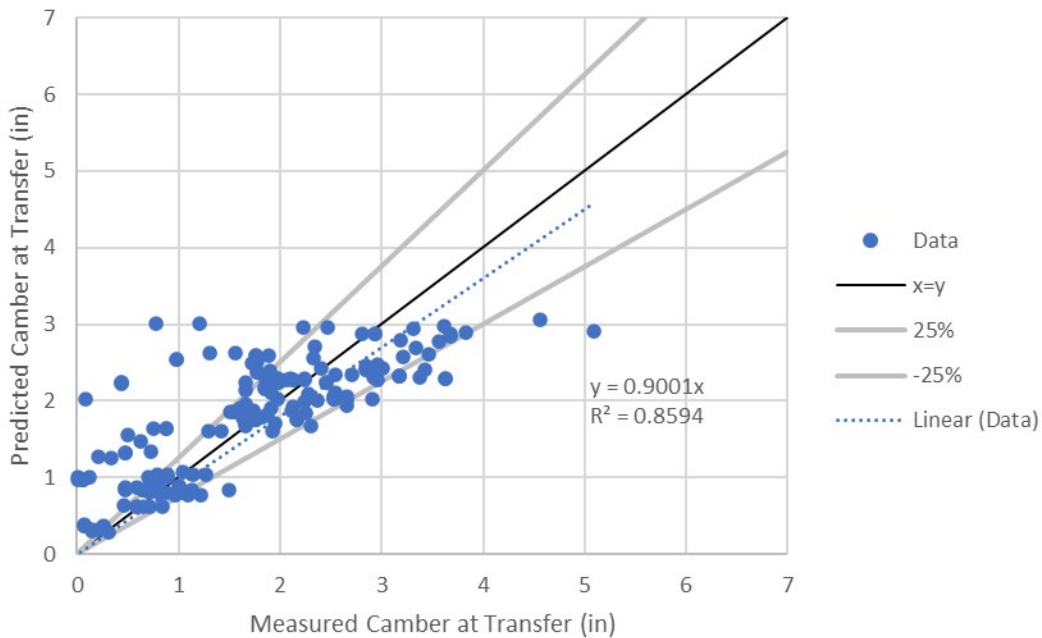


Figure 4-46. Predicted to measured camber with correction for sag in measurement line, overhang length, and actual concrete strength

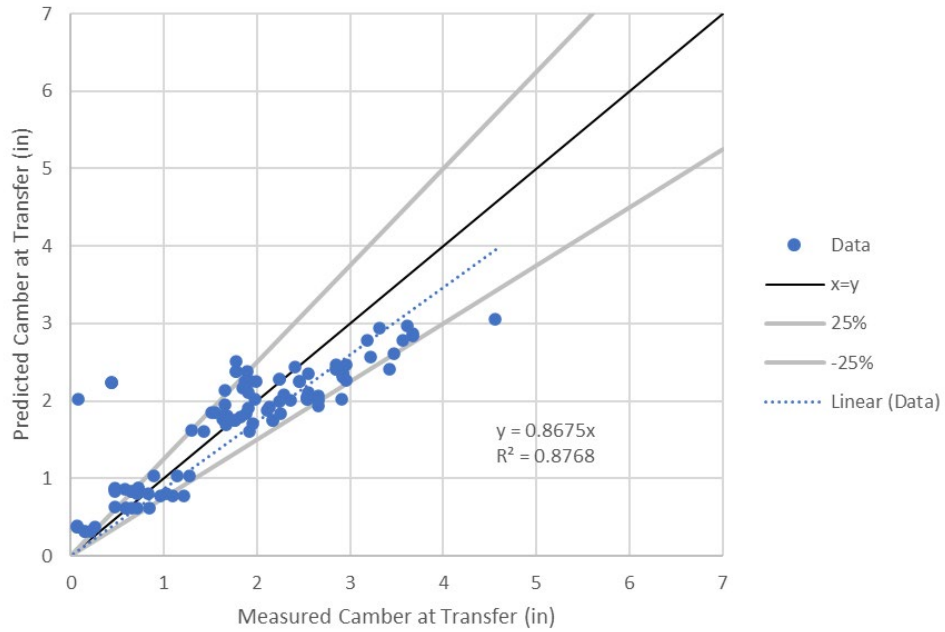


Figure 4-47. Predicted to measured camber with correction for sag in measurement line, overhang length, and actual concrete strength for only Plant #2 girders

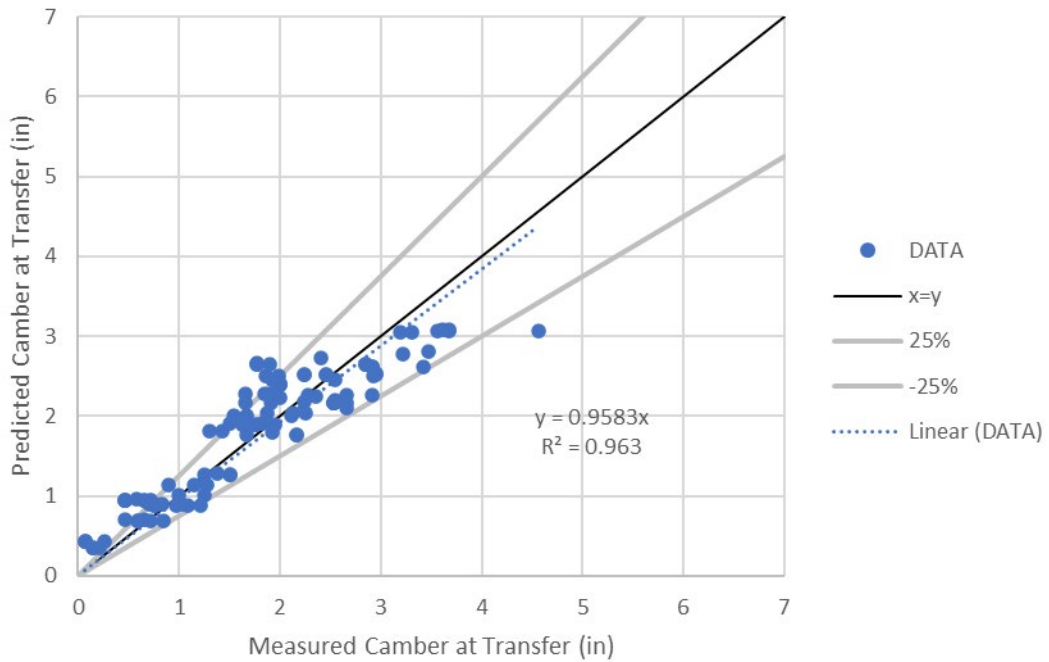


Figure 4-48. Predicted to measured camber with correction for sag in measurement line, overhang length, and design concrete strength for only Plant #2 girders

CHAPTER 5: PROPOSED CAMBER PREDICTION

This chapter presents a proposed approach to predict the prestressed girder camber. The main changes in the approach compared to the current MoDOT method are:

- Incremental time-step approach. Rather than determining camber at transfer, 7 days, and 90 days, camber can be determined at any point in time.
- Include effect of overhang length on camber.
- Additional options to include the effects of prestress loss due to elevated concrete temperatures during curing and daily temperature effects on camber.

5.1 *Calculation of Deflection and Camber*

Deflection and camber calculations shall consider all internal loads (i.e., prestressing, concrete creep, and shrinkage) and external loads such as dead loads, superimposed dead load, and live loads.

Camber is an upward displacement caused by movement due to prestressing forces. Deflection is a downward displacement due to external loads. Therefore, both camber and deflection shall be considered in making an appropriate adjustment for final profile grade on the bridge.

5.1.1 *Initial Camber at Transfer at Midspan*

Total initial camber at transfer due to self-weight of girder and prestressing forces shall be determined as:

$$\Delta_{IC} = -\Delta_{g1i} + \Delta_{g2i} + \Delta_{HS-j} + \Delta_{SS-j} \quad 5-1$$

where:

Δ_{IC} = initial camber at transfer,

Δ_{g1i} = deflection due to self-weight from support to end of girder,

Δ_{g2i} = deflection due to self-weight from support to girder midspan,

Δ_{SS-j} = camber due to prestressing straight strands, defined in 5.1.5,

Δ_{HS-j} = camber due to prestressing harped strands, defined in 5.1.5.

Note: Positive and negative values indicate downward and upward displacements, respectively.

5.1.2 Camber at Midspan After Strand Release

This section presents the long-term camber or the camber growth over time, while the girder is at the precast plant (after strand release and before hauling). The time variation of camber can be calculated as following:

$$\Delta_t = (\Delta_{g2} + \Delta_{ps1} + \Delta_{CR1t} + \Delta_{l1t})_{center} + (\Delta_{g1} + \Delta_{ps2} + \Delta_{CR2t} + \Delta_{l2t})_{overhang} \quad 5-2$$

$$\Delta_{ps1} = \Delta_{HS-j} + \Delta_{SS-j} \quad 5-3$$

$$\Delta_{ps2} = \Delta_{HS-j} + \Delta_{SS-j} - \Delta_{ps1} \quad 5-4$$

$$\Delta_{l1t} = \Delta_{ps1} * \frac{Losses}{f_{pj}} \quad 5-5$$

$$\Delta_{l2t} = \Delta_{ps2} * \frac{Losses}{f_{pj}} \quad 5-6$$

where:

Δ_t = camber at time t after strand release with creep,

Δ_{CRxt} = time-dependent camber due to creep at time t days, see 5.1.7,

Δ_{l1t} = time-dependent camber due to prestress losses (at center),

Δ_{l2t} = time-dependent camber due to prestress losses (at girder ends),

Note: Camber is typically calculated 7 days after strand release to allow sufficient time for inspection. Camber is also typically calculated at 90 days to estimate camber before hauling.

5.1.3 Final Camber at Midspan After Slab is Poured

Total deformation after the slab is poured can be determined as the sum of theoretical camber of girder after erection and deflections due to slab and concentrated loads (haunch, diaphragms, etc.) before composite action between slab and girder.

$$\Delta_{FC} = \Delta_t + \Delta_s + \sum \Delta_C + \Delta_{gh} \quad 5-7$$

where:

Δ_{FC} = final camber after slab is poured,

Δ_s = deflection due to weight of slab,

$\sum \Delta_C$ = deflection due to concentrated loads (haunch, diaphragms, etc.),

Δ_{gh} = change in girder self-weight deflection when changing the support locations (i.e., change from temporary support location to bearing pad support). See 5.1.6

5.1.4 Final Camber Along Span Length

Deformations along the span length can be approximately determined as a product of final camber at midspan times correction factors.

$$\Delta_{0.1} = 0.3140 \Delta_{FC} \text{ at span fraction of 0.10,}$$

$$\Delta_{0.2} = 0.5930 \Delta_{FC} \text{ at span fraction of 0.20,}$$

$$\Delta_{0.25} = 0.7125 \Delta_{FC} \text{ at span fraction of 0.25,}$$

$$\Delta_{0.3} = 0.8130 \Delta_{FC} \text{ at span fraction of 0.30,}$$

$$\Delta_{0.4} = 0.9520 \Delta_{FC} \text{ at span fraction of 0.40,}$$

$$\Delta_{0.5} = 1.0000 \Delta_{FC} \text{ at span fraction of 0.50.}$$

5.1.5 Calculation of Camber (Upward) Using Transformed Properties

Camber at midspan due to strand forces is determined as noted below:

For straight strands (there may be multiple groups as determined by debonding lengths),

$$\Delta_{SS} = \Delta_{SS-j} + \Delta_{SS-l} \quad 5-8$$

where:

$$\Delta_{SS-j} = - \frac{F_{1-j} e_1}{8E_{ci} I_{tri}} (L^2 - 4l_0^2) \quad 5-9$$

$$\Delta_{SS-l} = \Delta_{SS-j} \frac{\text{Initial Loss}}{f_{pj}} \quad 5-10$$

where:

F_{1-j} = total prestressing force of straight strand group just prior to transfer with initial relaxation losses (kips),

L = end to end prestressed girder length (in.),

E_{ci} = initial concrete modulus of elasticity (ksi),

I_{tri} = transformed moment of inertia of non-composite section (in⁴),

l_0 = debonded length of prestressed strands (in.),

e_1 = eccentricity between centroid of straight strand group (CSS) and center of gravity of transformed non-composite section (CGB) as shown in Figure below (in.),

f_{pj} = prestressing force in the strand just prior to transfer (ksi),

Initial Loss = summation of the time dependent losses. Losses include relaxation, creep, and shrinkage, but exclude elastic shortening. See section 5.1.8 for calculation of time dependent losses at time t (usually 7 or 90 days).

Note: Gross properties may be used to calculate losses and is consistent with AASHTO LRFD

5.9.3.4.

For two-point harped strands,

$$\Delta_{HS} = \Delta_{HS-j} + \Delta_{HS-l} \quad 5-11$$

where:

$$\Delta_{HS-j} = -\frac{F_{2-j}e_2L^2}{8E_{ci}I_{tri}} + \frac{F_{2-j}(e_2+e_3)a_h^2}{6E_{ci}I_{tri}} \quad 5-12$$

$$\Delta_{HS-l} = \Delta_{HS-j} \frac{\text{Initial Loss}}{f_{pj}} \quad 5-13$$

$$a_h = (L - b)/2 \quad 5-14$$

$$\Delta_l = \Delta_{SS-l} + \Delta_{HS-l} \quad 5-15$$

where:

F_{2-j} = total prestressing force of harped strand group just prior to transfer with initial relaxation losses, (kips),

b = length between harped points, (in.),

a_h = distance from end of girder to harped point,

e_2 = eccentricity between centroid of harped strands (CHS) and center of gravity of transformed non-composite section (CGB) at midspan as shown in Figure below, (in.),

e_3 = eccentricity between centroid of harped strands (CHS) and center of gravity of transformed non-composite section (CGB) at the end of girder as shown in Figure below, (in.).

Δ_l = Camber caused by prestress losses (in.).

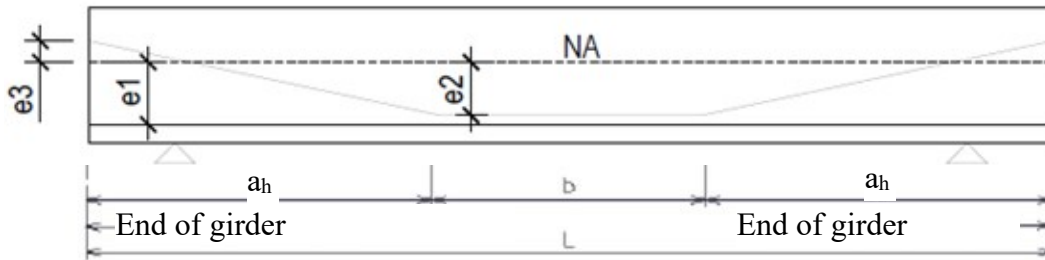


Figure 5-1. Girder details displaying the eccentricities and distances used in camber computations

5.1.6 Calculations of Deflections (Downward)

Deflections at midspan due to dead loads are determined as the following:

For self-weight of girder,

$$\Delta_{g1} = \frac{w_g \cdot a}{24E_c(t)I'_{tr}} [3a^2(a + 2L_s) - L_s^3] \quad 5-16$$

$$\Delta_{g2} = \frac{5w_g L_s^4}{384E_c(t)I'_{tr}} - \frac{w_g a^2 L_s^2}{16E_c(t)I'_{tr}} \quad 5-17$$

$$\Delta_{gh} = \Delta_{g3} - \Delta_{g1} - \Delta_{g2} \quad 5-18$$

$$\Delta_{g3} = \frac{5w_g L^4}{384E_c(t)I'_{tr}} \quad 5-19$$

where:

Δ_{g3} = deflection due to self-weight from end to end of girder,

Δ_{g1} = deflection due to self-weight from support to end of girder,

Δ_{g2} = deflection due to self-weight from support to girder midspan,

W_g = uniform load due to self-weight of girder (kip/in.),

E_c = final concrete modulus of elasticity based on f'_c (ksi),

L_s = length between temporary supports, (in.) as shown in Figure 5-2,

a = overhang length, (in.) as shown in Figure 5-2,

I'_{tr} = moment of inertia of transformed non-composite section based on E_c (in⁴),

L = length of the girder = $L_s + 2a$, (in.) as shown in Figure 5-2.

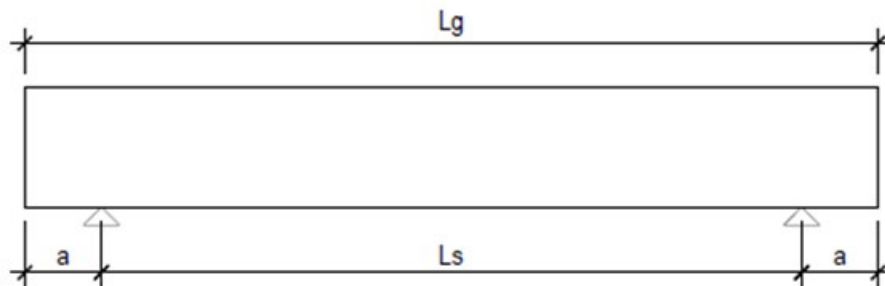


Figure 5-2. Girder dimensions

For self-weight of slab,

$$\Delta_s = \frac{5w_s L'^4}{384E_c I'_{tr}} \quad 5-20$$

where:

w_s = uniform load due to self-weight of slab and haunch (the mid span haunch thickness is used to calculate the haunch distributed load), (kip/in.),

L' = length between permanent supports of the prestressed girder, (in.),

Weight of additional slab haunch may be treated as uniform or concentrated load as appropriate.

Diaphragm weight should be treated as concentrated load.

For one concentrated load at midspan,

$$\Delta_d = \frac{P_d L^3}{48E_c I'_{tr}} \quad 5-21$$

For two equal concentrated loads,

$$\Delta_{as} = \frac{2P_{as}x}{48E_c I'_{tr}} (3L^2 - 4x^2) \quad 5-22$$

where:

P_d = concentrated load due to diaphragm (kips),

x = distance from the centerline of bearing pad to the applied load, P (in.),

P_{as} = concentrated load due to additional slab haunch (the thickness used is the difference in haunch thickness between the end and center of the girder.) (kips),

Δ_{as} = additional deflection due to additional slab haunch (kips),

Δ_d = deflection due to diaphragm weight (kips).

5.1.7 Creep Coefficient

Research has indicated that high strength concrete (HSC) undergoes less ultimate creep and shrinkage than conventional concrete. Creep is a time-dependent phenomenon in which deformation increases under a constant stress. Creep coefficient is a ratio of creep strain over elastic strain, and it can be estimated as follows per AASHTO LRFD 5.4.2.3.2 (2012):

$$\Psi(t, t_i) = 1.9k_s k_{hc} k_f k_{td} t_i^{-0.118} \quad 5-23$$

$$k_s = 1.45 - 0.13(v/s) \geq 1.0 \quad 5-24$$

$$k_{hc} = 1.56 - 0.008H \quad 5-25$$

$$k_f = 5/(1 + f'_{ci}) \quad 5-26$$

$$k_{td} = t / \left(\frac{12(100 - 4f'_{ci})}{f'_{ci} + 20} + t \right) \quad 5-27$$

where:

Ψ = creep coefficient,

H = 70, average annual ambient relative humidity,

t = maturity of concrete, (days), may use 7 days for camber design after strand release, use 90 days for camber design after erection,

t_i = age of concrete when a load is initially applied, (days) use 0.75 days for camber design,

v/s = volume-to-surface area ratio, (in.),

f'_{ci} = initial girder concrete compressive strength, (ksi).

k_s = volume to surface ratio correction factor,

k_{hc} = creep humidity correction factor,

k_f = concrete strength factor,

k_{td} = time development factor.

Using the creep coefficient, the change in deflection due to creep at any time t can be determined as:

$$\Delta_{CR1t} = (\Delta_{g2i} + \Delta_{ps1}) \Psi(t, t_i) + (\Delta_l)_1 0.7 \Psi(t, t_i) \quad 5-28$$

$$\Delta_{CR2t} = (\Delta_{g1i} + \Delta_{ps2}) \Psi(t, t_i) + (\Delta_l)_2 0.7 \Psi(t, t_i) \quad 5-29$$

5.1.8 Prestress Losses

$$Losses = \Delta f_{pSR} + \Delta f_{pCR} + \Delta f_{pR} + \Delta f_{pSD} + \Delta f_{pCD} + \Delta f_{pSS} \quad 5-30$$

Δf_{pSR} = prestress loss due to shrinkage of girder concrete between transfer and deck placement (ksi),

Δf_{pCR} = prestress loss due to creep of girder concrete between transfer and deck placement (ksi),

Δf_{pR} = prestress loss due to relaxation of prestressing strands (ksi),

Δf_{pSD} = prestress loss due to shrinkage of girder concrete between time of deck placement and final time (ksi),

Δf_{pCD} = prestress loss due to creep of girder concrete between time of deck placement and final time (ksi),

Δf_{pSS} = prestress gain due to shrinkage of deck in composite section (ksi).

5.1.9 Elastic Shortening

The loss due to elastic shortening in pretensioned members shall be taken as:

$$\Delta f_{pES} = \frac{E_p}{E_{ci}} f_{cgp} \quad 5-31$$

f_{cgp} = the concrete stress at the center of gravity of prestressing tendons due to the prestressing force immediately after transfer and the self-weight of the member at the section of maximum moment (ksi),

E_p = modulus of elasticity of prestressing steel (ksi),

E_{ci} = modulus of elasticity of concrete at transfer or, time of load application (ksi).

Note: This type of loss shall not be considered when using the transformed properties.

5.1.9.1 Relaxation Losses

A more accurate equation for prediction of relaxation loss between transfer and deck placement is given in Tadros et al. (2003):

$$\Delta f_{pR} = \frac{\log(24t)}{k'_L \log(24t_i)} K_{id} \left[1 - \frac{3(\Delta f_{pR} + \Delta f_{pR})}{f_{pj}} \right] \left[\frac{f_{pj}}{f_{py}} - 0.55 \right] f_{pj} \quad 5-32$$

where:

k'_L = factor accounting for type of steel, equal to 45 for low relaxation steel and 10 for stress relieved steel,

t = time in days between strand tensioning and deck placement,

K_{id} = transformed section coefficient that accounts for time-dependent interaction between concrete and bonded steel in the section being considered for time period between transfer and deck placement.

5.1.9.2 Shrinkage Losses of Girder

The prestress loss due to shrinkage of girder concrete between time of transfer and deck placement,

Δf_{pSR} , shall be determined as:

$$\Delta f_{pSR} = \varepsilon_{bid} E_p K_{id} \quad 5-33$$

in which:

$$\varepsilon_{bid} = -k_s k_{hs} k_f k_{td} * 0.48 * 10^{-3} \quad 5-34$$

$$K_{id} = \frac{1}{1 + \frac{E_p A_{ps}}{E_{ci} A_g} \left(1 + \frac{A_g e_{pg}^2}{I_g} \right) (1 + 0.7 \psi(t, t_i))} \quad 5-35$$

where:

ε_{bid} = concrete shrinkage strain of girder between the time of transfer and deck placement,

e_{pg} = eccentricity of prestressing force with respect to centroid of girder (in.); positive in common construction where it is below girder centroid,

$\psi(t, t_i)$ = girder creep coefficient at final time due to loading introduced at transfer as per section 5.1.7,

t = final age (days),

t_i = age at transfer (days),

k_s = volume to surface ratio correction factor as per section 5.1.7,

k_{hs} = shrinkage humidity correction factor, = $2.0 - 0.014H$,

k_f = concrete strength factor, = $5/(1+f'_{ci})$,

k_{td} = time development factor as per section 5.1.7.

5.1.9.3 Creep Losses of Girder

The prestress loss due to creep of girder concrete between time of transfer and deck placement,

Δf_{pCR} , shall be determined as:

$$\Delta f_{pCR} = E_p f_{cgp} \psi(t, t_i) K_{id} / E_{ci} \quad 5-36$$

5.1.9.4 Shrinkage Losses of Deck Concrete

The prestress loss due to shrinkage of girder concrete between time of deck placement and final

time, Δf_{pSD} , shall be determined as:

$$\Delta f_{pSD} = \varepsilon_{bdf} E_p K_{df} \quad 5-37$$

in which:

$$K_{df} = \frac{1}{1 + \frac{E_p A_{ps}}{E_{ci} A_c} \left(1 + \frac{A_c e_{pc}^2}{I_c} \right) (1 + 0.7 \psi(t_f, t_d))} \quad 5-38$$

where:

ϵ_{bdf} = shrinkage strain of girder between time of deck placement and final time,

K_{df} = transformed section coefficient that accounts for time-dependent interaction between concrete and bonded steel in the section being considered for time period between deck placement and final time,

e_{pc} = eccentricity of prestressing force with respect to centroid of composite section (in.), positive in typical construction where prestressing force is below centroid of section,

A_c = area of section calculated using the gross composite concrete section properties of the girder and the deck and the deck-to-girder modular ratio (in.²),

I_c = moment of inertia of section calculated using the gross composite concrete section properties of the girder and the deck and the deck-to girder modular ratio at service (in.⁴)

5.1.9.5 Creep Losses of Deck Concrete

The prestress loss due to creep of girder concrete between time of deck placement and final time,

Δf_{pSD} , shall be determined as:

$$\Delta f_{cdf} = \frac{\epsilon_{ddf} A_d E_{cd}}{1 + 0.7\psi(t_f, t_d)} \left(\frac{1}{A_c} + \frac{e_{pc} e_d}{I_c} \right) \quad 5-39$$

Δf_{cdf} = change in concrete stress at centroid of prestressing strands due to shrinkage of deck concrete (ksi),

ϵ_{ddf} = shrinkage strain of deck concrete between placement and final time,

A_d = area of deck concrete (in.²),

E_{cd} = modulus of elasticity of deck concrete (ksi),

e_d = eccentricity of deck with respect to the gross composite section, positive in typical construction where deck is above girder (in.),

$\psi(t_f, t_d)$ = creep coefficient of deck concrete at final time due to loading introduced shortly after deck placement.

5.1.10 Modulus of Elasticity

MoDOT currently uses the AASHTO formula for predicting the modulus of elasticity. In the proposed model, the AASHTO LRFD 5.4.2.4 equation is recommended for use:

$$E_c(t) = 33000k_1\gamma^{1.5}\sqrt{f'_c} \quad (\text{ksi}) \quad 5-40$$

where:

$E_c(t)$ = the time modulus of elasticity,

k_1 = correction factor, currently taken as 1.0,

γ = the concrete unit weight,

$f'_c(t)$ = the time compressive modulus.

5.1.11 Temperature Due to Concrete Curing

The prestress losses used in this approach are the same as MoDOT. However, the proposed model considers the losses caused by the increased temperature of the concrete during curing. The thermal increase during this stage causes the strands to relax. As a result, the girder camber is affected by these losses.

The influence of temperature impacts can be calculated according to the following:

$$\Delta f_p = E_p \mu_p \Delta T \quad 5-41$$

where:

μ_p = the thermal expansion coefficient of steel cable (8×10^{-6} strain / °F),

ΔT = the estimated change in temperature (assumed to be 60°F).

5.1.12 Change in Camber Due to Daily Temperature Variation

Differential heating during the day can result in extra camber in bridge girders.

The possible variation in camber in 12 hours can be estimated as (Nguyen et al. 2015):

$$\Delta_{camber} = \left(\frac{\alpha A_1}{h} \right) (T_{max} - T_{min}) \left(\frac{L^2}{8} \right) \quad 5-42$$

where:

T_{max} = maximum air temperature during the 24-hour period,

T_{min} = minimum air temperature during the 24-hour period,

α = coefficient of thermal conductivity $5.5 \times 10^{-6}/^\circ\text{F}$ ($9.9 \times 10^{-6}/^\circ\text{C}$),

A_1 = calibration factor, assumed to be 1.28,

L = length of the prestressed girder (in.),

h = the girder height (in.),

Δ_{camber} = camber variation due to temperature.

5.2 Camber Prediction Spreadsheet

This section presents guidelines for use of the spreadsheet for predicting camber-deflection history using the new methodology proposed in this study. This spreadsheet allows prediction of the camber-deflection history using the incremental time step approach. Input data like the girder type and geometries, the strands details and profile, the material properties and the debond length are indicated using yellow highlighted cells. The spreadsheet also provides the option to display the camber at transfer and at hauling.

5.2.1 Overview of the Spreadsheet

This section provides overview of the proposed spreadsheet. The details of each page will be discussed in the following subsections.

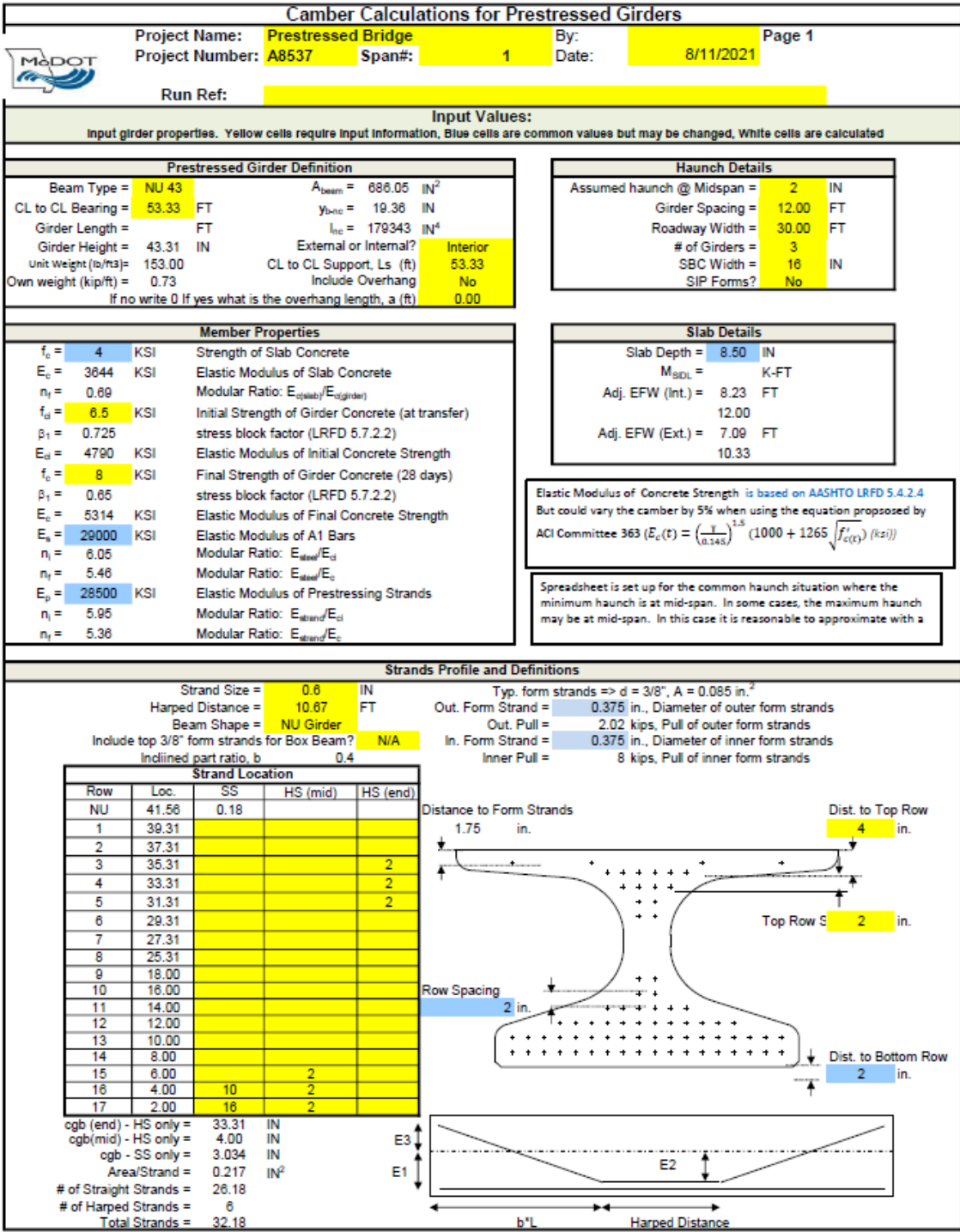


Figure 5-3. Proposed spreadsheet page 1

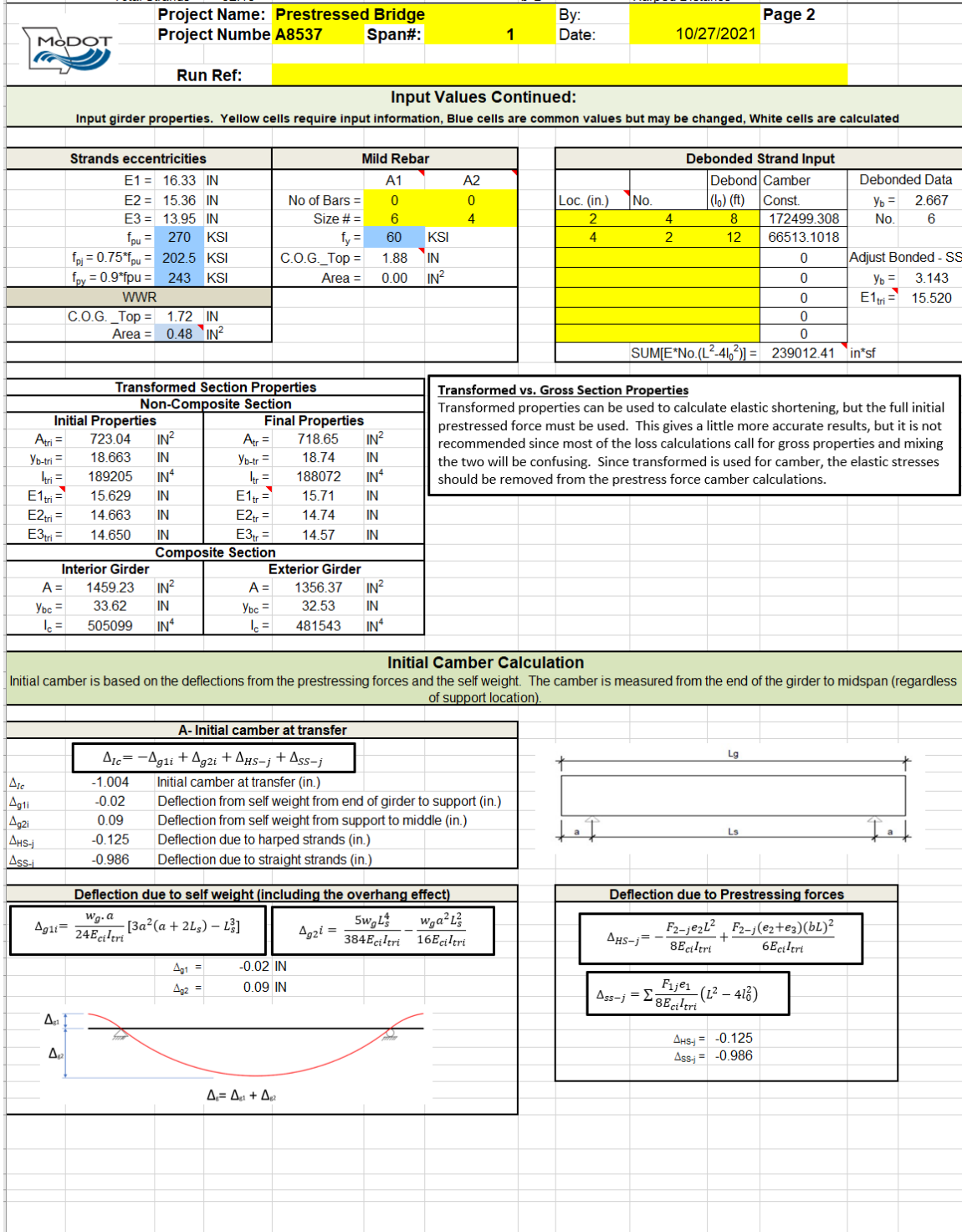


Figure 5-4. Proposed spreadsheet page 2


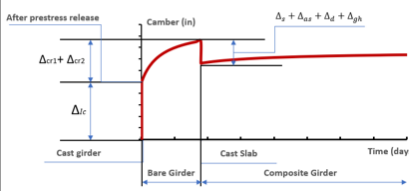
	Project Name: Prestressed Bridge	By:	Page 3																				
	Project Number: A8537 Span#: 1	Date: 10/27/2021																					
Run Ref:																							
Loss Estimation with time																							
The following describes the equations used in the estimation of camber with time. Estimation of camber with time includes the effect of losses. The losses in the concrete are grouped from time to deck placement, and after deck placement.																							
Prestress Losses Camber																							
$\Delta_{I1t} = \Delta_{ps1} * \frac{Losses}{f_{pj}}$		$\Delta_{I2t} = \Delta_{ps2} * \frac{Losses}{f_{pj}}$																					
$Losses = \Delta f_{pSR} + \Delta f_{pCR} + \Delta f_{pR} + \Delta f_{pSD} + \Delta f_{pCD} + \Delta f_{pSS}$																							
$\Delta_{I1t} = \text{camber due to prestressing losses at center (in)}$ $\Delta_{I2t} = \text{camber due to prestressing losses at end, (in)}$																							
LRFD 5.9.5.4.2 Losses: Time of Transfer to Time of Deck Placement																							
LRFD 5.9.5.2.3a Elastic Shortening		LRFD 5.9.5.4.2 Losses: creep and shrinkage of concrete																					
$\Delta f_{pES} = \frac{E_p}{E_c} f_{cgp}$		<table border="1"> <tr> <td>5.9.5.4.2a Shrinkage losses</td> <td>5.9.5.4.2b Creep losses</td> </tr> <tr> <td>$\Delta f_{pSR} = \epsilon_{bid} E_p K_{id}$</td> <td>$\Delta f_{pCR} = E_p f_{cgp} \Psi_{bid} K_{id} / E_{ci}$</td> </tr> <tr> <td>Humidity, H (%) 70</td> <td>Release time, ti (days) 1</td> </tr> <tr> <td colspan="2">Shrinkage strain (in/in), $\epsilon_{sh} = -K_s K_{hs} k_c k_{td} 0.48 * 10^{-3}$</td> </tr> <tr> <td colspan="2">Creep coefficient, $\Psi(t, t_i) = 1.9 K_s k_{hc} k_c k_{td} t^{-0.118}$</td> </tr> <tr> <td>V/s correction factor, ks = 1.45 - 0.13(v/s) >= 0.0</td> <td>1.05</td> </tr> <tr> <td>Creep humidity factor, khc = 1.56 - 0.008H</td> <td>1.00</td> </tr> <tr> <td>Shrinkage humidity factor, khs = 2.0 - 0.014H</td> <td>1.02</td> </tr> <tr> <td>Concrete strength factor, kf = 5/(1+fc)</td> <td>0.67</td> </tr> <tr> <td>Transformed section coefficient, K_{id}</td> <td>0.808</td> </tr> </table>		5.9.5.4.2a Shrinkage losses	5.9.5.4.2b Creep losses	$\Delta f_{pSR} = \epsilon_{bid} E_p K_{id}$	$\Delta f_{pCR} = E_p f_{cgp} \Psi_{bid} K_{id} / E_{ci}$	Humidity, H (%) 70	Release time, ti (days) 1	Shrinkage strain (in/in), $\epsilon_{sh} = -K_s K_{hs} k_c k_{td} 0.48 * 10^{-3}$		Creep coefficient, $\Psi(t, t_i) = 1.9 K_s k_{hc} k_c k_{td} t^{-0.118}$		V/s correction factor, ks = 1.45 - 0.13(v/s) >= 0.0	1.05	Creep humidity factor, khc = 1.56 - 0.008H	1.00	Shrinkage humidity factor, khs = 2.0 - 0.014H	1.02	Concrete strength factor, kf = 5/(1+fc)	0.67	Transformed section coefficient, K _{id}	0.808
5.9.5.4.2a Shrinkage losses	5.9.5.4.2b Creep losses																						
$\Delta f_{pSR} = \epsilon_{bid} E_p K_{id}$	$\Delta f_{pCR} = E_p f_{cgp} \Psi_{bid} K_{id} / E_{ci}$																						
Humidity, H (%) 70	Release time, ti (days) 1																						
Shrinkage strain (in/in), $\epsilon_{sh} = -K_s K_{hs} k_c k_{td} 0.48 * 10^{-3}$																							
Creep coefficient, $\Psi(t, t_i) = 1.9 K_s k_{hc} k_c k_{td} t^{-0.118}$																							
V/s correction factor, ks = 1.45 - 0.13(v/s) >= 0.0	1.05																						
Creep humidity factor, khc = 1.56 - 0.008H	1.00																						
Shrinkage humidity factor, khs = 2.0 - 0.014H	1.02																						
Concrete strength factor, kf = 5/(1+fc)	0.67																						
Transformed section coefficient, K _{id}	0.808																						
CG of Strands = 3.2141 IN Bending moment caused by the concrete beam, M _{beam} = -3109.70 K-IN Stress @ strand level by concrete beam, f _{beam} = -0.2800 KSI Stress @ strand level by strands, f _{ps} = 4.12 KSI Stress @ strand level by strands, f _{cgp} = 3.84 KSI Elastic Shortening losses, Δf_{pES} = 22.83 KSI																							
5.9.5.4.3c Relaxation losses																							
$\Delta f_{pR} = \frac{\log(24t)}{45 \log(24t_i)} K_{id} \left[1 - \frac{3(\Delta f_{pR} + \Delta f_{pR})}{f_{pj}} \right] \left[\frac{f_{pj}}{f_{py}} - 0.55 \right] f_{pj}$		$K_{id} = \frac{1}{1 + \frac{E_p A_{ps}}{E_{ci} A_g} \left(1 + \frac{A_g e_{pg}^2}{I_g} \right) (1 + 0.7 \psi_{bit})}$																					
t = concrete age in days		Time development factor, k _{td} = t/(61-4f _{ci} +t)																					
Δf_{pR} = Time relaxation losses		Creep coefficient at final time, Ψ_{bit} (25yrs,1days) = 1.374																					
LRFD 5.9.5.4.3 Losses: Time of Deck Placement to Final Time																							
5.9.5.4.3a Shrinkage of Girder Concrete		5.9.5.4.3b Creep of Girder Concrete																					
Time of Deck placement, t _d 90 $\Delta f_{pSD} = \epsilon_{bid} E_p K_{df}$		$\Delta f_{pCD} = E_p / E_{ci} * f_{cgp} * (\Psi_{bit} - \Psi_{bid}) * K_{df} + E_p / E_{ci} * \Delta f_{cd} * \Psi_{bit} * K_{df}$ Ψ_{bit} (td,1days) = 0.99 Ps losses = 25.78 Int. Gdr. Ext. Gdr. $\Delta f_{CD} = -0.94 \quad -0.94$																					
$K_{df} = \frac{1}{1 + \frac{E_p A_{ps}}{E_{ci} A_c} \left(1 + \frac{A_c e_{pc}^2}{I_c} \right) (1 + 0.7 \psi_{bit})}$		$\Delta f_{cd} = \frac{\epsilon_{ddf} A_d E_{cd}}{1 + 0.7 \psi_{df}} \left(\frac{1}{A_c} + \frac{e_{pc} e_d}{I_c} \right)$																					
Transformed section coefficient, K _{df} Int. Gdr. Ext. Gdr. K _{df} = 0.830 0.830 ϵ_{bid} (td days) = 2E-04 Δf_{pSR} (td days) = 5.697		Int. Gdr. Ext. Gdr. e _d = -14.94 -16.04 in. A _d = 1224.0 1054.0 in. ²																					
Construction Deflections																							
The following describes the information needed to estimate camber through the construction process																							
		Slab Wt. + Haunch Deflection																					
		$\Delta_s = \frac{5W_s L^4}{384 E_c I_{tr}}$																					
		SIP Forms Variable Joint Filler? Yes 0.00 klf - Int 0.00 klf - Ext Assumed Joint Filler Width = 3" per side deflection due to self-weight of Slab and haunch int. girder, Δ_{s-int} = 0.23 IN deflection due to self-weight of Slab and haunch ext. girder, Δ_{s-ext} = 0.20 IN																					

Figure 5-5. Proposed spreadsheet page 3

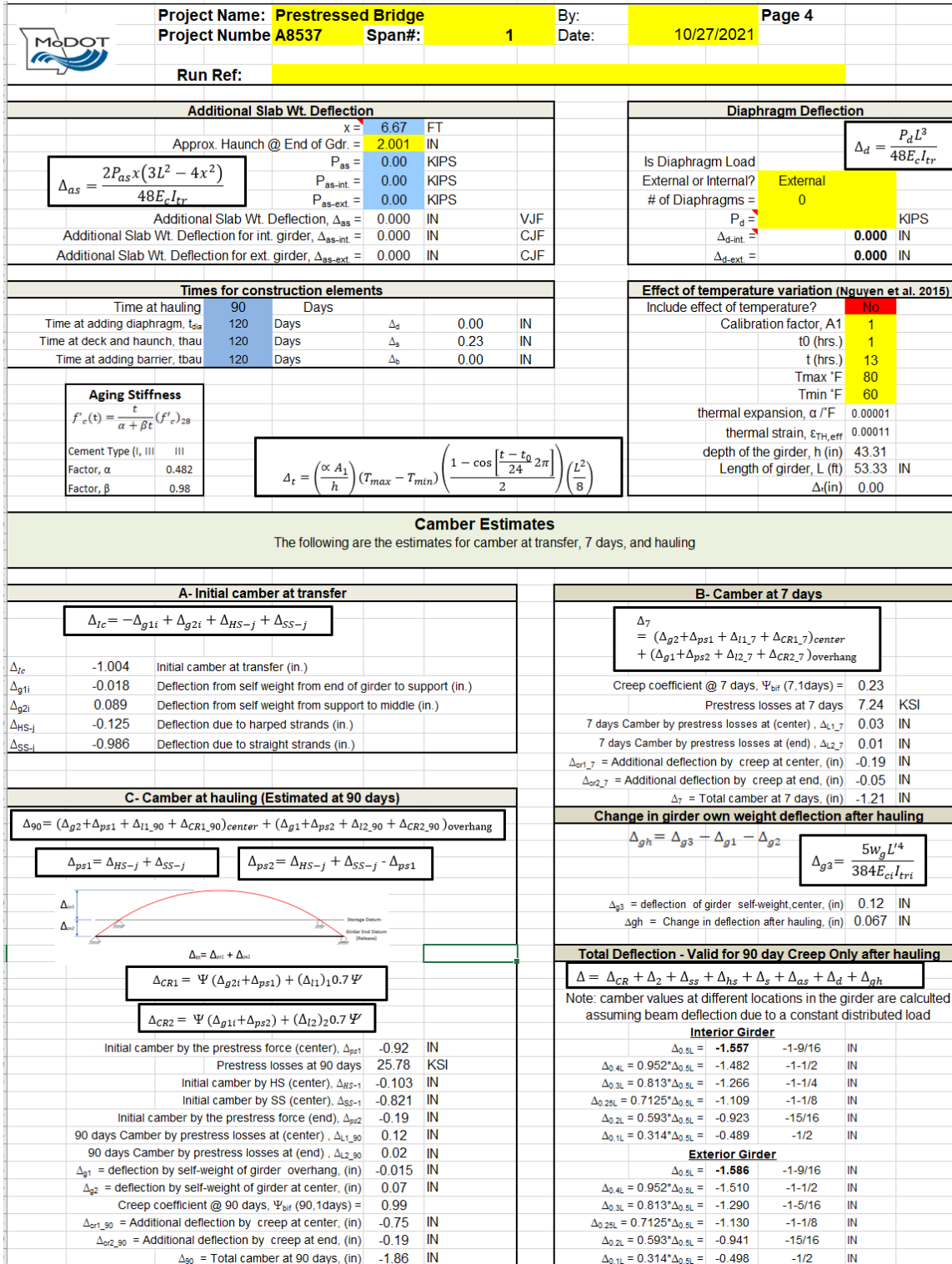


Figure 5-6. Proposed spreadsheet page 4



Time Step Camber Analysis

t (days)	K _{gl} (Girder)	ε _{sh} (Girder)	K _{wd} (Deck)	ε _{sh} (Deck)	Δf _{cdf} (Ksi)	Δf _{psH} (Ksi)	Ψ _{sl} (f,f,t)	Ψ _{sl} (f,f,t ₀)	Δf _{psH} (Ksi)	Δf _{psH} (Ksi)	TL (ksi)	f _{ps} (t) (ksi)	Δ _{so} (in)	Δ _{sl} (in)	E _c (t) (ksi)	Δ _s (in)	Δ _o (in)	Δ _i (in)
0																		0
1																		0
1	0.03	0.00001	0.00	0.00000	0.00	0.22	0.04	0.00	0.63	1.12	1.97	200.53	0.01	0.001	4789.55	0.147	-0.04	-0.99
2	0.05	0.00002	0.00	0.00000	0.00	0.43	0.07	0.00	1.23	1.35	3.00	199.50	0.01	0.002	5240.96	0.135	-0.07	-1.03
3	0.08	0.00003	0.00	0.00000	0.00	0.62	0.11	0.00	1.79	1.47	3.89	198.61	0.02	0.002	5422.37	0.130	-0.10	-1.06
4	0.10	0.00004	0.00	0.00000	0.00	0.81	0.14	0.00	2.33	1.55	4.69	197.81	0.02	0.003	5520.43	0.128	-0.13	-1.09
5	0.13	0.00004	0.00	0.00000	0.00	0.99	0.17	0.00	2.84	1.61	5.44	197.06	0.03	0.003	5581.89	0.126	-0.16	-1.12
6	0.15	0.00005	0.00	0.00000	0.00	1.16	0.20	0.00	3.32	1.65	6.13	196.37	0.03	0.004	5624.02	0.125	-0.19	-1.14
7	0.17	0.00006	0.00	0.00000	0.00	1.32	0.23	0.00	3.78	1.69	6.79	195.71	0.03	0.004	5654.71	0.125	-0.22	-1.16
10	0.22	0.00008	0.00	0.00000	0.00	1.76	0.31	0.00	5.04	1.76	8.56	193.94	0.04	0.005	5711.23	0.124	-0.29	-1.23
13	0.27	0.00009	0.00	0.00000	0.00	2.14	0.37	0.00	6.15	1.80	10.09	192.41	0.05	0.006	5742.37	0.123	-0.35	-1.28
16	0.31	0.00011	0.00	0.00000	0.00	2.48	0.43	0.00	7.12	1.82	11.42	191.08	0.06	0.007	5762.10	0.122	-0.40	-1.32
19	0.35	0.00012	0.00	0.00000	0.00	2.78	0.49	0.00	7.99	1.83	12.61	189.89	0.06	0.008	5775.71	0.122	-0.44	-1.36
22	0.39	0.00013	0.00	0.00000	0.00	3.05	0.53	0.00	8.76	1.84	13.66	188.84	0.07	0.008	5785.68	0.122	-0.49	-1.40
25	0.42	0.00014	0.00	0.00000	0.00	3.30	0.57	0.00	9.46	1.85	14.60	187.90	0.07	0.009	5793.28	0.122	-0.52	-1.43
28	0.44	0.00015	0.00	0.00000	0.00	3.52	0.61	0.00	10.09	1.85	15.46	187.04	0.08	0.010	5799.28	0.122	-0.55	-1.46
34	0.49	0.00017	0.00	0.00000	0.00	3.90	0.68	0.00	11.18	1.86	16.94	185.56	0.08	0.010	5808.13	0.121	-0.61	-1.51
41	0.54	0.00019	0.00	0.00000	0.00	4.27	0.74	0.00	12.24	1.86	18.37	184.13	0.09	0.011	5815.22	0.121	-0.67	-1.55
48	0.58	0.00020	0.00	0.00000	0.00	4.58	0.80	0.00	13.13	1.85	19.56	182.94	0.1	0.012	5820.25	0.121	-0.71	-1.59
55	0.61	0.00021	0.00	0.00000	0.00	4.84	0.84	0.00	13.87	1.85	20.56	181.94	0.1	0.013	5824.01	0.121	-0.75	-1.62
62	0.64	0.00022	0.00	0.00000	0.00	5.06	0.88	0.00	14.51	1.85	21.42	181.08	0.1	0.013	5826.93	0.121	-0.78	-1.65
69	0.66	0.00023	0.00	0.00000	0.00	5.25	0.92	0.00	15.06	1.85	22.16	180.34	0.11	0.014	5829.25	0.121	-0.80	-1.67
76	0.68	0.00024	0.00	0.00000	0.00	5.42	0.94	0.00	15.54	1.85	22.80	179.70	0.11	0.014	5831.15	0.121	-0.83	-1.69
83	0.70	0.00024	0.00	0.00000	0.00	5.57	0.97	0.00	15.97	1.84	23.38	179.12	0.11	0.014	5832.74	0.121	-0.85	-1.71
90	0.72	0.00025	0.00	0.00000	0.00	5.70	0.99	0.00	16.34	1.84	23.88	178.62	0.12	0.015	5834.07	0.121	-0.87	-1.73
90	0.72	0.00025	0.00	0.00000	0.00	5.70	0.99	0.00	16.34	1.84	23.88	178.62	0.12	0.015	5834.07	0.121	-0.87	-1.48
92	0.72	0.00025	0.04	0.00002	-0.01	5.68	1.00	0.57	14.16	1.94	21.79	180.71	0.11	0.013	5834.42	0.121	-0.88	-1.36
120	0.77	0.00027	0.40	0.00022	-0.08	5.66	1.07	0.61	15.17	1.96	22.80	179.70	0.11	0.014	5838.04	0.121	-0.94	-1.40
160	0.82	0.00028	0.61	0.00033	-0.13	5.79	1.13	0.64	16.10	1.99	23.88	178.62	0.12	0.015	5841.02	0.121	-0.99	-1.44
200	0.85	0.00029	0.71	0.00038	-0.15	5.92	1.17	0.67	16.72	2.01	24.65	177.85	0.12	0.015	5842.81	0.121	-1.02	-1.46
240	0.87	0.00030	0.77	0.00042	-0.16	6.03	1.20	0.68	17.15	2.03	25.21	177.29	0.12	0.016	5844.01	0.121	-1.04	-1.48
280	0.89	0.00031	0.81	0.00044	-0.17	6.11	1.23	0.70	17.48	2.04	25.64	176.86	0.12	0.016	5844.86	0.121	-1.06	-1.49
320	0.90	0.00031	0.84	0.00045	-0.18	6.18	1.24	0.71	17.73	2.06	25.97	176.53	0.13	0.016	5845.50	0.121	-1.08	-1.50
360	0.91	0.00031	0.86	0.00046	-0.18	6.24	1.26	0.71	17.93	2.07	26.25	176.25	0.13	0.016	5846.00	0.121	-1.09	-1.51
400	0.92	0.00032	0.87	0.00047	-0.18	6.29	1.27	0.72	18.10	2.09	26.47	176.03	0.13	0.016	5846.40	0.121	-1.09	-1.51
9125	1.00	0.00034	1.00	0.00054	-0.21	6.76	1.37	0.78	19.64	2.67	29.08	173.42	0.14	0.018	5849.83	0.121	-1.17	-1.56

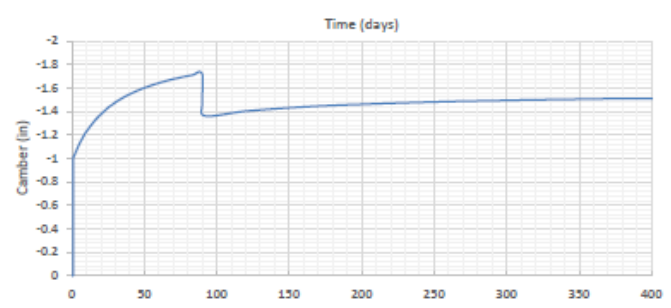


Figure 5-7. Proposed spreadsheet page 5

5.2.1.1 Spreadsheet Page Heading

The heading of each page in the spreadsheet contains some general information about the girder. These are the project name, designer name, project number, span number, page number, date, and the run reference (see Figure 5-8) to help identify the prestressed girder for which camber is calculated.


Camber Calculations for Prestressed Girders				
	Project Name:	Prestressed Bridge	By:	Page 1
	Project Number:	A8537	Span#:	1
	Date:	8/11/2021		
	Run Ref:			

Figure 5-8. Page heading in the spreadsheet

5.2.1.2 Prestressed Girder Definition

This section contains the geometric information of the prestressed girder. The input data in this section are the beam type, beam length, and overhang length (see Figure 5-9). The white cells are calculated automatically based on tables of standard beam types in another tab of the workbook. In addition, there is an option whether to include the overhang effect or not. If the option is yes, the user must insert the overhang length details.

Prestressed Girder Definition				
Girder Type =	NU 43		$A_{beam} =$	686.05 IN ²
Girder Length, L =	53.33 FT		$y_{b-nc} =$	19.36 IN
			$I_{nc} =$	179343 IN ⁴
Girder Depth=	43.31 IN		External or Internal?	Interior
Unit Weight=	153.00 lb/ft3		CL to CL Support, Ls (ft)	53.33
Wg : Self Weight =	0.73 kip/ft		Include Overhang	No
	If no write 0 If yes what is the overhang length , a (ft)			0.00

Figure 5-9. Prestressed girder definition

5.2.1.3 Cross-Section and Haunch Details

Haunch details are also defined in the calculation of the camber as the haunch causes a dead load, which will cause downward deflection. The haunch thickness, girder spacing, the roadway depth, and number of girders must be filled by the user in the part of haunch details in the proposed spreadsheet (see Figure 5-10).

Haunch Details		
Assumed haunch @ Midspan =	2	IN
Girder Spacing =	12.00	FT
Roadway Width =	30.00	FT
# of Girders =	3	
SBC Width =	16	IN
SIP Forms?	No	

Figure 5-10. Haunch details

5.2.1.4 Slab Weight

To consider the deflection caused by the slab weight after the deck is added, the slab details are defined in the spreadsheet (see Figure 5-11). The proposed spreadsheet allows the user to identify the slab thickness.

Slab Details		
Slab Depth =	8.50	IN
M_{SIDL} =		K-FT
Adj. EFW (Int.) =	8.23	FT
	12.00	
Adj. EFW (Ext.) =	7.09	FT
	10.33	

Figure 5-11. Slab details

5.2.1.5 Material Properties

The properties of concrete of slab and prestressed girder, steel, and prestressed strands are defined in this section (see Figure 5-12). The user must fill the initial and 28-day compressive strength of the concrete used in the prestressed girder. In addition, the user may revise the concrete compressive strength of slab and the elastic modulus for steel and prestressed strands.

Material Properties			
$f_c =$	4	KSI	Strength of Slab Concrete
$E_c =$	3644	KSI	Elastic Modulus of Slab Concrete
$n_{fc} =$	0.69		Modular Ratio: $E_{c(\text{slab})}/E_{c(\text{girder})}$
$f_{ci} =$	6.5	KSI	Initial Strength of Girder Concrete (at transfer)
$\beta_1 =$	0.725		stress block factor (LRFD 5.7.2.2)
$E_{ci} =$	4790	KSI	Elastic Modulus of Initial Concrete Strength
$f_c =$	8	KSI	Final Strength of Girder Concrete (28 days)
$\beta_1 =$	0.65		stress block factor (LRFD 5.7.2.2)
$E_c =$	5314	KSI	Elastic Modulus of Final Concrete Strength
$E_s =$	29000	KSI	Elastic Modulus of A1 Bars
$n_{is} =$	6.05		Modular Ratio: E_{steel}/E_{ci}
$n_{fs} =$	5.46		Modular Ratio: E_{steel}/E_c
$E_p =$	28500	KSI	Elastic Modulus of Prestressing Strands
$n_{ip} =$	5.95		Modular Ratio: E_{strand}/E_{ci}
$n_{fp} =$	5.36		Modular Ratio: E_{strand}/E_c

Figure 5-12. Material properties

5.2.1.6 Strand Profile and Definition

The strand profile and definition are important to calculate the exact camber caused by the prestressing strands. The window highlighted in Figure 5-13 allows the user to input the location of each strand (harped as well as straight) in the girder, as well as the number and their diameter. The average eccentricities are automatically calculated in the part of strand eccentricities (see

Figure 5-14). These calculations also consider the effect of debonded length of the strands on the camber (see Figure 5-15). These definitions enable more accurate calculation of the camber.

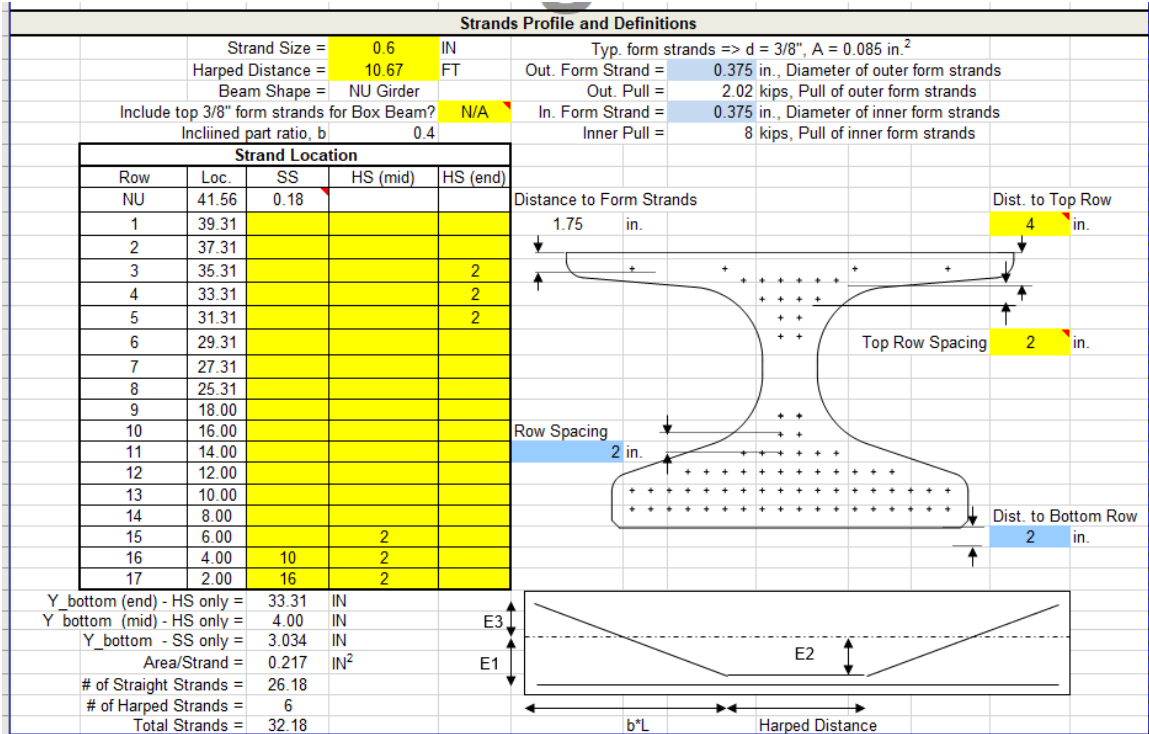


Figure 5-13. Strand profile and definition

Strands eccentricities	
E1 =	16.33 IN
E2 =	15.36 IN
E3 =	13.95 IN
f_{pu} =	270 KSI
$f_{pj} = 0.75 * f_{pu}$ =	202.5 KSI
$f_{py} = 0.9 * f_{pu}$ =	243 KSI

Figure 5-14. Strand eccentricities

Debonded Strand Input					
Loc. (in.)	No.	Debond (l ₀) (ft)	Camber Const.	Debonded Data	
2	4	8	172499.3	y _b =	2.667
4	2	12	66513.1	No.	6
			0	Adjust Bonded - SS	
			0	y _b =	3.143
			0	E _{1tri} =	15.520
			0		
			0		
SUM[E*No.(L ² -4l ₀ ²)] =			239012.4	in*sf	

Figure 5-15. Input to account for debonded strands

5.2.1.7 Transformed Section Properties Calculation

The proposed calculations use the transformed section properties. The section of spreadsheet shown in Figure 5-16 presents the calculated transformed properties for non-composite section, girder without slab, and composite section, girder with slab. For the non-composite section, these properties are calculated using the initial material properties and final material properties. These are calculated for the interior and exterior girders, after pouring the deck slab.

Transformed Section Properties					
Non-Composite Section					
Initial Properties			Final Properties		
$A_{tri} =$	723.04	IN ²	$A_{tr} =$	718.65	IN ²
$y_{b-tri} =$	18.663	IN	$y_{b-tr} =$	18.74	IN
$I_{tri} =$	189205	IN ⁴	$I_{tr} =$	188072	IN ⁴
$E1_{tri} =$	15.629	IN	$E1_{tr} =$	15.71	IN
$E2_{tri} =$	14.663	IN	$E2_{tr} =$	14.74	IN
$E3_{tri} =$	14.650	IN	$E3_{tr} =$	14.57	IN
Composite Section					
Interior Girder			Exterior Girder		
$A =$	1459.23	IN ²	$A =$	1356.37	IN ²
$y_{bc} =$	33.62	IN	$y_{bc} =$	32.53	IN
$I_c =$	505099	IN ⁴	$I_c =$	481543	IN ⁴

Figure 5-16. Transformed section properties

5.2.1.8 Initial Camber Calculations

Initial camber is based on the deflections from the prestressing forces and the self-weight. The camber is measured from the end of the girder to midspan (regardless of support location). This section presents the part of the spreadsheet in which the initial camber is calculated (see Figure 5-17). The procedures of these calculation are presented in detail in section 5.1.

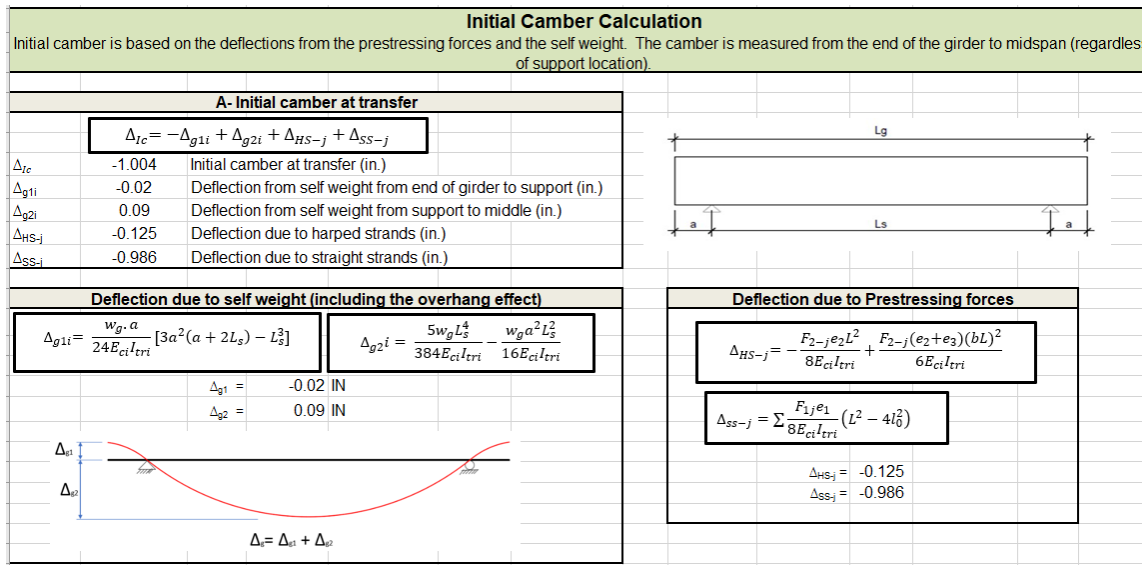


Figure 5-17. Initial camber calculations

5.2.1.9 Loss Estimation

This section describes the equations used in the estimation of camber (according to AASHTO LRFD 5.9.5) with time and calculates it (see Figure 5-18). Estimation of camber with time must include the effect of prestress losses. The losses in the concrete are grouped from time to deck placement, and after deck placement.

5.2.1.10 Additional Deflection

The additional deflections caused by different components, like the haunch and slab, are also considered in the proposed spreadsheet (see Figure 5-19). It is important to compute how much change occurs in the camber due to the weight of the deck slab.

Loss Estimation with time																																																					
The following describes the equations used in the estimation of camber with time. Estimation of camber with time includes the effect of losses. The losses in the concrete are grouped from time to deck placement, and after deck placement.																																																					
<table border="1" style="width: 100%;"> <thead> <tr> <th colspan="2" style="text-align: center;">Prestress Losses Camber</th> </tr> </thead> <tbody> <tr> <td style="text-align: center;">$\Delta_{11t} = \Delta_{ps1} * \frac{Losses}{f_{pj}}$</td> <td style="text-align: center;">$\Delta_{12t} = \Delta_{ps2} * \frac{Losses}{f_{pj}}$</td> </tr> <tr> <td colspan="2" style="text-align: center;"> $Losses = \Delta f_{pSR} + \Delta f_{pCR} + \Delta f_{pR} + \Delta f_{pSD} + \Delta f_{pCD} + \Delta f_{pSS}$ </td> </tr> <tr> <td colspan="2" style="text-align: center;"> Δ_{11t} = camber due to prestressing losses at center (in) Δ_{12t} = camber due to prestressing losses at end. (in) </td> </tr> </tbody> </table>		Prestress Losses Camber		$\Delta_{11t} = \Delta_{ps1} * \frac{Losses}{f_{pj}}$	$\Delta_{12t} = \Delta_{ps2} * \frac{Losses}{f_{pj}}$	$Losses = \Delta f_{pSR} + \Delta f_{pCR} + \Delta f_{pR} + \Delta f_{pSD} + \Delta f_{pCD} + \Delta f_{pSS}$		Δ_{11t} = camber due to prestressing losses at center (in) Δ_{12t} = camber due to prestressing losses at end. (in)																																													
Prestress Losses Camber																																																					
$\Delta_{11t} = \Delta_{ps1} * \frac{Losses}{f_{pj}}$	$\Delta_{12t} = \Delta_{ps2} * \frac{Losses}{f_{pj}}$																																																				
$Losses = \Delta f_{pSR} + \Delta f_{pCR} + \Delta f_{pR} + \Delta f_{pSD} + \Delta f_{pCD} + \Delta f_{pSS}$																																																					
Δ_{11t} = camber due to prestressing losses at center (in) Δ_{12t} = camber due to prestressing losses at end. (in)																																																					
LRFD 5.9.5.4.2 Losses: Time of Transfer to Time of Deck Placement																																																					
<table border="1" style="width: 100%;"> <thead> <tr> <th colspan="2" style="text-align: center;">LRFD 5.9.5.2.3a Elastic Shortening</th> </tr> </thead> <tbody> <tr> <td colspan="2" style="text-align: center;">$\Delta f_{pES} = \frac{E_p}{E_c} f_{cgp}$</td> </tr> <tr> <td colspan="2">CG of Strands = 3.2141 IN</td> </tr> <tr> <td colspan="2">Bending moment caused by the concrete beam, $M_{beam} = -3109.70$ K-IN</td> </tr> <tr> <td colspan="2">Stress @ strand level by concrete beam, $f_{beam} = -0.2800$ KSI</td> </tr> <tr> <td colspan="2">Stress @ strand level by strands, $f_{ps} = 4.12$ KSI</td> </tr> <tr> <td colspan="2">Stress @ strand level by strands, $f_{cgp} = 3.84$ KSI</td> </tr> <tr> <td colspan="2">Elastic Shortening losses, $\Delta f_{pES} = 22.83$ KSI</td> </tr> </tbody> </table> <table border="1" style="width: 100%;"> <thead> <tr> <th colspan="2" style="text-align: center;">5.9.5.4.3c Relaxation losses</th> </tr> </thead> <tbody> <tr> <td colspan="2" style="text-align: center;"> $\Delta f_{pR} = \frac{\log(24t)}{45 \log(24t_i)} K_{id} \left[1 - \frac{3(\Delta f_{pR} + \Delta f_{pR})}{f_{pj}} \right] \left[\frac{f_{pj}}{f_{py}} - 0.55 \right] f_{pj}$ </td> </tr> <tr> <td>t =</td> <td>concrete age in days</td> </tr> <tr> <td>Δf_{pR} =</td> <td>Time relaxation losses</td> </tr> </tbody> </table>	LRFD 5.9.5.2.3a Elastic Shortening		$\Delta f_{pES} = \frac{E_p}{E_c} f_{cgp}$		CG of Strands = 3.2141 IN		Bending moment caused by the concrete beam, $M_{beam} = -3109.70$ K-IN		Stress @ strand level by concrete beam, $f_{beam} = -0.2800$ KSI		Stress @ strand level by strands, $f_{ps} = 4.12$ KSI		Stress @ strand level by strands, $f_{cgp} = 3.84$ KSI		Elastic Shortening losses, $\Delta f_{pES} = 22.83$ KSI		5.9.5.4.3c Relaxation losses		$\Delta f_{pR} = \frac{\log(24t)}{45 \log(24t_i)} K_{id} \left[1 - \frac{3(\Delta f_{pR} + \Delta f_{pR})}{f_{pj}} \right] \left[\frac{f_{pj}}{f_{py}} - 0.55 \right] f_{pj}$		t =	concrete age in days	Δf_{pR} =	Time relaxation losses	<table border="1" style="width: 100%;"> <thead> <tr> <th colspan="2" style="text-align: center;">LRFD 5.9.5.4.2 Losses: creep and shrinkage of concrete</th> </tr> </thead> <tbody> <tr> <td style="text-align: center;">5.9.5.4.2a Shrinkage losses</td> <td style="text-align: center;">5.9.5.4.2b Creep losses</td> </tr> <tr> <td>$\Delta f_{pSR} = \epsilon_{bid} E_p K_{id}$</td> <td>$\Delta f_{pCR} = E_p f_{cgp} \Psi_{bid} K_{id} / E_{ci}$</td> </tr> <tr> <td>Humidity, H (%) = 70</td> <td>Release time, t_i (days) = 1</td> </tr> <tr> <td colspan="2">Shrinkage strain (in/in), $\epsilon_{sh} = -k_s k_{hs} k_{k_{id}} 0.48 * 10^{-3}$</td> </tr> <tr> <td colspan="2">Creep coefficient, $\Psi(t, t_i) = 1.9 k_s k_{hc} k_{k_{id}} t_i^{-0.118}$</td> </tr> <tr> <td>V/s correction factor, $k_s = 1.45 - 0.13(v/s) \geq 0.0$</td> <td>1.05</td> </tr> <tr> <td>Creep humidity factor, $k_{hc} = 1.56 - 0.008H$</td> <td>1.00</td> </tr> <tr> <td>Shrinkage humidity factor, $k_{hs} = 2.0 - 0.014H$</td> <td>1.02</td> </tr> <tr> <td>Concrete strength factor, $k_f = 5/(1+f_{ci})$</td> <td>0.67</td> </tr> <tr> <td colspan="2" style="text-align: center;">Transformed section coefficient, K_{id}</td> </tr> <tr> <td colspan="2" style="text-align: center;"> $K_{id} = \frac{1}{1 + \frac{E_p A_{ps}}{E_{ci} A_g} \left(1 + \frac{A_g e_{pg}^2}{I_g} \right) (1 + 0.7 \psi_{bit})}$ </td> </tr> <tr> <td>Time development factor, k_{td}</td> <td>$t/(61-4f_{ci}t)$</td> </tr> <tr> <td>Creep coefficient at final time, Ψ_{bit} (25yrs, 1days) =</td> <td>1.374</td> </tr> </tbody> </table>	LRFD 5.9.5.4.2 Losses: creep and shrinkage of concrete		5.9.5.4.2a Shrinkage losses	5.9.5.4.2b Creep losses	$\Delta f_{pSR} = \epsilon_{bid} E_p K_{id}$	$\Delta f_{pCR} = E_p f_{cgp} \Psi_{bid} K_{id} / E_{ci}$	Humidity, H (%) = 70	Release time, t_i (days) = 1	Shrinkage strain (in/in), $\epsilon_{sh} = -k_s k_{hs} k_{k_{id}} 0.48 * 10^{-3}$		Creep coefficient, $\Psi(t, t_i) = 1.9 k_s k_{hc} k_{k_{id}} t_i^{-0.118}$		V/s correction factor, $k_s = 1.45 - 0.13(v/s) \geq 0.0$	1.05	Creep humidity factor, $k_{hc} = 1.56 - 0.008H$	1.00	Shrinkage humidity factor, $k_{hs} = 2.0 - 0.014H$	1.02	Concrete strength factor, $k_f = 5/(1+f_{ci})$	0.67	Transformed section coefficient, K_{id}		$K_{id} = \frac{1}{1 + \frac{E_p A_{ps}}{E_{ci} A_g} \left(1 + \frac{A_g e_{pg}^2}{I_g} \right) (1 + 0.7 \psi_{bit})}$		Time development factor, k_{td}	$t/(61-4f_{ci}t)$	Creep coefficient at final time, Ψ_{bit} (25yrs, 1days) =	1.374
LRFD 5.9.5.2.3a Elastic Shortening																																																					
$\Delta f_{pES} = \frac{E_p}{E_c} f_{cgp}$																																																					
CG of Strands = 3.2141 IN																																																					
Bending moment caused by the concrete beam, $M_{beam} = -3109.70$ K-IN																																																					
Stress @ strand level by concrete beam, $f_{beam} = -0.2800$ KSI																																																					
Stress @ strand level by strands, $f_{ps} = 4.12$ KSI																																																					
Stress @ strand level by strands, $f_{cgp} = 3.84$ KSI																																																					
Elastic Shortening losses, $\Delta f_{pES} = 22.83$ KSI																																																					
5.9.5.4.3c Relaxation losses																																																					
$\Delta f_{pR} = \frac{\log(24t)}{45 \log(24t_i)} K_{id} \left[1 - \frac{3(\Delta f_{pR} + \Delta f_{pR})}{f_{pj}} \right] \left[\frac{f_{pj}}{f_{py}} - 0.55 \right] f_{pj}$																																																					
t =	concrete age in days																																																				
Δf_{pR} =	Time relaxation losses																																																				
LRFD 5.9.5.4.2 Losses: creep and shrinkage of concrete																																																					
5.9.5.4.2a Shrinkage losses	5.9.5.4.2b Creep losses																																																				
$\Delta f_{pSR} = \epsilon_{bid} E_p K_{id}$	$\Delta f_{pCR} = E_p f_{cgp} \Psi_{bid} K_{id} / E_{ci}$																																																				
Humidity, H (%) = 70	Release time, t_i (days) = 1																																																				
Shrinkage strain (in/in), $\epsilon_{sh} = -k_s k_{hs} k_{k_{id}} 0.48 * 10^{-3}$																																																					
Creep coefficient, $\Psi(t, t_i) = 1.9 k_s k_{hc} k_{k_{id}} t_i^{-0.118}$																																																					
V/s correction factor, $k_s = 1.45 - 0.13(v/s) \geq 0.0$	1.05																																																				
Creep humidity factor, $k_{hc} = 1.56 - 0.008H$	1.00																																																				
Shrinkage humidity factor, $k_{hs} = 2.0 - 0.014H$	1.02																																																				
Concrete strength factor, $k_f = 5/(1+f_{ci})$	0.67																																																				
Transformed section coefficient, K_{id}																																																					
$K_{id} = \frac{1}{1 + \frac{E_p A_{ps}}{E_{ci} A_g} \left(1 + \frac{A_g e_{pg}^2}{I_g} \right) (1 + 0.7 \psi_{bit})}$																																																					
Time development factor, k_{td}	$t/(61-4f_{ci}t)$																																																				
Creep coefficient at final time, Ψ_{bit} (25yrs, 1days) =	1.374																																																				
LRFD 5.9.5.4.3 Losses: Time of Deck Placement to Final Time																																																					
<table border="1" style="width: 100%;"> <thead> <tr> <th colspan="2" style="text-align: center;">5.9.5.4.3a Shrinkage of Girder Concrete</th> </tr> </thead> <tbody> <tr> <td>Time of Deck placement, t_d</td> <td>90</td> </tr> <tr> <td colspan="2" style="text-align: center;">$\Delta f_{pSD} = \epsilon_{bid} E_p K_{id}$</td> </tr> <tr> <td colspan="2" style="text-align: center;"> $K_{id} = \frac{1}{1 + \frac{E_p A_{ps}}{E_{ci} A_c} \left(1 + \frac{A_c e_{pc}^2}{I_c} \right) (1 + 0.7 \psi_{bit})}$ </td> </tr> <tr> <td colspan="2">Transformed section coefficient, K_{df}</td> </tr> <tr> <td>Int. Gdr.</td> <td>Ext. Gdr.</td> </tr> <tr> <td>$K_{df} = 0.830$</td> <td>0.830</td> </tr> <tr> <td>ϵ_{bid} (td days) =</td> <td>0.0002</td> </tr> <tr> <td>Δf_{pSR} (td days) =</td> <td>5.6974</td> </tr> </tbody> </table>	5.9.5.4.3a Shrinkage of Girder Concrete		Time of Deck placement, t_d	90	$\Delta f_{pSD} = \epsilon_{bid} E_p K_{id}$		$K_{id} = \frac{1}{1 + \frac{E_p A_{ps}}{E_{ci} A_c} \left(1 + \frac{A_c e_{pc}^2}{I_c} \right) (1 + 0.7 \psi_{bit})}$		Transformed section coefficient, K_{df}		Int. Gdr.	Ext. Gdr.	$K_{df} = 0.830$	0.830	ϵ_{bid} (td days) =	0.0002	Δf_{pSR} (td days) =	5.6974	<table border="1" style="width: 100%;"> <thead> <tr> <th colspan="2" style="text-align: center;">5.9.5.4.3b Creep of Girder Concrete</th> </tr> </thead> <tbody> <tr> <td colspan="2" style="text-align: center;">$\Delta f_{pCD} = E_p / E_{ci} * f_{cgp} * (\Psi_{bit} - \Psi_{bid}) * K_{df} + E_p / E_c * \Delta f_{cd} * \Psi_{bit} * K_{df}$</td> </tr> <tr> <td>$\Psi_{bit}$ (td, 1days) =</td> <td>0.99</td> </tr> <tr> <td>Ps losses =</td> <td>25.78</td> </tr> <tr> <td>Int. Gdr.</td> <td>Ext. Gdr.</td> </tr> <tr> <td>$\Delta f_{CD} = -0.94$</td> <td>-0.94</td> </tr> <tr> <td colspan="2" style="text-align: center;"> $\Delta f_{cd} = \frac{(e_d)(gdr_spac)(0.15k/ft^2)L^2}{8} \times \frac{(y_b - t_r - C.G.strands)}{I_{tr}} + (PS_losses)(A_{ps}) \left(\frac{1}{A_{beam}} + \frac{(y_b - t_{ri} - C.G.strands)^2}{I_{tri}} \right)$ </td> </tr> </tbody> </table>	5.9.5.4.3b Creep of Girder Concrete		$\Delta f_{pCD} = E_p / E_{ci} * f_{cgp} * (\Psi_{bit} - \Psi_{bid}) * K_{df} + E_p / E_c * \Delta f_{cd} * \Psi_{bit} * K_{df}$		Ψ_{bit} (td, 1days) =	0.99	Ps losses =	25.78	Int. Gdr.	Ext. Gdr.	$\Delta f_{CD} = -0.94$	-0.94	$\Delta f_{cd} = \frac{(e_d)(gdr_spac)(0.15k/ft^2)L^2}{8} \times \frac{(y_b - t_r - C.G.strands)}{I_{tr}} + (PS_losses)(A_{ps}) \left(\frac{1}{A_{beam}} + \frac{(y_b - t_{ri} - C.G.strands)^2}{I_{tri}} \right)$		<table border="1" style="width: 100%;"> <thead> <tr> <th colspan="2" style="text-align: center;">5.9.5.4.3d Shrinkage of Deck Concrete</th> </tr> </thead> <tbody> <tr> <td colspan="2" style="text-align: center;">$\Delta f_{pSS} = E_p / E_c * \Delta f_{cd} K_{id} (1 + 0.7 \Psi_{bit})$</td> </tr> <tr> <td colspan="2" style="text-align: center;"> $\Delta f_{cdf} = \frac{\epsilon_{add} A_d E_{cd} \left(\frac{1}{A_c} + \frac{e_{pc} e_d}{I_c} \right)}{1 + 0.7 \psi_{df}}$ </td> </tr> <tr> <td>Int. Gdr.</td> <td>Ext. Gdr.</td> </tr> <tr> <td>$e_d = -14.94$</td> <td>-16.04 in.</td> </tr> <tr> <td>$A_d = 1224.0$</td> <td>1054.0 in.²</td> </tr> </tbody> </table>	5.9.5.4.3d Shrinkage of Deck Concrete		$\Delta f_{pSS} = E_p / E_c * \Delta f_{cd} K_{id} (1 + 0.7 \Psi_{bit})$		$\Delta f_{cdf} = \frac{\epsilon_{add} A_d E_{cd} \left(\frac{1}{A_c} + \frac{e_{pc} e_d}{I_c} \right)}{1 + 0.7 \psi_{df}}$		Int. Gdr.	Ext. Gdr.	$e_d = -14.94$	-16.04 in.	$A_d = 1224.0$	1054.0 in. ²							
5.9.5.4.3a Shrinkage of Girder Concrete																																																					
Time of Deck placement, t_d	90																																																				
$\Delta f_{pSD} = \epsilon_{bid} E_p K_{id}$																																																					
$K_{id} = \frac{1}{1 + \frac{E_p A_{ps}}{E_{ci} A_c} \left(1 + \frac{A_c e_{pc}^2}{I_c} \right) (1 + 0.7 \psi_{bit})}$																																																					
Transformed section coefficient, K_{df}																																																					
Int. Gdr.	Ext. Gdr.																																																				
$K_{df} = 0.830$	0.830																																																				
ϵ_{bid} (td days) =	0.0002																																																				
Δf_{pSR} (td days) =	5.6974																																																				
5.9.5.4.3b Creep of Girder Concrete																																																					
$\Delta f_{pCD} = E_p / E_{ci} * f_{cgp} * (\Psi_{bit} - \Psi_{bid}) * K_{df} + E_p / E_c * \Delta f_{cd} * \Psi_{bit} * K_{df}$																																																					
Ψ_{bit} (td, 1days) =	0.99																																																				
Ps losses =	25.78																																																				
Int. Gdr.	Ext. Gdr.																																																				
$\Delta f_{CD} = -0.94$	-0.94																																																				
$\Delta f_{cd} = \frac{(e_d)(gdr_spac)(0.15k/ft^2)L^2}{8} \times \frac{(y_b - t_r - C.G.strands)}{I_{tr}} + (PS_losses)(A_{ps}) \left(\frac{1}{A_{beam}} + \frac{(y_b - t_{ri} - C.G.strands)^2}{I_{tri}} \right)$																																																					
5.9.5.4.3d Shrinkage of Deck Concrete																																																					
$\Delta f_{pSS} = E_p / E_c * \Delta f_{cd} K_{id} (1 + 0.7 \Psi_{bit})$																																																					
$\Delta f_{cdf} = \frac{\epsilon_{add} A_d E_{cd} \left(\frac{1}{A_c} + \frac{e_{pc} e_d}{I_c} \right)}{1 + 0.7 \psi_{df}}$																																																					
Int. Gdr.	Ext. Gdr.																																																				
$e_d = -14.94$	-16.04 in.																																																				
$A_d = 1224.0$	1054.0 in. ²																																																				

Figure 5-18. Loss estimation

Additional Slab Wt. Deflection		Diaphragm Deflection	
$\Delta_{as} = \frac{2P_{as} x (3L^2 - 4x^2)}{48E_c I_{tr}}$		$\Delta_d = \frac{P_d L^3}{48E_c I_{tr}}$	
Approx. Haunch @ End of Gdr. =	2.001 IN	Is Diaphragm Load	External
P_{as} =	0.00 KIPS	External or Internal?	External
$P_{as, int.}$ =	0.00 KIPS	# of Diaphragms =	0
$P_{as, ext.}$ =	0.00 KIPS	P_d =	0.000 KIPS
Additional Slab Wt. Deflection, Δ_{as} =		$\Delta_{d, int.}$ =	0.000 IN
Additional Slab Wt. Deflection for int. girder, $\Delta_{as, int.}$ =		$\Delta_{d, ext.}$ =	0.000 IN
Additional Slab Wt. Deflection for ext. girder, $\Delta_{as, ext.}$ =			

Figure 5-19. Additional deflection

5.2.2 Time Camber Estimates (Discrete Time-Step)

This part of the spreadsheet presents the calculated camber at different times (see Figure 5-20). These are camber at transfer, 7 days, and hauling, which are most important time stages during construction. In addition, the camber is presented along the girder length.

Camber Estimates			
The following are the estimates for camber at transfer, 7 days, and hauling			
A- Initial camber at transfer		B- Camber at 7 days	
$\Delta_{Ic} = -\Delta_{g1i} + \Delta_{g2i} + \Delta_{HS-j} + \Delta_{SS-j}$			
Δ_{Ic}	-1.004	Initial camber at transfer (in.)	$\Delta_7 = (\Delta_{g2} + \Delta_{ps1} + \Delta_{I1,7} + \Delta_{CR1,7})_{center} + (\Delta_{g1} + \Delta_{ps2} + \Delta_{I2,7} + \Delta_{CR2,7})_{overhang}$
Δ_{g1i}	-0.018	Deflection from self weight from end of girder to support (in.)	
Δ_{g2i}	0.089	Deflection from self weight from support to middle (in.)	
Δ_{HS-j}	-0.125	Deflection due to harped strands (in.)	
Δ_{SS-j}	-0.986	Deflection due to straight strands (in.)	
C- Camber at hauling (Estimated at 90 days)		Change in girder own weight deflection after hauling	
$\Delta_{90} = (\Delta_{g2} + \Delta_{ps1} + \Delta_{I1,90} + \Delta_{CR1,90})_{center} + (\Delta_{g1} + \Delta_{ps2} + \Delta_{I2,90} + \Delta_{CR2,90})_{overhang}$			
$\Delta_{ps1} = \Delta_{HS-j} + \Delta_{SS-j}$		$\Delta_{ps2} = \Delta_{HS-j} + \Delta_{SS-j} - \Delta_{ps1}$	
$\Delta_{CR1} = \Psi (\Delta_{g2i} + \Delta_{ps1}) + (\Delta_{I1})_1 0.7 \Psi$			
$\Delta_{CR2} = \Psi (\Delta_{g1i} + \Delta_{ps2}) + (\Delta_{I2})_2 0.7 \Psi$			
$\Delta_{gh} = \Delta_{g3} - \Delta_{g1} - \Delta_{g2}$			
$\Delta_{g3} = \frac{5W_g L^4}{384 E_{ci} I_{tri}}$			
$\Delta = \Delta_{CR} + \Delta_2 + \Delta_{SS} + \Delta_{hs} + \Delta_s + \Delta_{as} + \Delta_d + \Delta_{gh}$			
Note: camber values at different locations in the girder are calculated assuming beam deflection due to a constant distributed load			
Interior Girder			
$\Delta_{0.5L} = -1.557 \quad -1-9/16 \quad IN$			
$\Delta_{0.4L} = 0.952^* \Delta_{0.5L} = -1.482 \quad -1-1/2 \quad IN$			
$\Delta_{0.3L} = 0.813^* \Delta_{0.5L} = -1.266 \quad -1-1/4 \quad IN$			
$\Delta_{0.25L} = 0.7125^* \Delta_{0.5L} = -1.109 \quad -1-1/8 \quad IN$			
$\Delta_{0.2L} = 0.593^* \Delta_{0.5L} = -0.923 \quad -15/16 \quad IN$			
$\Delta_{0.1L} = 0.314^* \Delta_{0.5L} = -0.489 \quad -1/2 \quad IN$			
Exterior Girder			
$\Delta_{0.5L} = -1.586 \quad -1-9/16 \quad IN$			
$\Delta_{0.4L} = 0.952^* \Delta_{0.5L} = -1.510 \quad -1-1/2 \quad IN$			
$\Delta_{0.3L} = 0.813^* \Delta_{0.5L} = -1.290 \quad -1-5/16 \quad IN$			
$\Delta_{0.25L} = 0.7125^* \Delta_{0.5L} = -1.130 \quad -1-1/8 \quad IN$			
$\Delta_{0.2L} = 0.593^* \Delta_{0.5L} = -0.941 \quad -15/16 \quad IN$			
$\Delta_{0.1L} = 0.314^* \Delta_{0.5L} = -0.498 \quad -1/2 \quad IN$			

Figure 5-20. Time camber estimates (discrete time-step)

5.2.3 Time Camber Estimates (Time-Step)

This part of the spreadsheet presents the time-step calculated camber (see Figure 5-21). The time losses including shrinkage, creep, and relaxation losses are calculated in this section in addition to

the effects from the aging concrete modulus. Finally, the camber time-history is also presented in a chart form.

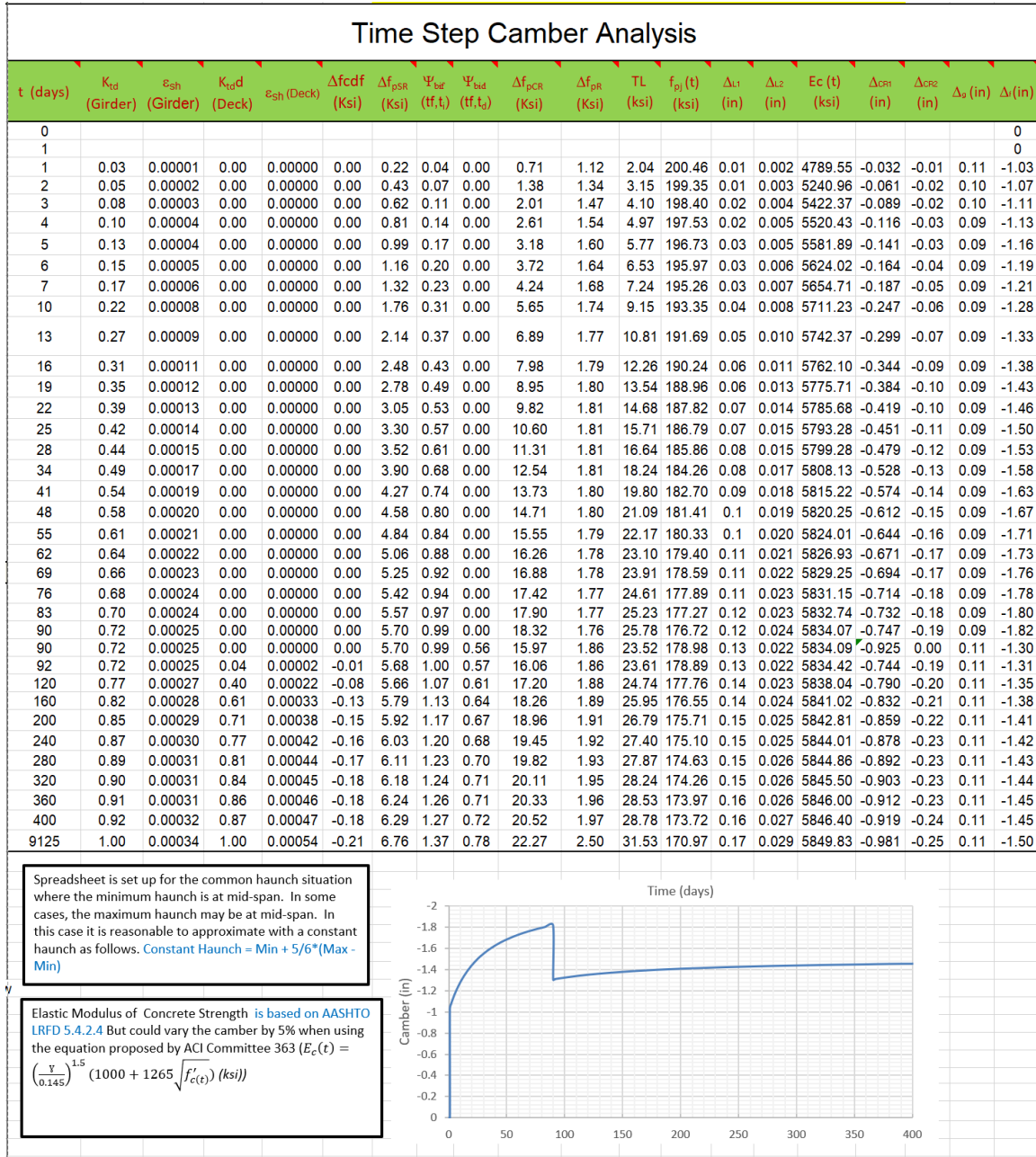


Figure 5-21. Time camber estimates (time-step)

5.2.4 Sensitivity Analysis

Although the proposed method gives more accurate camber prediction, there are several factors that will affect the camber. It is hard to control some of these factors during construction. So, the sensitivity analysis was added as a part of the spreadsheet to understand the effect of changing these factors on the camber calculation at transfer and at 90 days (see Figure 5-22). These factors include the initial compressive strength, aging strength factors, k_1 factor for elasticity modulus, overhang length, daily temperature change, density of concrete, creep coefficient, and losses due to concrete curing. The user must hit the run button to facilitate the sensitivity analysis. Note that + sign means decrease in the camber and – sign means increase in the camber.

	Initial Compressive strength (ksi)	Change in camber (in.)		AGING STRENGTH (α and β)		Change in camber (in.)		Eci (K1)	Change in camber (in.)		over hang length (ft)	Change in camber (in.)		Run	
		Initial	90 days	Initial	90 days	Initial	90 days		Initial	90 days		Initial	90 days		
	7	0.08	0.19	0.482	0.98	0.04	0.11	0.85	-0.11	-0.13	3.61	0.07	0.10		
	7.5	0.11	0.27	2.3	0.92	0.11	0.10	0.9	-0.05	-0.04	2.71	0.06	0.10		
	8	0.14	0.34	1	0.95	0.07	0.11	0.95	0.00	0.04	1.80	0.06	0.10		
	8.5	0.17	0.40	0.7	0.98	0.05	0.11	1.05	0.08	0.17	0.90	0.05	0.11		
	9	0.19	0.45	1.4	0.95	0.08	0.11	1.1	0.12	0.23	4.51	0.07	0.09		
Max		0.19	0.45			0.11	0.11		0.12	0.23		0.07	0.11		
Min		0.00	0.00			0.00	0.00		-0.11	-0.13		0.00	0.00		
	Daily temperature change	Change in camber (in.)		Density factor	Change in camber (in.)		Strand eccentricity (in.)	Change in camber (in.)		creep coefficient	Change in camber (in.)		Temperature due to concrete curing	Change in camber (in.)	
		Initial	90 days		Initial	90 days		Initial	90 days		Initial	90 days		Initial	90 days
	10	0.11	0.17	0.95	0.03	0.09	0.0625	0.0419	0.1063	0.8	0.05	0.25	60	0.12	0.23
	20	0.17	0.24				-0.0625	0.0430	0.1082	0.9	0.05	0.18			
	30	0.24	0.30							1.1	0.04	0.04			
										1.2	0.04	-0.03			
Max		0.24	0.30		0.03	0.09		0.04	0.11		0.05	0.25		0.12	0.23
Min		0.00	0.00		0.00	0.00		0.00	0.00		0.00	-0.03		0.00	0.00

Figure 5-22. Sensitivity analysis

5.3 Spreadsheet Verification

The accuracy of the spreadsheet was verified by running an independent analysis of 2 girders (a NU girder and a Tx girder) and comparing the results to PGSuper and Lusas (Figure 5-23 and

Figure 5-24). The results show that at transfer PGSuper was about 4% lower and Lusas about 21% higher than the spreadsheet. At 90 days (before deck) PGSuper was 21% higher and Lusas 3% lower. At 90 days (after deck) PG super was 60% higher and Lusas 4% higher. All predictions were within approximately ½ in. These results indicate that the spreadsheet was able to accurately determine the camber. Possible reasons for differences include: difference in models to predict elastic modulus and compressive strengths at early ages (under 28 days), moment of inertia used to calculate deflections, support locations used during deflection calculations, and equations used to predict prestress losses: approximate vs refined estimates.

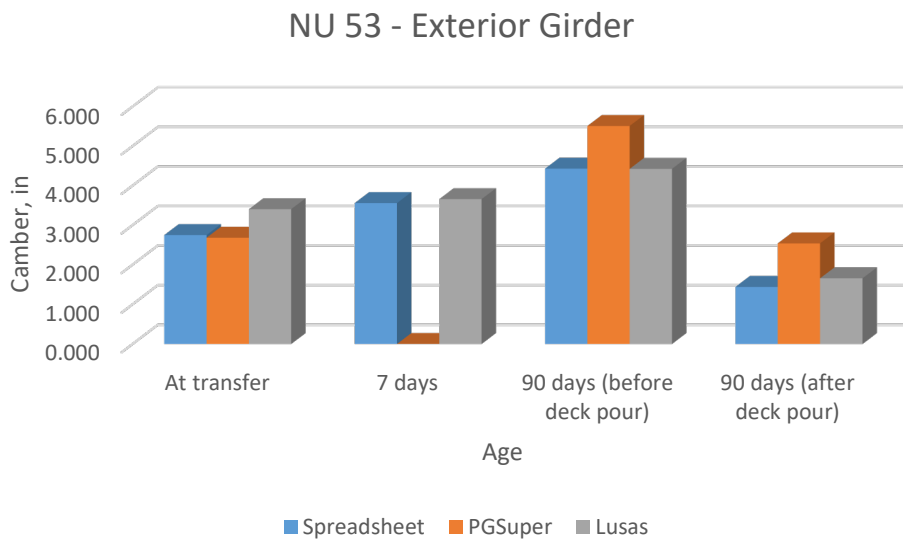
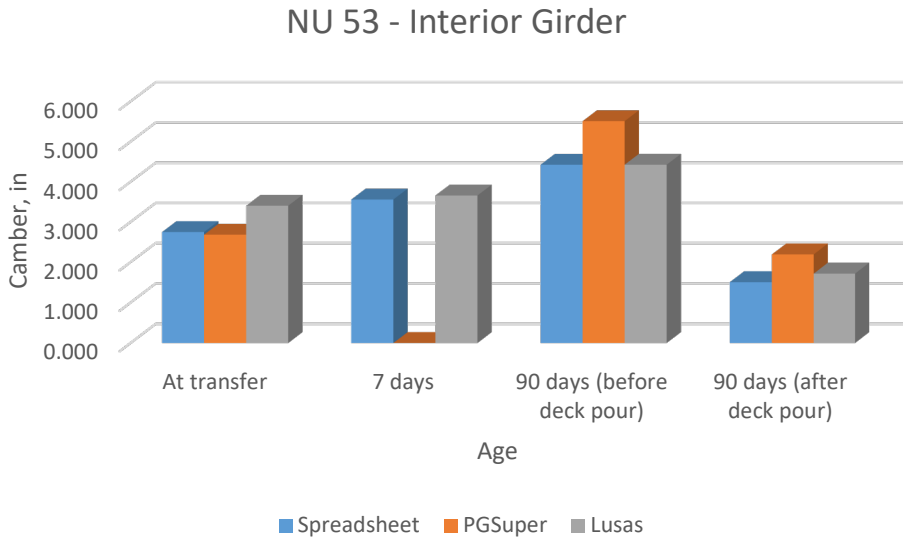


Figure 5-23. Comparison of Spreadsheet results vs PGSuper and Lusas for NU girder

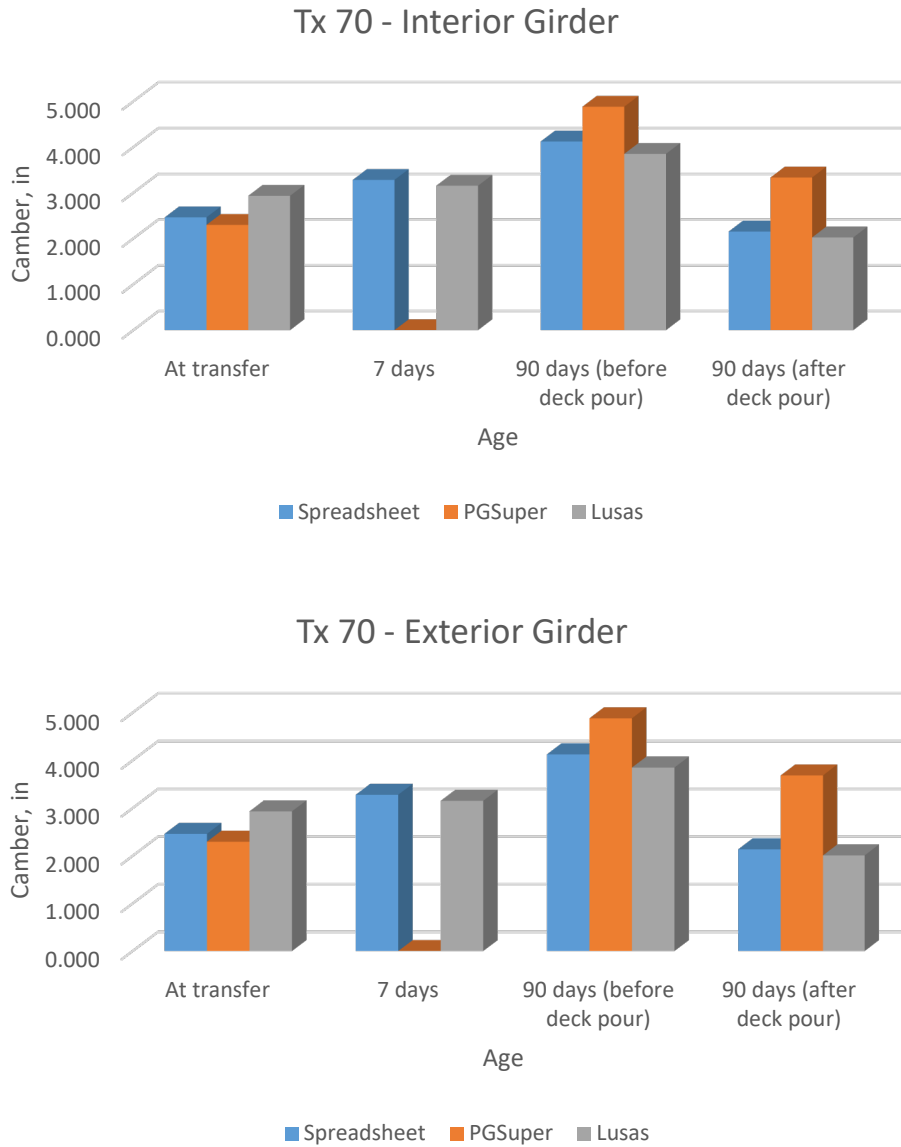


Figure 5-24. Comparison of Spreadsheet results vs PGSuper and Lusas for Tx girder

5.4 *Proposed Camber Measurement*

The accurate measurement of the camber is also critical for the evaluation of the girder. The following recommendations outline a method for camber measurement using a string line.

- Use a string line with the least possible self-weight. The self-weight is directly proportional to the amount of sag. An 80-lb. braided fishing line or similar can be used with negligible sag effect.
- For more accurate measurement and to mitigate the effect of sag in the string line, reference marks can be placed on the girder before the strands are cut.
- Consistent pull forces are needed to reduce variability in camber measurement. A hanging scale to measure the amount of pull, or a pulley and weight system are recommended to apply consistent tension. The recommended level of force is between 20 and 30 lbs. With a braided fishing line this will reduce the sag to less than 0.1 in. over 100 ft.
- According to Tadros (2015) the tolerance for predicted cambers of less than 1 in. is $\pm\frac{1}{2}$ in. For predicted cambers larger than 1 in. the tolerance is $\pm 50\%$ of the predicted camber. If a girder falls outside of tolerance, then a more accurate method, such as use of a rotary laser level, is recommended to confirm the camber measurement.
- Measurements should be taken in the morning before temperature gradients due to daily heating cause additional camber.
- Measurements taken before 72 hours after curing may have reduced camber (~12%) due to increased concrete temperature reducing the prestressing force.

CHAPTER 6: SUMMARY AND CONCLUSIONS

Accurate bridge camber in prestressed concrete girders is a critical design component in the ride, appearance, maintenance requirements, slab placement, and overall life of a concrete bridge superstructure. This study looked closely at possible contributors to the causes for error in camber, including concrete properties (e.g. strength, modulus, time-dependent characteristics of concrete due to aging, creep, and shrinkage), prestressing tendon relaxation, beam storage conditions, and camber measurement methods. The study evaluated the sources of error in camber prediction and measurement, and developed a modified calculation model validated with measured field data.

A literature review found several previous studies that have highlighted the difficulties in predicting initial and long-term camber. Even with improvements to equations, accuracy was only in the $\pm 15\%$ range. The primary causes of camber error were:

- Concrete compressive strength (on the order of 22% higher at release),
- Concrete modulus (many studies recommended the AASHTO 2010 equation for modulus with k_1 factors from 0.85 to 1.2),
- Temperature (differences in ambient and curing temperatures causing reduction of prestress force at release, and daily temperature variations causing as much as 0.75 in. change in camber),
- Creep and shrinkage parameters (most studies recommend use of AASHTO creep and shrinkage models but some (Honarvar et al. 2015, Stallings et al. 2003) used modification factors,

- Support geometry during storage: overhang length in storage affects the girder camber and most studies recommend including the effect,
- Variability in initial prestress and girder self-weight.

Data from 189 girders with initial camber and 33 girders with later camber measurements before hauling were analyzed to evaluate the accuracy of the camber calculation procedure. In addition, field measurements were conducted on four girders, including material characterization tests for concrete strength gain with time, modulus, and creep.

The girders selected for this study were found to be reasonably representative of the inventory of NU girders in Missouri. The current camber measurement showed an average under-prediction of the camber by about 23%. The camber measurement method in two precast plants were compared. It was found that the self-weight of the string line used to measure camber caused a significant sag and led to larger than actual camber measurements. Field measurements were made on four girders from two separate pours and cylinder strength, modulus, and creep data taken. The field cambers showed an over-prediction of camber for one set of girders, while the other was well predicted.

A systematic look at the parameters affecting the accuracy of the initial and long-term camber predictions was undertaken. The following conclusions are made based on that analysis:

- An evaluation of the current MoDOT camber prediction method found that the current method under-predicts the camber by about 23%.
- The method of camber measurement is critical to the accuracy of the camber measurement. The current heavy Kevlar string line used by Plant #2 produced a line sag of 0.56 in. under a 45 lb. pull force for a 100 ft. girder. If the camber

measurement is corrected for possible sag in the string line, then the under-prediction of camber is reduced to 4%.

- Consistency of the camber measurement is also important. Plant #2 had a more consistent measurement method and less variability than Plant #1.
- The length of the overhang (distance past temporary supports) does affect camber. A change in overhang length from 0 ft. to 4 ft. can cause an average change in camber of about 20% in the girder data set. Analysis equations used in PGSuper can be used to include the effect of overhang in the initial camber. In addition, the location of temporary supports should be consistent, possibly under locations of lifting loops, to reduce variability in camber predictions.
- Concrete compressive strength at prestress transfer is typically higher than the design initial concrete strength. The average initial compressive strength of the field bridges was 8.58 ± 1.17 ksi, about 32% higher than the design strength (6.5 ksi).
- The increased compressive strength affects the modulus of the concrete, and thereby the predicted camber. Using the measured compressive strength, the trendline slope of the measured to predicted camber decreases by 10%.
- Equations used to calculate concrete modulus from concrete compressive strength were evaluated. Using the AASHTO LRFD 5.4.2.3.2 (2012) equations vs. the ACI Committee 209 (1997) changed the camber by only 4%.
- Both elevated temperatures during curing and daily temperature changes affect camber. Increased temperatures during curing can temporarily reduce prestress forces and reduce camber by about 12%. Daily temperature changes cause a

thermal gradient in the girder and can increase camber by 25% with a 25 °F temperature change.

- Variability in initial prestress force, concrete density, type of section property used (gross vs. transformed) and strand eccentricity results in a change of camber of only approximately 5%.
- The current AASHTO discrete time-step approach can predict the long-term camber.

Based on the analysis of camber prediction methods and comparison to Missouri bridge data, the following recommendations are made:

- Procedures and tolerances for the measurement of camber at prestress girder plants are needed.
- The length of the overhang (distance past temporary supports) needs to be included in the camber analysis. It is recommended that the equations found in PGSuper be used to account for the overhang length. Procedures for consistent placement of temporary supports are needed.
- While concrete compressive strength (and related modulus) affects camber, it is not possible to predict the actual strength beforehand. Therefore, design initial concrete strength can still be used. If initial concrete strength is increased to 8,500 psi there would be an average 10% reduction in camber.
- The effect of temperature should be considered in the camber results. In order to negate the effect of temperature, camber can be measured at least 72 hours after form release, and in the morning (Tadros 2015).

- Other factors affect camber to a lesser degree (initial prestress force, concrete density, type of section property used (gross vs. transformed) and strand eccentricity) and need not be modified in predicting camber.

The main changes in the camber calculation equations compared to the current MoDOT method are:

- Incremental time-step approach. Rather than determining camber at transfer, 7 days, and 90 days, camber can thus be determined at any point in the life of the girder. Spreadsheet still calculates specific time points (7 day, 90 day) for bridge plans.
- Include effect of overhang length on camber while girder is in storage. Spreadsheet allows adjustment of length to centerline of bearing when girder is placed.
- Additional options to include the effects of prestress loss due to elevated concrete temperatures during curing and daily temperature effects on camber.

The modifications to the camber calculation reduced the underprediction of camber to less than 4% on average (when sag in the string line measurement was accounted for) and decreased the RMSE from 0.81 in. to 0.30 in. and the average error from 35% to 20%. This yielded predictions that were in most cases within $\pm 25\%$ of the measured camber. The proposed method was implemented into a computer spreadsheet for easy calculation.

REFERENCES

- AASHTO. (2012). *AASHTO LRFD bridge design specifications, customary U.S. units. AASHTO load and resistance factor design bridge design specifications.*
- AASHTO. (2014). *AASHTO LRFD bridge design specifications. customary U.S. units.*
- American Concrete Institute (ACI) Committee 209. (1997). "Prediction of Creep, Shrinkage and Temperature Effects in Concrete Structures." *ACI Committee 209 Report, 92(Reapproved),* 47.
- Brice, R. (2020). " Precast, Prestress Bridge Girder Design Example, PGSuper Training"
- Brown, K. M. (1998). "Camber growth prediction in precast prestressed concrete bridge girders." (December).
- Byle, K. A., Burns, N. H., and Ramón L. Carrasquillo. (1997). *Module 03 – High Performance Computing. TEXAS.*
- CEB-FIB. (1999). *fib Model Code for Concrete Structures. fib journal, Structural Concrete.*
- CEB-FIB. (2010). *fib Model Code for Concrete Structures. fib journal, Structural Concrete.*
- French, C. E., and O'Neill, C. R. (2012). *Validation of Prestressed Concrete I-Beam Deflection and Camber Estimates. Minnesota.*
- Garber, D., Gallardo, J., Deschenes, D., Dunkman, D., and Oguzhan, B. (2012). *Effect of New Prestressed Loss Estimation on Prestressed Concrete Bridge Girder Design. Travel*

Behaviour Research, Texas City.

Gilbertson, C. G., and Ahlborn, T. M. (2004). “A probabilistic comparison of prestress loss methods in prestressed concrete beams.” *PCI journal*, 49(5).

Gopalaratnam, V., and Eatherton, M. R. (2001). “INSTRUMENTATION AND MONITORING OF HIGH PERFORMANCE CONCRETE PRESTRESSED BRIDGE GIRDERS.” *undefined*.

Honarvar, E., Nervig, J., and Rouse, J. M. (2015). *Improving the accuracy of camber predictions for precast pretensioned concrete beams. DOT National Transportation Integrated Search - ROSA P*.

Jayaseela, H., and Bruce, W. R. (2007). *Prestress losses and the estimation of long-term deflections and camber for prestressed concrete bridges final report. Design*, Oklahoma State.

Mohammedi, A., and Hale, M. (2018). *Estimating Camber, Deflections, and Prestress Losses in Precast Prestressed Bridge Girders*.

Naaman, A. E. (2012). *Prestressed Concrete Analysis and Design - Fundamentals*. Techno Press.

Nguyen, H., Stanton, J., Eberhard, M., and Chapman, D. (2015). “The effect of temperature variations on the camber of precast, prestressed concrete girders.” *PCI Journal*, 60(5), 48–64.

Rizkalla, S., and Zia, P. (2011). *Predicting Camber, Deflection, and Prestress Losses in*

Prestressed Concrete Members. North Carolina.

Rosa, M. A., Stanton, J. F., and Eberhard, M. O. (2007). *Improving Predictions for Camber in Precast , Prestressed Concrete Bridge Girders* by. WASHINGTON, D.C.

Stallings, J. M., Barnes, R. W., and Eskildsen, S. (2003). “Camber and Prestress Losses in Alabama HPC Bridge Girders.” *PCI Journal*, 48(5), 90–104.

Tadros, M. K., Al-Omaishi, N., Seguirant, S. J., and Gallt, J. G. (2003). *Prestress Losses in Pretensioned High-Strength Concrete Bridge Girders*. WASHINGTON, D.C.

Tadros, M. K., Fawzy, F. F., and Hanna, K. E. (2011). “Precast, prestressed girder camber variability.” *PCI journal*, 56(1).

Tadros, M.K. (2015) “Camber Variability in Prestressed Concrete Bridge Beams” *Concrete Bridge Technology, ASPIRE Spring 2015, pp. 38-42*

Tomley, D. A. (2019). *Best Practices for Estimating Camber of Bulb T and Florida Girders*.

Yang, Y., and Myers, J. J. (2005). “Prestress loss measurements in Missouri’s first fully instrumented high-performance concrete bridge.” *Transportation Research Record*, 118–125.

Appendix A

A-1 Current MoDOT Method

MoDOT suggests using a discrete-time-step approach which means to calculate the camber at different time points. These time points are at prestress transfer, 7 days after strand release, 90 days after strand release, and after the slab is poured. Also, MoDOT suggests using transformed properties in the calculation in which the relaxation losses aren't considered, and considers the effect of debond length. The existing method used by MoDOT is as follows:

Initial Camber at Transfer

The initial camber at prestress transfer is the combination of the deflections due to the girder self-weight and prestressing forces from harped and straight strands:

$$\Delta_{Ic} = \Delta_g + \Delta_{HS} + \Delta_{SS}$$

where:

Δ_{Ic} = initial camber at transfer,

Δ_g = deflection due to self-weight of girder (not including overhang),

Δ_{SS} = camber due to prestressing straight strands,

Δ_{HS} = camber due to prestressing harped strands,

Note: Negative and positive values indicate upward camber and downward deflections, respectively. Details of deflection calculations are given in Section 1.5.

Camber at Midspan After Strand Release (Estimated at 7 days)

The girder camber 7 days after strand release is the initial camber plus the effect of creep over 7 days:

$$\Delta_7 = \Delta_{Ic} + \Delta_{CR \text{ at } 7 \text{ days}}$$

where:

Δ_7 = the girder camber at 7 days after prestress strand release with creep,

$\Delta_{CR \text{ at } 7 \text{ days}}$ = time - dependent camber caused by creep at 7 days.

Camber at Midspan After Erection (Estimated at 90 days)

The girder camber 90 days after strand release is the initial camber plus the time-dependent camber effect over 90 days:

$$\Delta_{90} = \Delta_{Ic} + \Delta_{CR \text{ at } 90 \text{ days}}$$

where:

Δ_{90} = the girder camber at 90 days after prestress strand release with creep,

$\Delta_{CR \text{ at } 90 \text{ days}}$ = time - dependent camber caused by creep at 90 days.

Final Camber at Midspan After Pouring the Slab

Total camber after pouring the slab can be calculated as the sum of the girder camber after erection (90 days) and displacements caused by slab and concentrated loads (diaphragms, haunch, etc.) before composite action between girder and slab.

$$\Delta_{FC} = \Delta_{90} + \Delta_S + \sum \Delta_C$$

where:

Δ_{FC} = final camber after pouring the slab,

Δ_S = displacement caused by slab weight,

$\sum \Delta_C$ = displacement caused concentrated loads (diaphragms, haunch, etc.).

Calculation of Camber (Upward) Using Transformed Properties.

Camber at midspan due to strand forces are determined by the following:

For straight strands,

$$\Delta_{SS} = \Delta_{SS-j} + \Delta_{SS-l}$$

$$\Delta_{SS-j} = \frac{F_{1-j} e_1}{8E_{ci}I_{tri}} (L^2 - 4l_0^2)$$

$$\Delta_{SS-l} = \Delta_{SS-j} \frac{\text{Initial losses}}{f_{pj}}$$

where:

F_{1-j} = total prestressing force of straight strand group just prior to transfer (kips),

L = distance between centerlines of bearing pads (in.),

l_0 = debond length of straight strand group from end of girder (in.),

E_{ci} = initial concrete modulus of elasticity,

I_{tri} = moment of inertia of transformed non-composite section (in.4),

e_1 = eccentricity between centroid of straight strand group (CSS) and center of gravity of transformed non-composite section (CGB) as shown in Figure below (in.),

f_{pj} = prestressing force in the strand just prior to transfer (ksi),

Initial losses = Summation of the time dependent losses (7 or 90 day). Losses include relaxation, creep, and shrinkage, but exclude elastic shortening.

$$\text{Losses} = \Delta f_{pSR} + \Delta f_{pCR} + \Delta f_{pR} + \Delta f_{pSD} + \Delta f_{pCD} + \Delta f_{pSS}$$

$$\Delta f_{pES} = \frac{E_p}{E_{ci}} f_{cgp}$$

$$\Delta f_{pR} = \frac{\log(24t)}{45 \log(24t_i)} K_{id} \left[1 - \frac{3(\Delta f_{pR} + \Delta f_{pR})}{f_{pj}} \right] \left[\frac{f_{pj}}{f_{py}} - 0.55 \right] f_{pj}$$

$$\Delta f_{pSR} = \varepsilon_{bid} E_p K_{id}$$

$$\Delta f_{pSD} = \varepsilon_{bdf} E_p K_{df}$$

$$\Delta f_{pCR} = E_p f_{cgp} \Psi_{bid} K_{id} / E_{ci}$$

$$\Delta f_{cdf} = \frac{\varepsilon_{ddf} A_d E_{cd}}{1 + 0.7 \psi_{df}} \left(\frac{1}{A_c} + \frac{e_{pc} e_d}{I_c} \right)$$

For harped strands:

$$\Delta_{HS} = \Delta_{HS-j} + \Delta_{HS-l}$$

$$\Delta_{HS-j} = \frac{F_{2-j} e_2 L^2}{8 E_{ci} I_{tri}} - \frac{F_{2-j} (e_2 + e_3) a^2}{6 E_{ci} I_{tri}}$$

$$\Delta_{HS-l} = \Delta_{HS-j} \frac{\text{Initial losses}}{f_{pj}}$$

$$a = (L - b) / 2$$

where:

Δ_{HS-j} = total prestressing force of harped strands just prior to transfer (kips),

b = length between harped points (in.),

e_2 = eccentricity between centroid of harped strands (CHS) and center of gravity of transformed non-composite section (CGB) at midspan as shown in Figure below (in.),

e_3 = eccentricity between centroid of harped strands (CHS) and center of gravity of transformed non-composite section (CGB) at the end of girder as shown in Figure below (in.).

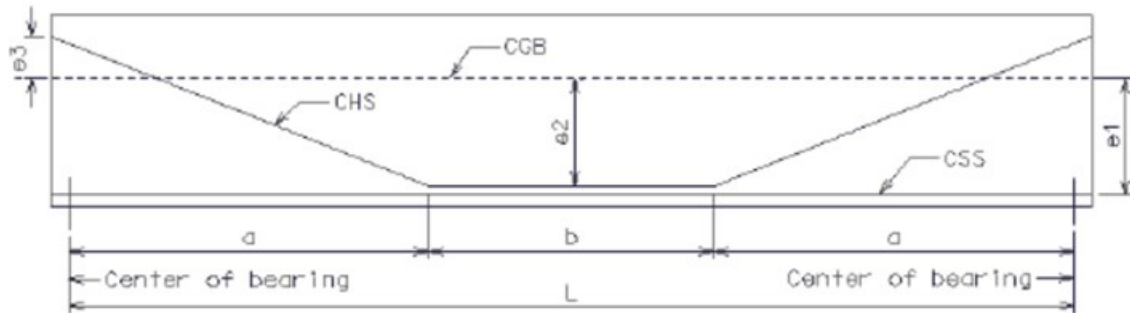


Figure 1. Girder details displaying the eccentricities and distances used in camber computations

Calculations of Deflections (Downward)

Deflections at midspan due to dead loads are determined as the following:

For self-weight of girder,

$$\Delta_g = \frac{5w_g L^4}{385E_{ci}I_{tri}}$$

where:

w_g = uniform load due to self-weight of girder, (kip/in.)

For self-weight of slab,

$$\Delta_s = \frac{5w_s L^4}{385E_c I'_{tri}}$$

where:

w_s = uniform load due to self-weight of slab (kip/in.),

E_c = final concrete modulus of elasticity based on f_c (ksi),

I'_{tri} = moment of inertia of transformed non-composite section (in.4).

Weight of additional slab haunch may be treated as uniform or concentrated load as appropriate.

Diaphragm weight should be treated as concentrated load.

For one concentrated load at midspan,

$$\Delta_c = \frac{PL^3}{48E_c I'_{tri}}$$

For two equal concentrated loads,

$$\Delta_c = \frac{Px}{48E_c I'_{tri}} (3L^2 - dx^2)$$

where:

P = concentrated load due to diaphragm and/or additional slab haunch (kips),

x = distance from the centerline of bearing pad to the applied load, P (in.).

Creep Coefficient

Research has indicated that high strength concrete (HSC) undergoes less ultimate creep and shrinkage than conventional concrete. Creep is a time-dependent phenomenon in which deformation increases under a constant stress. Creep coefficient is a ratio of creep strain over elastic strain, and it can be estimated as follows:

$$\Psi(t, t_i) = 1.9k_s k_{hc} k_f k_{td} t_i^{-0.118}$$

$$k_s = 1.45 - 0.13(v/s) \geq 1.0$$

$$k_{hc} = 1.56 - 0.008H$$

$$k_f = 5/(1 + f'_{ci})$$

$$k_{td} = t / \left(\frac{12(100 - 4f'_{ci})}{f'_{ci} + 20} + t \right)$$

where:

Ψ = creep coefficient,

H = 70, average annual ambient relative humidity,

t = maturity of concrete, (days), use 7 days for camber design after strand release, use 90 days for camber design after erection,

t_i = age of concrete when a load is initially applied, (days) use 0.75 days for camber design,

v/s = volume-to-surface area ratio (in.),

f'_{ci} = initial girder concrete compressive strength (ksi).

$$\Delta_{CR} = (\Delta_{SS-j} + \Delta_{HS-j} + \Delta_g) \Psi + (\Delta_{SS-i} + \Delta_{HS-i}) 0.7 \Psi$$

A-2 PGSuper Method

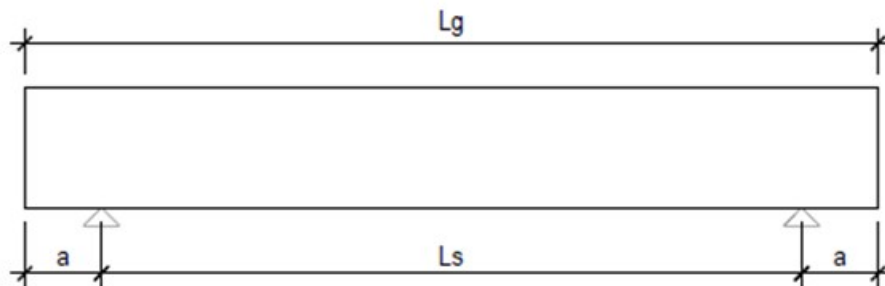


Figure 2. Girder dimensions

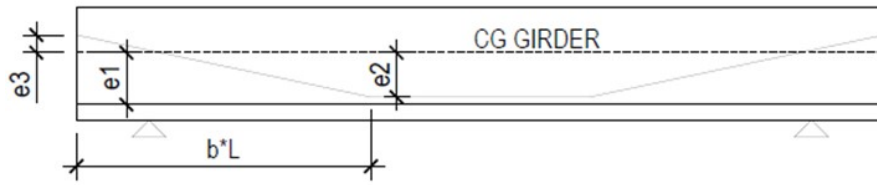


Figure 3. Optimum strand arrangement

The discrete time-step approach used in PGSuper allows to calculate the camber at prestress transfer, 90 days after strand release, and after the slab is poured. Also, PGSuper suggests using gross properties in the calculation in which the relaxation losses are considered. In addition, it is suggested by MoDOT to consider the effect of overhang length. The existing method used by PGSuper is as follow:

Initial Camber at Transfer

The initial camber at prestress transfer due the girder self-weight and prestressing forces from harped and straight strands shall be determined as:

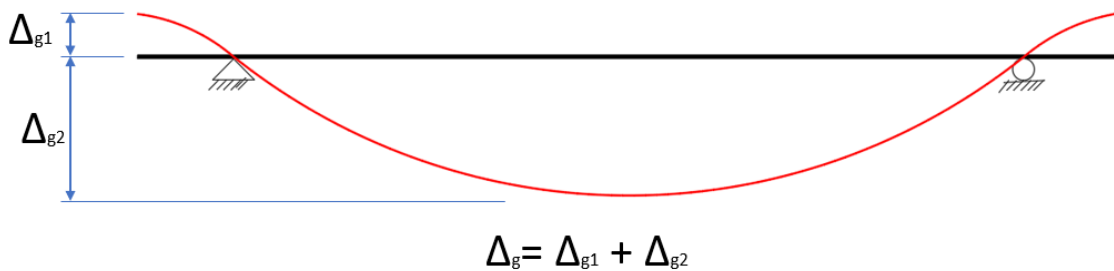


Figure 4. Girder self-weight deflection during lifting (Brice 2020)

$$\Delta_{Ic} = \Delta_{g1i} - \Delta_{g2i} + \Delta_{PS}$$

$$\Delta_{ps} = \Delta_{HS} + \Delta_{SS}$$

where:

Δ_{Ic} = initial camber at transfer,

Δ_{g1i} = deflection due to self-weight of girder at the overhang part,

Δ_{g2i} = deflection due to self-weight of girder at the middle part,

Δ_{SS} = camber due to prestressing straight strands,

Δ_{HS} = camber due to prestressing harped strands.

Note: negative and positive values indicate upward camber and downward deflections, respectively.

Factor	Equation
Δ_{g1i}	$\Delta_{g1} = \frac{w_g \cdot a}{24E_{ci}I_x} [3a^2(a + 2L_s) - L_s^3]$
Δ_{g2i}	$\Delta_{g2} = \frac{5w_g L_s^4}{384E_{ci}I_x} - \frac{w_g a^2 L_s^2}{16E_{ci}I_x}$
Δ_{SS}	$\Delta_{SS} = \frac{P_s e_1 L^2}{8E_{ci}I_x}$
Δ_{HS}	$\Delta_{HS} = \frac{b(3 - 4b^2)NL^3}{24E_{ci}I_x} + \frac{P_h e_3 L^2}{8E_{ci}I_x}$ $N = \frac{P(e_2 + e_3)}{bL}$

where:

P_s = total prestressing force of straight strand group just prior to transfer with considering the elastic shortening and initial relaxation losses, (kips),

P_h = total prestressing force of harped strand group just prior to transfer with considering the elastic shortening and initial relaxation losses, (kips),

L = distance between centerlines of bearing pads, (in.),

E_{ci} = initial concrete modulus of elasticity,

I_x = gross moment of inertia of non-composite section, (in.4),

Camber at Hauling (Estimated at 90 days)

The camber at hauling is equal to the camber at the end of storage, plus the change in dead load deflection due to the different support conditions between storage and hauling. Transportation is generally assumed to occur at 90 days.

$$\Delta_{90} = (\Delta_{g1} + \Delta_{ps1} + \Delta_{CR1 \text{ at } 90 \text{ days}})_{\text{mid-span}} + (\Delta_{g2} + \Delta_{ps2} + \Delta_{CR2 \text{ at } 90 \text{ days}})_{\text{end}}$$

$$\Delta_{CR1 \text{ at } 90 \text{ days}} = \Psi(\Delta_{g1i} + \Delta_{ps1})$$

$$\Delta_{CR2 \text{ at } 90 \text{ days}} = \Psi(\Delta_{g2i} + \Delta_{ps2})$$

where:

Ψ = the creep coefficient and can be calculated using the AASHTO LRFD 5.4.2.3.2.

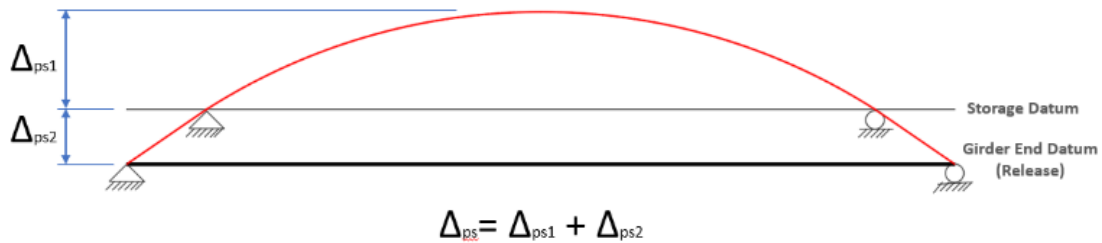


Figure 5. Prestress induced deflection based on storage datum (Brice (2020))

where:

Δ_{90} = the girder camber at 90 days after prestress strand release with creep,

$\Delta_{CR1 \text{ at } 90 \text{ days}}$ = time - dependent camber caused by creep at 90 days at girder mid-span,

$\Delta_{CR2 \text{ at } 90 \text{ days}}$ = time - dependent camber caused by creep at 90 days at girder end.

Factor	Equation
Δ_{g1}	$\Delta_{g1} = \frac{w_g \cdot a}{24E_c I_x} [3a^2(a + 2L_s) - L_s^3]$
Δ_{SS1}	$\Delta_{SS} = \frac{P_s e_1 L_s^2}{8E_{ci} I_x}$
Δ_{HS1}	$\Delta_{HS} = \frac{b(3 - 4b^2)NL_s^3}{24E_{ci} I_x} + \frac{P_h e_3 L_s^2}{8E_{ci} I_x}$ $N = \frac{P_h(e_2 + e_3)}{bL}$
Δ_{PS2}	$\Delta_{PS2} = \Delta_{HS1} + \Delta_{SS1} - \Delta_{PS}$

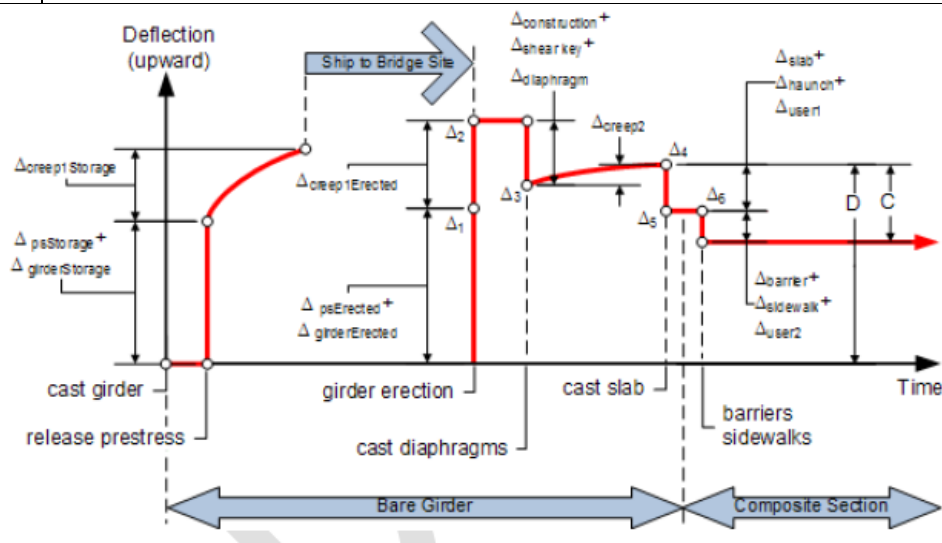


Figure 6. Camber diagram

Δ_{girder} = deflection caused by the girder self- weight,

Δ_{ps} = deflection caused by permanent prestressing, based on the in-place span length,

$$\Delta_{creep1} = \Psi(t_e, t_i)(\Delta_{girder} + \Delta_{ps})$$

Δ_{dia} =deflection caused by the self-weight of diaphragm,

δ_{girder} =incremental girder deflection caused by change in support between storage and erection,

$$\Delta_{creep2} = (\Psi(t_d, t_i) - \Psi(t_e, t_i))(\Delta_{girder} + \Delta_{ps}) + \Psi(t_d, t_e)(\Delta_{dia} + \delta_{girder})$$

Δ_{deck} =deflection caused by the self-weight of deck,

Δ_{haunch} =deflection caused by the self-weight of haunch,

$\Delta_{barrier}$ =deflection caused by the self-weight of traffic barrier,

Δ_{excess} =excess camber,

$$\Delta_1 = (\Delta_{girder} + \Delta_{ps})$$

$$\Delta_2 = (\Delta_1 + \Delta_{creep1})$$

$$\Delta_3 = (\Delta_2 + \Delta_{dia})$$

$$\Delta_4 = (\Delta_3 + \Delta_{creep2})$$

$$\Delta_5 = (\Delta_4 + \Delta_{deck} + \Delta_{haunch})$$

$$\Delta_6 = (\Delta_5 + \Delta_{barrier})$$

A-3 Incremental time-step approach Stallings et al. (2003)

Incremental time-step analysis can be used for the determination of prestressed girder deflection and camber over time. This kind of calculation is practical by using a computer program, for example, a spreadsheet. Compared to the discrete approach, this method can give camber at any time point. The camber at any time after the transfer of the prestress force is determined by:

$$\delta(t) = \delta_e(t) + 0.5[\delta_e(t) + \delta_i]C(t) + \delta_D[1 + C(t)]$$

where δ_i is the camber caused by the initial prestress force instantaneously after transfer, $\delta_e(t)$ is the camber caused by the effective prestress force at any time, $C(t)$ is the creep coefficient, δ_D is the immediate deflection caused by the different types of dead loads, and $\delta(t)$ is the overall camber at any time. The camber caused by prestress losses and dead loads can be calculated using the same equations used by MoDOT.

$\delta_e(t)$ is calculated using the time-dependent prestress forces considering the effects of shrinkage and creep. The current calculation uses ACI equations and parameters for these effects as follows:

$$C(t) = \frac{t^\Psi}{d + t^\Psi} C_u \gamma_c$$

where C_u is the ultimate creep coefficient; Ψ and d are constants; and γ_c is the product of correction factors for loading age, type of curing, relative humidity, the volume-to-surface ratio of the member, slump, and component materials of the concrete mixture.

A-4 Incremental time-step approach Tadros et al. (2011)

Tadros et al. (2011) recommended the overhang effect to be considered in the calculation of the camber during the erection stage. He proposed a prediction method was proposed which considers that the prestressed girder is located on temporary supports at the storage yard that is a few feet into the span from the girder's ends. In addition, this method includes the effect of debond strands and transfer length. The long-term camber can be calculated with the same equation used by MoDOT. The creep coefficient can be calculated using the AASHTO LRFD 5.4.2.3.2.

The equations used in this method for predicting the initial camber are listed below in table 1. However, these equations give the deflection from the support to the middle of the girder. An additional term would need to be added to include the deflection from the end of the girder to the support.

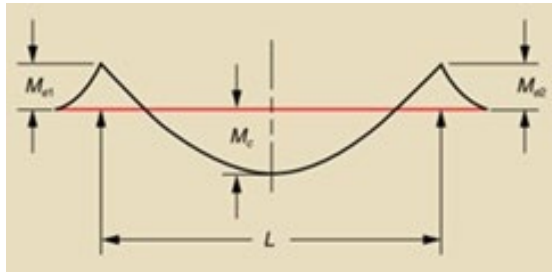


Figure 7. Bending moment diagram due to girder own weight

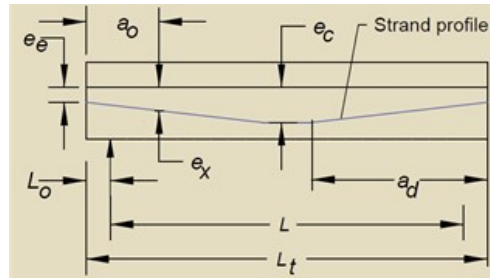


Figure 8. Optimum strand arrangement used in Tadros method

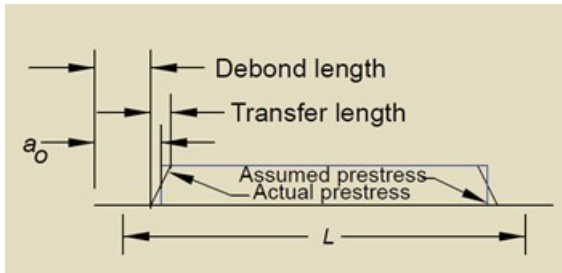


Figure 9. Debond and transfer length

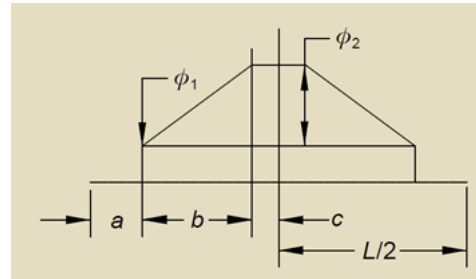


Figure 10. The curvature distribution due to the initial prestress

Table 1. Equation used in the initial camber prediction proposed by Tadros et al. 2001

Factor	Equation
Δ_d	$\Delta_d = \frac{5L^2}{48E_{ci}I_x} (0.1M_{e1} + M_c + 0.1M_{e2})$
Δ_s	$\Delta_s = \frac{\phi_1}{2} (b + c)(2a + b + c) + \frac{\phi_2}{6} (3ab + 2b^2 + 6ac + 3c^2)$
	$\phi_1 = \frac{P_i e_x}{E_{ci} l_{ti}} \quad \phi_2 = \frac{P_i (e_c + e_x)}{E_{ci} l_{ti}}$
a	$a = a_0 - L_0, \quad L_0 = \frac{L_t - L}{2}$
b	$b = a_d - a_0$

c	$c = \frac{L}{2} - a - b$
e_x	$e_x = e_e + \frac{a_0}{a_d} (e - e_e)$

where:

Δ_d = deflection caused by the dead load of the girder,

Δ_s = camber caused by the straight and harped strands,

M_{e1} = moment at left support, negative if overhang exists, zero if overhang ignored,

M_{e2} = moment at right support, negative if overhang exists, zero if overhang ignored,

M_c = midspan moment,

L_o = overhang length,

L_t = total member length,

a = distance between the support and the assumed start of prestress in girder,

a_0 = modified debond length = (actual debond length + transfer length/2),

a_d = distance from member end to hold-down point,

c = distance from the start of curvature to the midspan,

e_x = eccentricity of strand group at point of debonding,

ϕ_1 = curvature due to straight strands,

ϕ_2 = curvature due to harped strands.

A-5 Incremental time-step approach Naaman (2012)

Incremental time-step analysis can be used for the determination of prestressed girder deflection and camber over time. These kinds of calculations are made practical by using a computer program, for example, a spreadsheet. Compared to the discrete approach this method can give camber at any time point.

An incremental time-step approach, even though somewhat cumbersome, provides a more realistic and accurate estimate of the contribution of these coupled nonlinear effects. The theoretical approach that can be used for the incremental time-dependent analysis integrates prestress loss

prediction due to time-dependent effects along with the prediction of the time-dependent deflection time histories. This is accomplished in the following steps:

1. Divide the timespan of the prestressed member into several time segments (t_i, t_j), with significantly shorter intervals early in its life, when all of the time-dependent effects are more significant and when there are also more changes to the environmental and loading conditions during the early fabrication and construction stages (e.g. 1, 7, 14, 28, 90, 365..... days). Note t_i is the time at the start of the interval and t_j is the time at the end of the time interval under consideration. These times can additionally be chosen to also reflect practical fabrication/construction timelines.
2. Compute the top and bottom strains, $\varepsilon_{ct}(t_i)$, and $\varepsilon_{cb}(t_i)$, at the important cross-sections (support and hold-down points) at the start of the time interval, t_i , based on material properties at this time and basic mechanics.

$$\varepsilon_{ct}(t) = \frac{F(t)}{E_{ce}(t)A_c} \left(1 - \frac{e_c}{k_b}\right)$$

$$\varepsilon_{cb}(t) = \frac{F(t)}{E_{ce}(t)A_c} \left(1 - \frac{e_c}{k_t}\right)$$

$$E_{ce}(t) = \frac{E_c(t)}{1 + C_c(t - t')}$$

$$E_c(t) = 33\gamma_c^{1.5} \sqrt{f'_c(t)} = E_c \sqrt{\frac{t}{b + ct}}$$

$$C_c(t - t') = \frac{(t - t')^{0.6}}{10 + (t - t')^{0.6}} C_{CU} K_{CH} K_{CS} K_{CA}$$

3. For the time interval under consideration, (t_i, t_j), assume that the loading and environmental conditions remain unchanged from the start (t_i) to the finish (t_j). Determine the change in the

top and bottom strains due to aging, creep, shrinkage, relaxation, and prestress losses ($\Delta\varepsilon_{ct}(t_i, t_j)$ and $\Delta\varepsilon_{cb}(t_i, t_j)$) during the time interval $(t_j - t_i)$. Update the strain at the top and the bottom at the support and at the hold-down points ($\varepsilon_{ct}(t_j) = \varepsilon_{ct}(t_i) + \Delta\varepsilon_{ct}(t_i, t_j)$, $\varepsilon_{cb}(t_j) = \varepsilon_{cb}(t_i) + \Delta\varepsilon_{cb}(t_i, t_j)$), and , to enable curvature and deflection computations.

$$\Phi = \frac{\varepsilon_{ct} - \varepsilon_{cb}}{h}$$

4. Use the updated magnitude of the strains as the starting values of the next time interval.

where:

$E_{ce}(t)$ = the equivalent concrete elasticity modulus as affected by creep,

e_c = the eccentricity of the C-force at the section,

M = the externally applied moment,

$F(t)$ = the time prestressing force,

$E_c(t)$ = concrete elasticity modulus at time t ,

t = concrete age (days),

t' = concrete age at prestressing release (days),

$C_c(t - t')$ = creep coefficient at $(t - t')$,

C_{CU} = Nominal ultimate creep coefficient (2.35),

K_{CH} = Ambient relative humidity factor = $1.27 - 0.67h$,

K_{CS} = Volume-to-surface ratio factor = $\frac{2}{3} \cdot \left(1 + 1.13e^{\left(-0.54\left(\frac{v}{s}\right)\right)} \right)$,

K_{CA} = Age application of load factor = $1.13t_i^{-0.094}$.

b and c are empirical constants which are functions cement type and curing conditions.

The time camber caused by the prestressing force and deflection caused by dead load can be calculated as following:

Factor	Equation
$\Delta_g(t)$	$\Delta_{g1} = \frac{w_g \cdot L^4}{384 E_{ce}(t) I_x}$
$\Delta_{SS}(t)$	$\Delta_{SS} = \frac{\Phi_{SS} L^2}{8}$
$\Delta_{HS}(t)$	$\Delta_{HS} = \frac{\Phi_{Hsc} L^2}{8} + (\Phi_{Hse} - \Phi_{Hsc}) * \frac{a^2}{6}$
$\Delta(t)$	$\Delta(t) = \Delta_{g1}(t) + \Delta_{SS}(t) + \Delta_{HS}(t)$

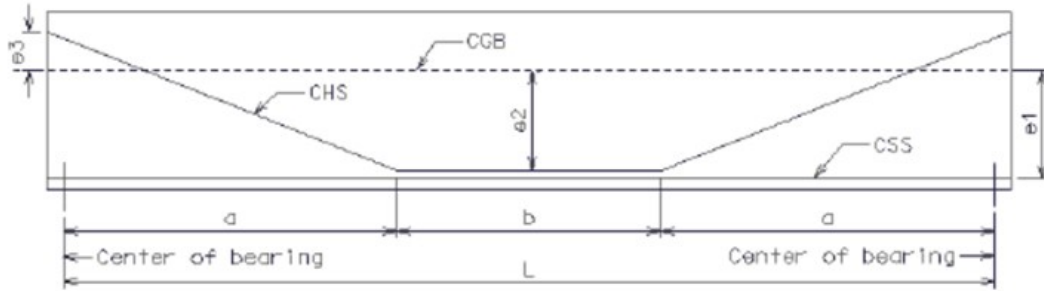


Figure 11: Girder details displaying the eccentricities and distances used in camber computations

where:

Φ_{SS} = curvature caused by straight strands,

Φ_{Hse} = curvature caused by harped strands at the end of the prestressed girder,

Φ_{Hsc} = curvature caused by harped strands at the mid-span of the prestressed girder,

$\Delta_g(t)$ = time deflection caused by girder own weight,

$\Delta_{SS}(t)$ = time camber caused by straight strands,

$\Delta_{HS}(t)$ = time camber caused by harped strands,

$\Delta(t)$ = time camber.